

UNIVERSIDADE DE LISBOA
FACULDADE DE CIÊNCIAS
DEPARTAMENTO DE BIOLOGIA VEGETAL



**Ciências
ULisboa**

Studying mechanisms of antifungal resistance in *Candida glabrata* clinical isolates: emphasis on the role of the CgPdr1 transcription factor

Danielle de Sotti Novais

Mestrado em Microbiologia Aplicada

Dissertação orientada por:
Prof. Doutor Nuno P. Mira
Prof. Doutora Margarida Barata

2017

Acknowledgements

Firstly, I would like to express my gratitude to Professor Nuno Mira for having accepted to be my supervisor at the Institute for Bioengineering and Biosciences (iBB), Instituto Superior Técnico (IST), University of Lisbon, where my work was conducted. In particular, I would like to thank him for his guidance, encouragement, suggestions and mainly for his knowledge and scientific enthusiasm that were of the most valuable for my scientific formation. I would also like to thank Professor Margarida Barata for always being available to help any time it was needed.

Furthermore, I would like to acknowledge Professor Isabel Sá-Correia, for allowing me to do my project in Biological Sciences Research Group and for providing the necessary conditions to realize this thesis. My acknowledgements are also going to Professor Fernanda Carvalho from the Centro de Química Estrutural, Instituto Superior Técnico, for kindly providing me the compounds used in this thesis. I also would like to acknowledge the funding received by iBB-Institute for Bioengineering and Biosciences from FCT-Portuguese Foundation for Science and Technology (UID/BIO/04565/2013), from Programa Operacional Regional de Lisboa 2020 (Project N. 007317).

A special thanks goes to Sara Salazar for her patience in guiding me in the lab, even when she sometimes had to interrupt her on work in order to help me with mine. It would have been truly difficult to advance with my work without her help so I really appreciate all the time she took to support me. I also want to express my gratitude to Pedro Pais, Ana Vila-Santa and Mafalda Cavalheiro for being ready to listen me and for helping me during my journey in the lab. In conclusion, I am most grateful for all my colleagues of the BSRG group for the given support and especially for all the laughs (and sense of humor) that motivated me to continue my project.

Moreover, I want to say thank to my friends outside the lab, specially, Ruth, Iara, Íris, Lígia and Filipa who helped me to keep my mental health during this year and for being always ready to listen to me even in more difficult times. Also, I want to say thank to my colleagues from work.

At last, I want to express my sincere gratitude to my mom and Fernando for all the support during my master degree. I know how difficult it was sometimes, particularly for my mom. I will never be able to thank her enough for the effort she made so that I could finish my studies.

Studying mechanisms of antifungal resistance in *Candida glabrata* clinical isolates: emphasis on the role of the CgPdr1 transcription factor

Danielle de Sotti Novais
2017

This thesis was fully performed at Biological Sciences Research Group (BSRG), Institute for Biotechnology and Bioengineering (IBB), Instituto Superior Técnico, University of Lisbon under the direct supervision of Prof. Dr. Nuno P. Mira. Prof.^a Dra. Margarida Barata was the internal designated supervisor in the scope of the Master in Applied Microbiology of the Faculty of Sciences of the University of Lisbon.

Resumo

Nos últimos anos tem-se verificado um aumento significativo na incidência de infecções causadas por espécies do género *Candida*, entre outras razões, devido ao aumento significativo da população imunocomprometida^{1 2 3}. *C. albicans* é a principal espécie causadora de infecções fúngicas, que variam desde infecções superficiais nas mucosas até infecções sistêmicas, potencialmente letais. No entanto, nos últimos tempos tem-se verificado um aumento significativo nas infecções originadas por outras espécies do género *Candida*, geralmente conhecidas por NCAC (*Non-Candida albicans Candida species*)¹. Entre estas, *C. glabrata* tem emergido de forma particular sendo a segunda principal espécie causadora de infecções fúngicas invasivas^{8 9}, com uma taxa de letalidade a rondar os 40 %^{10 11}. A emergência de estirpes NCAC (e, particularmente, de *C. glabrata*) resistentes a azóis, os principais antifúngicos usados na prática clínica¹, tem contribuído de forma significativa para a mudança da etiologia observada nas infecções causadas por *Candida*. Os azóis têm como alvo a enzima citocromo P450_{14DM} envolvida na biossíntese de ergosterol^{22 23}. Em *C. glabrata* esta enzima é codificada pelo gene *ERG11* e a inibição desse gene pelos azóis sabe-se levar à diminuição da síntese do ergosterol o que resulta na concomitante acumulação de esteróis metilados na posição 14 α , altamente tóxicos para célula por levarem a alterações significativas na integridade da membrana plasmática^{22 23 25}. Um dos principais mecanismos de resistência aos azóis observado em estirpes clínicas de *C. glabrata* é a sobre-expressão de genes que codificam transportadores de múltiplas drogas pertencentes à Superfamília ABC (*ATP-binding cassette*) como sejam Cdr1 ou Cdr2²⁹. Um dos mecanismos moleculares subjacentes à sobre-expressão dessas bombas de efluxo em isolados clínicos resistentes está relacionada com aparecimento de mutações ganho de função no gene que codifica o factor de transcrição Pdr1⁶⁸. Vários estudos têm reportado diferentes mutações de ganho de função no gene *CgPDR1*^{47 68 70 73 80}, mutações estas que conduzem a uma ativação constante do regulador mesmo na ausência de qualquer droga. Estas mutações localizam-se em vários domínios da proteína incluindo o domínio de regulação (e.g. R376W e L328F) ou o domínio de ativação (e.g. D1082Q e E1083Q). A identificação destas mutações de ganho de função reveste-se de especial importância para tornar mais rápida a identificação de pacientes que possam estar colonizados com estirpes que serão intrinsecamente resistentes a azóis e que, portanto, vão necessitar de ser tratados com outro tipo de antifúngicos aos quais o regulador CgPdr1 não responde. Neste trabalho foram comparadas as sequências codificantes do gene *CgPDR1* de um conjunto de isolados clínicos de *C. glabrata* resistentes a fluconazol e voriconazol, com a sequência da estirpe de referência CBS138 que se sabe ser sensível a estes mesmos azóis. Na sequência dessa análise foram identificadas duas mutações, I392M e R35K, como possíveis candidatas a corresponderem a novas mutações de ganho de função de *CgPDR1*. Tal hipótese é suportada pelo fenótipo de resistência dos isolados clínicos e também pelo facto de se observar uma sobre-expressão dos genes *CgCDR1* e *CgPUP1* nesses mesmos isolados, por comparação com os níveis de expressão observados na estirpe CBS138. A substituição de aminoácido I392M está localizada no domínio regulatório inibitório (localizado entre os resíduos 322-465), pelo que é possível que a alteração da isoleucina para a metionina resulte, de uma alguma forma, numa redução da inibição deste domínio permitindo assim aumentar a atividade de CgPdr1. Este domínio regulatório verificou-se também conter o domínio de ligação a xenobióticos, uma região responsável pela ativação de CgPdr1 por ligação a drogas, incluindo azóis⁷⁷. Assim, outra hipótese para uma eventual híper-ativação de *CgPDR1* no mutante I392M pode resultar por uma alteração nesse domínio de ligação a drogas da proteína, fazendo um *bypass* à necessidade de haver ligação da droga à proteína para que ocorra ativação da mesma. A variante R35K está localizada no domínio de ligação ao DNA do *CgPDR1* (localizado entre os resíduos 26 e 59) e está responsável pela ligação do regulador ao motivo de DNA PDRE (*Pleiotropic drug resistance element*) encontrada na região promotora dos genes alvos⁷⁵. Até ao momento não foram descritas variantes de CgPdr1 híper-ativas com alterações no DBD de *CgPDR1*, pelo que serão necessários mais estudos para avaliar de que forma a mutação R35K contribui para uma híper-ativação de CgPdr1.

A constante emergência de estirpes resistentes a azóis torna essencial o desenvolvimento de novas moléculas com potencial antifúngico mas que tenham alvos de acção diferentes dos azóis, para ser assim possível sensibilizar estirpes resistentes. Nesse sentido, neste trabalho foi aprofundado o estudo de um conjunto de complexos organometálicos derivados de Ag e de cânfora, recentemente demonstrados como tendo potencial antimicrobiano ⁸⁷, como agentes anti-*Candida* e, em particular, como agentes capazes de sensibilizar isolados de *C. glabrata* resistentes a azóis. Os compostos foram obtidos usando uma combinação de nitrato de prata e derivados de cânfora, que são dois tipos de compostos com propriedades farmacêuticas reconhecidas ^{89 90}. Os 3 compostos Ag(I)-camphorimine usados neste estudo apresentaram uma elevada atividade contra a estirpe de referência *C. glabrata* CBS138 (MIC na ordem de 15,63 mg/L para os compostos B e C, e 31,25 mg/L para o composto A), sendo esta atividade particularmente notória em condições de pH neutro. Os valores de MIC obtidos para os isolados clínicos resistentes a fluconazol e voriconazol foram numa gama semelhante aos dos obtidos para a estirpe de referência (na gama entre os 15,63 mg/L e os 62,5 mg/L) indicando assim uma elevada capacidade dos compostos Ag(I)-camphorimine em sensibilizar as estirpes resistentes. Foi também observado que a presença dos compostos Ag(I)-camphorimine aumenta o efeito inibitório do fluconazol, incluindo nas estirpes resistentes, indicando assim um efeito sinérgico significativo. Estes dois resultados e também o facto de *CgPDR1* e o seu gene alvo *CgCDR1* se terem verificado ser dispensáveis para a tolerância de *C. glabrata* contra os compostos Ag(I)-camphorimine, indica que o mecanismo de acção destes compostos e dos azóis são diferentes. Por fim, foi observado que o efeito sinérgico observado não resulta de um aumento da concentração intracelular de fluconazol nas células potenciado pela presença dos compostos Ag(I)-camphorimine.

Até ao momento, o efeito inibitório de Ag(I) ou de químicos derivados de Ag(I) tem sido pouco estudado em *Candida glabrata* e a maior parte desses estudos tem abordado somente o uso de nanopartículas. Os estudos que mostram a atividade desses compostos indicam que existe uma inibição significativa das células sendo os principais motivos, a inibição de formação de hifas, alteração da superfície celular levando a formação de poros na célula e também a alteração da parede celular dessas estirpes ^{87 104 105}. Por este motivo no futuro, a fim de promover a implementação dos compostos Ag(I)-camphorimine aqui estudados, como um possível tratamento da candidíase, estudos adicionais serão necessários de modo a elucidar quais os mecanismos de acção desses compostos em células de *C. glabrata*. Também é requerido obter informação quanto toxicidade desses químicos contra células mamíferas, tanto a nível local e sistémica.

Concluindo, considerando que o atraso no diagnóstico de estirpes resistentes aos antifúngicos e posterior ajuste dos tratamentos utilizados é um dos fatores com maior impacto na determinação da taxa de mortalidade de pacientes infetados com candidíase, o conhecimento obtido neste trabalho constitui uma contribuição significativa para melhorar o sucesso da atualidade estratégias utilizadas no tratamento da candidíase.

Palavras-Chaves: *CgPdr1*, Resistência aos azóis, *Candida Glabrata*, Complexos Ag(I)-Camphorimine, variantes ganho de função de *CgPdr1*

Abstract

Candida glabrata is emerging as a human pathogen, being the second major cause of invasive fungal infections. Part of the success of *C. glabrata* as a pathogen rely on its rapid acquisition of resistance to azoles, the front line therapy used in prophylactic and active treatment of candidiasis. Acquisition of azole resistance in *C. glabrata* results, among other mechanisms, from alterations in the coding sequence of the transcriptional regulator CgPdr1 that result in gain-of-function (GOF) variants of this protein that are constitutively active, even in the absence of azoles. In the present work the sequence of *CgPDR1* alleles encoded by eight *C. glabrata* isolates found to be resistant to fluconazole and voriconazole was determined and compared with the sequence of the reference strain CBS138, susceptible to azoles. Two mutations, I392M and R35K, were identified and hypothesized to represent new gain-of-function *CgPDR1* variants. *CgCDR1* and *CgPUP1*, two known CgPdr1-targets, were found to be over-expressed in isolates FFUL412, FFUL443 and FFUL866 during growth in drug-free medium, reinforcing the idea that the identified mutations lead to constitutive activation of *CgPDR1*.

The efficacy of a set of Ag(I)-camphorimine complexes against *C. glabrata*, including against azole resistant clinical isolates (including those harboring *CgPDR1* GOF variants), was also examined in this work. The results obtained showed a potent effect of Ag(I)-camphorimine complexes in inhibiting growth of *C. glabrata*, more marked at a near neutral pH. Remarkable, the level of inhibition of the azole resistant isolates was similar to the one registered for azole susceptible strains suggesting that the mechanism of action of azoles and of Ag(I)-camphorimine differs. A synergistic effect between Ag(I)-camphorimine complexes and fluconazole in inhibiting growth of *C. glabrata*, including of the azole-resistant isolates was also demonstrated, a strategy that could be used to improve the efficacy of azole-based therapies in the treatment of candidiasis.

Keywords: CgPdr1, *CgPDR1* GOF variants, azole resistance, *Candida glabrata*, Ag(I)-camphorimine complexes

Table of contents

Acknowledgements	I
Resumo	III
Abstract	V
Table of contents	VI
List of figures	VIII
List of tables	XIII
Abbreviations	XIV
1. Introduction	1
1.1. Overview	1
1.2. A general overview on the molecular mechanisms of azole functioning in <i>Candida</i> cells and underlying resistance mechanisms	2
1.2.1. The CgPdr1-dependent regulatory network and its role in azole-resistance in <i>C. glabrata</i>	5
1.3. Introduction to the theme of thesis	8
2. Materials and Methods	10
2.1. Strains and growth media	10
2.2. Preparation of antifungal drugs and of camphorimine-derived chemicals	10
2.3. Genomic DNA extraction	11
2.4. PCR reaction and DNA sequencing by Sanger method of <i>CgPDR1</i> gene	11
2.5. Cloning of <i>CgPDR1</i> gene	12
2.6. Assessment of gene expression based on real time RT-PCR	14
2.7. Quantification of MIC ₅₀ using the microdilution method	15
2.8. Growth curves in the presence of camphorimine complexes	16
2.9. Synergy assays between the camphorimine compound and fluconazole	16
2.10. [³ H]- Fluconazole accumulation assay	16
3. Results	17
3.1. Unveiling new gain-of-function mutations in <i>CgPDR1</i>	17
3.1.1. Cloning of <i>CgPDR1</i> gene of the reference strain and of the resistant clinical isolates FFUL412, FFUL443 and FFUL866	19
3.2. Study on the antimicrobial effect against <i>C. glabrata</i> of Ag(I) camphorimine complexes	21
3.2.1. Assessment of the activity of compound A, B and C against <i>C. glabrata</i> azole-resistant clinical isolates	23
3.2.2. Synergistic effect of Ag(I)-camphorimine complexes with fluconazole	25

3.2.3. The synergistic effect between Ag(I)-camphorimine complexes and fluconazole does not result from increased accumulation of the azole inside <i>C. glabrata</i> cells.....	29
4. Discussion and Future Perspectives	30
References	33
Annex A	40
Annex B.....	41
Annex C.....	42
Annex D	43
Annex E.....	44
Annex F	45
Annex G	46
Annex H	47
Annex I.....	48
Annex J.....	49
Annex K	50
Annex L.....	51
Annex M.....	53
Annex N	54
Annex O	55

List of figures

Figure 1.1: Targets of antifungal drugs not present in mammalian cells. A. Azoles inhibits fungal cytochrome P450_{14DM} (14 α -demethylase) which is encoded by *ERG11* and catalyzes a late step in the biosynthesis of ergosterol blocking the production of ergosterol and causing the accumulation of a toxic sterol intermediate¹⁸. B. Polyenes intercalates into ergosterol-containing fungal membranes, thereby forming membrane-spanning channels that lead to the leakage of cellular components and cell death. D. Echinocandins Interferes with fungal cell-wall biosynthesis by inhibiting β -(1,3)-d-glucan synthase¹⁹. The image was altered from Kathiravan et al. 2012²⁰.

Figure 1.2: Chemical structural of fluconazole, voriconazole and miconazole. Image was modified from Mast et al. 2013²⁶ and Snell et al. 2012²⁷.

Figure 1.3: Ergosterol biosynthesis pathway. The enzyme Erg11 targeted by azoles is highlighted in the red box. *ERG1*, *ERG4* and *ERG6* genes sites are shown. Deletions of these genes increased susceptibility to azoles in *C. glabrata* showing that function of these enzymes in the ergosterol biosynthetic pathway is required for maximal tolerance of this yeast species to azoles^{32 34}. Image was modified from Akins, Robert A., 2005³³.

Figure 1.4: Domain arrangement of the ABC transporters and a schematic representation of the predicted topology of the ABC transporter Cdr1p. Image was modified from Cannon D., Richard et al., 2009⁴⁸.

Figure 1.5: Domain arrangement of MFS transporters and a schematic representation of the predicted topology of the MFS transporter Mdr1p. Image was modified from Cannon D., Richard et al., 2009⁴⁸.

Figure 1.6: Example of a functional model of a new compound (iKIX1) that show to sensitize azole-resistant strains by hampering the Pdr1-Med interaction. The iKIX1 molecule block the azole-induce recruitment of Gal11/Med15-Mediator to Pdr1 target genes upon azole treatment. This blocking prevent the upregulation of Pdr1 target genes, including those which encode drug efflux pumps which result to a restoration of the sensitivity to the azole antifungal. Image was retrieved from Nishikawa, J et al., 2016⁷⁸.

Figure 1.7: Described *C. glabrata* PDR1 gain-of-function mutations. The domains shown were based on the homology between *S. cerevisiae* Pdr1p and CgPdr1p retrieved from Tsai, H., et al., 2010⁷⁰. DBD – DNA-binding domain; RD – Regulatory Domain; FSTFD – Fungus-specific Transcription factor Domain; AD – Activation Domain. Mutations described according from the information available in Tsai H., et al.,2006,⁶⁸ Torelli, B., et al.,2008,⁴⁷ Ferrari, S., et al., 2009,⁸⁰ Tsai, H., et al., 2010,⁷⁰ Berila, N. and Subik, J., 2010,⁸¹ Caudle K., et al.,2011,⁷³ Vale-Silva, L., et al.,2015,⁸² Garnaud, C., et al,2015,⁸³ Katiyar, S., et al.,2016,⁸⁴ Healey, K., et al.,2016⁵⁵.

Figure 1.8: Measured MIC values for the antifungals fluconazole, voriconazole of the cohort clinical isolates used in the previous work (Salazar, S., 2015)⁸⁶ and the reference strains CBS138 (White). Resistant isolates are market in black, while isolates classified as being susceptible or intermediately resistant are marked in grey.

Figure 2.1: Schematic representation of the procedure used to prepare the 96-multiwell plates used to determine MIC of 3 different compounds for the different *C. glabrata* isolates. B: blank; GC: control. Image altered from EUCAST discussion document E.Dis 7.1¹⁰². In the case of the com-

pounds the same methodology was applied with the difference that the initial stock concentration was of 1000 mg/L.

Figure 3.1: Example of the result obtained after amplification of *CgPDR1* gene using primer FW1 and REV1. Lane 1 represents the ladder (1 kb plus DNA Ladder) - The black arrows show the 3 kb fragment and the 4 kb fragment.

Figure 3.2: Comparison of the transcript levels of *CgCDR1* and *CgPUP1* genes in CBS138, FFUL29, FFUL412, FFUL443, FFUL830, FFUL866 and FFU878. Cells of the different isolates were cultivated in RPMI growth medium until mid-exponential phase after which the expression of *CgCDR1* and *CgPUP1* genes was compared by qRT-PCR. The values represented for the isolates strains are relative to the value obtained for the CBS138 strain, which was considered to be equal to 1. Gene expression was calculated using *RDN25* as an internal control. For the statistical analysis the results obtained for the resistant isolates strains were compared with those gathered for CBS138. * p-value below 0.05, ** p-value below 0,001, *** p-value below 0.0001.

Figure 3.3: Genetic engineering strategy scheme used to clone *CgPDR1* gene encoded by the CBS138 and FFUL887. 1 – Amplification of *CgPDR1* by PCR; 2 – Digestion of plasmid with Sall; 3 – Homologous recombination in *S. cerevisiae* (representation of linearized plasmid after insertion of the *CgPdr1*: black rectangle refers to *CgPdr1*)

Figure 3.4: PCR products fragments expected after amplification of *CgPDR1* and separated by an agarose gel electrophoresis. The amplification of *CgPDR1* gene was done using the genomic DNA of the CBS138 (lane 3), FFUL412 (lane 4), FFUL443 (lane 5), FFUL866 (lane 8) and FFUL887 (lane10). Lane 1 represents the ladder (Nzy Ladder III) – The black arrows show the 3 kb fragment and the 4 kb fragment.

Figure 3.5: PCR colony of potential candidates of CBS138 and FFUL887. Lane 1 and 13 represents the ladder (Nzy Ladder III). Lanes 2 to 6 represents CBS138 candidates and lanes 8 to 12 FFUL887 candidates. The expect fragment should be approximately 4500 bp. Black arrows show the 4 kb fragment and the 5 kb fragment.

Figure 3.6: Microdilution assay performed in several condition of the growth medium RPMI supplemented with compound A against the reference strain CBS138. a) Growth medium RPMI (pH 7) prepared as recommended by EUCAST (for more information see materials and methods), b) RPMI (pH 5.38) prepared as recommended by EUCAST, c) RPMI (pH 7) with TrisBase instead of MOPS, d) RPMI (pH 5,38) with TrisBase instead of MOPS, e) RPMI (pH 7) without MOPS buffer, f) RPMI (pH 5.38) without MOPS buffer. The MIC₅₀ was determined comparing the values of the different isolates in the supplemented medium with chemical and the one registered in control conditions after 24 h of cultivation at 37 °C in RPMI growth medium (pH 7), as described in materials and methods. The MIC₅₀ value in indicated by a black arrows and the 50 % reduction of the growth registered in the absence of the chemicals is indicated by the red line.

Figure 3.7: Growth curves of KUE100 (●), Δ pdr1 (■) and Δ cdr1 (▲) in growth medium RPMI (pH7), or with the same medium supplemented with compound A (7.81 mg/L and 31.25mg/L), B, and C (7.81 mg/L and 15.63 mg/L). The growth was followed during approximately 40 h and the absorbance of the growth increasing was measured in OD595 nm.

Figure 3.8: Heatmaps obtained in the synergism assay used to assess the potential of the synergistic effect of fluconazole and camphorimine compound A, B and C. Darker green means a larger growth and red a greater inhibition.

Figure 3.9: Graphic representation of the ODs obtained in the assays to assess the effects of the potential synergistic combination of compound A and fluconazole against *C. glabrata* strains. In the graphic is represented a control column (w/o FLC or A) with the growth medium without stress, or the medium supplemented only with compound A (only A), or with the concentration of the breakpoint value (32 mg/L for CBS138 (only 32) and 64 mg/L for the resistant isolates (only 64)), and one concentration below (16 mg/L for CBS138 (only 16) and 32 mg/L for the resistant isolates (only 32)) and at last a combination of the compound plus each one of the concentrations of fluconazole. Three non-inhibitory concentrations of the compound was used, 1.95 mg/L, 3.91 mg/L and 7.81 mg/L.

Figure 3.10: Graphic representation of the ODs obtained in the assays to assess the effects of the potential synergistic combination of compound B and fluconazole against *C. glabrata* strains. In the graphic is represented a control column (w/o FLC or B) with the growth medium without stress, or the medium supplemented only with compound B (only B), or with the concentration of the breakpoint value (32 mg/L for CBS138 (only 32) and 64 mg/L for the resistant isolate (only 64)), and one concentration below (16 mg/L for CBS138 (only 16) and 32 mg/L for the resistant isolate (only 32)) and at last a combination of the compound plus each one of the concentrations of fluconazole. Three non-inhibitory concentrations of the compound was used, 7.81 mg/L, 3.91 mg/L and 1.95 mg/L.

Figure 3.11: Graphic representation of the ODs obtained in the assays to assess the effects of the potential synergistic combination of compound C and fluconazole against *C. glabrata* strains. In the graphic is represented a control column (control) with the growth medium without stress, or the medium supplemented only with compound C (only C), or with the concentration of the breakpoint value (32 mg/L for CBS138 (only 32) and 64 mg/L for the resistant isolate (only 64)), and one concentration below (16 mg/L for CBS138 (only 16) and 32 mg/L for the resistant isolate (only 32)) and at last a combination of the compound plus each one of the concentrations of fluconazole. Three non-inhibitory concentrations of the compound was used, 7.81 mg/L, 3.91 mg/L and 1.95 mg/L.

Figure 3.12: Intracellular concentration of fluconazole inside the *Candida glabrata* cells potentiated by the Ag(I)-based drugs. *Candida glabrata* cells don't accumulate more fluconazole intracellular with the RPMI supplemented with camphorimine compound than cells without the supplementation. The results obtained were representative of, at least, three independent experiments.

Figure 4.1: Described GOF mutations and two aminoacid substitutions candidates to be new GOF variants of CgPdr1. A - Location of the described *C. glabrata* PDR1 GOF mutations B – Location of the R35K and I392M replacement candidates to be new GOF variants of CgPdr1. The domains shown were based on the homology between *S. cerevisiae* Pdr1p and CgPdr1p retrieved from Tsai, H., et al., 2010⁷⁰. DBD – DNA-binding domain; RD – Regulatory Domain; FSTFD – Fungus-specific Transcription factor Domain; AD – Activation Domain.

Annex A: Alignment of the sequence of *CgPDR1* from isolate FFUL29 obtained with the sequence of the CBS138 reference strain. The sequencing reaction was performed by STABVIDA as a paid service and Clustal Omega was used for sequence alignment. Aminoacids substitutions are represented by a black rectangle.

Annex B: Alignment of the sequence of *CgPDR1* from isolate FFUL412 obtained with the sequence of the CBS138 reference strain. The sequencing reaction was performed by STABVIDA as a paid

service and Clustal Omega was used for sequence alignment. Aminoacids substitutions are represented by a black rectangle.

Annex C: Alignment of the sequence of *CgPDR1* from isolate FFUL443 obtained with the sequence of the CBS138 reference strain. The sequencing reaction was performed by STABVIDA as a paid service and Clustal Omega was used for sequence alignment. Aminoacids substitutions are represented by a black rectangle.

Annex D: Alignment of the sequence of *CgPDR1* from isolate FFUL674 obtained with the sequence of the CBS138 reference strain. The sequencing reaction was performed by STABVIDA as a paid service and Clustal Omega was used for sequence alignment. Aminoacids substitutions are represented by a black rectangle.

Annex E: Alignment of the sequence of *CgPDR1* from isolate FFUL677 obtained with the sequence of the CBS138 reference strain. The sequencing reaction was performed by STABVIDA as a paid service and Clustal Omega was used for sequence alignment. Aminoacids substitutions are represented by a black rectangle.

Annex F: Alignment of the sequence of *CgPDR1* from isolate FFUL830 obtained with the sequence of the CBS138 reference strain. The sequencing reaction was performed by STABVIDA as a paid service and Clustal Omega was used for sequence alignment. Aminoacids substitutions are represented by a black rectangle.

Annex G: Alignment of the sequence of *CgPDR1* from isolate FFUL866 obtained with the sequence of the CBS138 reference strain. The sequencing reaction was performed by STABVIDA as a paid service and Clustal Omega was used for sequence alignment. Aminoacids substitutions are represented by a black rectangle.

Annex H: Alignment of the sequence of *CgPDR1* from isolate FFUL878 obtained with the sequence of the CBS138 reference strain. The sequencing reaction was performed by STABVIDA as a paid service and Clustal Omega was used for sequence alignment. Aminoacids substitutions are represented by a black rectangle.

Annex I: Antifungal activity of compound A against the resistant clinical isolates, FFUL29, FFUL674, FFUL830, FFUL866, FFUL878, FFLU887 and the reference strain CBS138. The MIC₅₀ was determined comparing the values of the different isolates in the supplemented medium with chemical and the one registered in control conditions after 24 h of cultivation at 37 °C in RPMI growth medium (pH 7), as described in materials and methods. The MIC₅₀ value is indicated by a black arrow and the 50% reduction of the growth registered in the absence of the chemicals is indicated by the red line.

Annex J: Antifungal activity of compound B against the resistant clinical isolates, FFUL29, FFUL674, FFUL830, FFUL866, FFUL878, FFLU887 and the reference strain CBS138. The MIC₅₀ was determined comparing the values of the different isolates in the supplemented medium with chemical and the one registered in control conditions after 24 h of cultivation at 37 °C in RPMI growth medium (pH 7), as described in materials and methods. The MIC₅₀ value is indicated by a black arrow and the 50% reduction of the growth registered in the absence of the chemicals is indicated by the red line.

Annex K: Antifungal activity of compound C against the resistant clinical isolates, FFUL29, FFUL674, FFUL830, FFUL866, FFUL878, FFLU887 and the reference strain CBS138. The MIC₅₀ was determined comparing the values of the different isolates in the supplemented medium with chemical and the one registered in control conditions after 24 h of cultivation at 37 °C in RPMI growth medium (pH 7), as described in materials and methods. The MIC₅₀ value is indicated by a black arrow and the 50% reduction of the growth registered in the absence of the chemicals is indicated by the red line.

Annex L: Heatmaps obtained in the synergism assay used to assess the potential of the synergistic effect of fluconazole and camphorimine compound A. Darker green means a larger growth and red a greater inhibition.

Annex M: Graphic representation of the ODs obtained in the assays to assess the effects of the potential synergistic combination of compound A and fluconazole against *C. glabrata* clinical isolates. In the graphic is represented a control column (w/o FLC or A) with the growth medium without stress, or the medium supplemented only with compound A (only A), or with the concentration of the breakpoint value (32 mg/L for CBS138 (only 32) and 64 mg/L for the resistant isolate (only 64)), and one concentration below (16 mg/L for CBS138 (only 16) and 32 mg/L for the resistant isolate (only 32)) and at last a combination of the compound plus each one of the concentrations of fluconazole. Three non-inhibitory concentrations of the compound was used, 1.95 mg/L, 3.91 mg/L and 7.81 mg/L.

Annex N: Graphic representation of the ODs obtained in the assays to assess the effects of the potential synergistic combination of compound B and fluconazole against *C. glabrata* clinical isolates. In the graphic is represented a control column (w/o FLC or B) with the growth medium without stress, or the medium supplemented only with compound B (only B), or with the concentration of the breakpoint value (32 mg/L for CBS138 (only 32) and 64 mg/L for the resistant isolate (only 64)), and one concentration below (16 mg/L for CBS138 (only 16) and 32 mg/L for the resistant isolate (only 32)) and at last a combination of the compound plus each one of the concentrations of fluconazole. Three non-inhibitory concentrations of the compound was used, 1.95 mg/L, 3.91 mg/L and 7.81 mg/L.

Annex O: Graphic representation of the ODs obtained in the assays to assess the effects of the potential synergistic combination of compound C and fluconazole against *C. glabrata* clinical isolates. In the graphic is represented a control column (w/o FLC or C) with the growth medium without stress, or the medium supplemented only with compound C (only C), or with the concentration of the breakpoint value (32 mg/L for CBS138 (only 32) and 64 mg/L for the resistant isolate (only 64)), and one concentration below (16 mg/L for CBS138 (only 16) and 32 mg/L for the resistant isolate (only 32)) and at last a combination of the compound plus each one of the concentrations of fluconazole. Three non-inhibitory concentrations of the compound was used, 1.95 mg/L, 3.91 mg/L and 7.81 mg/L.

List of tables

Table 1.1: Biological class of genes regulated by CgPdr1. Information was retrieved from Claude, K., et al., 2011 ⁷³, Tsai, H., et al., 2010⁷⁰, Vermitsky, J., et al., 2006 ⁶⁹ and Ferrari, S., et al., 2011 ⁷⁴.

Table 2.1: Description of the group of strains used in this work

Table 2.2: Primers sequences used to amplify the selected regions of *CgPDR1* gene of the *C. glabrata* resistant isolates.

Table 2.3: Reaction mixture used for the amplification of the selected regions of *CgPDR1* gene.

Table 2.4: Conditions of the PCR cycles for amplification of the selected regions of *CgPDR1* gene.

Table 2.5: Primers used for the amplification of the *CgPDR1* gene.

Table 2.6: Reaction mixture used for the amplification of the *CgPDR1* gene.

Table 2.7: Conditions of the PCR cycles for amplification of the *CgPDR1* gene.

Table 2.8: Primer sequences used to measure expression of *CgPDR1* gene using real time RT-PCR.

Table 3.1: Alterations in the amino acid sequence of CgPdr1 transcription factor encoded by FFUL29, FFUL412, FFUL443, FFUL674, FFUL677, FFUL830, FFUL866, FFUL878, FFUL887, FFUL4012, when compared to its counter-partners encoded by the CBS138 strain. In green the susceptible mutations and in blue and lighter red the non-described mutations. * Represent the candidates to be new GOF variants of CgPdr1. In red is shown the GOF mutations found in other studies. The described mutations was retrieved from Ferrari, S., et al., 2009 ⁸⁰ Caudle, K., et al., 2011 ⁷³ Katiyar, S., et al., 2016 ⁸⁴ and Salazar, S., et al., 2015 ⁸⁶.

Table 3.2: MIC₅₀ values (mg/L) for Ag(I) camphor complexes A, B and C against the azoles resistant isolates FFUL29, FFUL412, FFUL674, FFUL830, FFUL866, FFUL878 FFUL887, FFUL4012 and reference strain CBS138 based on the EUCAST microdilution method.

Abbreviations

ABC	ATP-binding Cassette
AD	Activation Domain
<i>C. glabrata</i>	<i>Candida glabrata</i>
<i>C. albicans</i>	<i>Candida albicans</i>
cDNA	Complementary Deoxyribonucleic Acid
CDR	Candida drug resistance
CFU	Colony Forming Units
ddH₂O	Double Distilled Water
DMSO	Dimethyl Sulfoxide
DNA	Deoxyribonucleic Acid
DBD	DNA-binding Domain
FSTFD	Fungus-specific Transcription factor Domain
GOF	Gain of function
MDR	Multi-drug Resistance
MFS	Major Facilitator (MF) Superfamily
MIC	Minimum Inhibitory Concentration
NCAC	Non-Candida albicans Candida Species
OD	Optical Density
ORF	Open Reading Frame
PDH	Pleiomorphic Drug Resistance Homolog
PDR	Pleiotropic Drug Resistance
PDRE	Pleiotropic Drug Response Elements
PUP	PDR1 Upregulated and Encoding a Mitochondrial Protein
RD	Regulatory Domain
RNA	Ribonucleic Acid
RPMI	Roswell Park Memorial Institute Medium
RT-PCR	Reverse Transcription Polymerase Chain Reaction
<i>S. cerevisiae</i>	<i>Saccharomyces cerevisiae</i>
spp.	<i>Species</i>
TRIS	Tris (Hydroxymethyl) Aminomethane
YPD	Yeast Peptone Dextrose

1. Introduction

1.1. Overview

The incidence of infections caused by Fungi has risen in the past decades emerging now as one of the main concerns in health. This increase has several origins out of which the increase in the size of the population of risk (*e.g.* immunocompromised patients undergoing aggressive therapeutic treatments that prolong patient's stays in hospitals, sometimes in a fragile condition, or the elderly) stands out ^{1 2 3}.

Fungal infections range from superficial rashes affecting the mucosas to life-threatening systemic infections in which the cells cross the bloodstream and may colonize any major internal organ ¹. Almost 10 % of the bloodstream infections reported today are attributed to fungi, these having associated high rates of mortality and contributing to increase hospital stays, which together with the high costs associated with antifungal therapies, leads to a massive economic burden for public healthcare systems ^{4 5 6}. Invasive infections caused by species of the *Candida* genus, generally known as candidemia or invasive candidiasis, are responsible for more fatalities than any other systemic mycosis having an associated lethality rate of around 40 % ⁴. Around 2/3 of the invasive candidemias reported are thought to result from healthcare associated-infections, the main risk factors for this being the use of central venous catheters, long term parenteral nutrition, surgery and transfer of the yeasts via nursing staff handling ^{1 2 3 7}. Epidemiological surveys show that *C. albicans* is the more relevant causative agent of invasive and superficial fungal infections; however, in the recent years the number of infections caused by non *albicans* *Candida* species (NCAC) has been raising significantly ¹. In specific, *C. glabrata* has been emerging as a major pathogen being the second major cause of invasive fungal infections ^{8 9}. The mortality of infections caused by *C. glabrata* is around 40 %, these rates being comparable with those reported for *C. albicans* ^{10 11}. However, in cases of delayed diagnosis the outcomes of patients with candidemia caused by *C. glabrata* are more severe than those observed for patients colonized with *C. albicans* ¹⁰. One of the reasons underlying this emergence of infections caused by NCAC and, in particular, by *C. glabrata*, relates with the high resistance of this yeast species to fluconazole, the frontline drug used for both active and prophylactic treatments of candidiasis. In this context, the massive use of fluconazole in the clinical practice led to the selection of the more tolerant species, *C. glabrata* among them ¹. More recently, the widespread use of agricultural fungicides structurally similar to azoles used in the clinical practice was also demonstrated to be on the basis of the emergence of resistant strains, including those belonging to the *C. glabrata* species ¹². *C. glabrata* was also found to acquire resistance to antifungals at a higher rate than any other *Candida* spp. ^{13 14}. To overcome this problem of azole-resistance, drugs alternative to fluconazole have been developed including new azoles (*e.g.* voriconazole) and echinocandins ¹⁵. Nevertheless, the number of strains resistant to these drugs is increasing ¹⁶ thereby rendering clear that a thorough understanding of the mechanisms underlying the development of acquired resistance to azoles is urgent so that appropriate responses could be developed. Furthermore it is also recognized the need of developing new antifungal drugs targeting proteins other than those that are affected by azole drugs. The overall goal of this thesis is to contribute for both these two issues, either by deepening the study on the role played by the transcriptional regulator CgPdr1, a key player in mediating azole resistance in *C. glabrata*, and also to assess the efficacy of Ag-based chemicals as putative anti-*Candida* agents.

1.2. A general overview on the molecular mechanisms of azole functioning in *Candida* cells and underlying resistance mechanisms

Being eukaryotic cells, fungal cells share many proteins with those found in mammalian cells which poses a great challenge in the design of antifungal drugs. For that reason, most of the currently used antifungal drugs target the cell wall and/or the properties of the plasma membrane that are not present in mammalian cells, as shown in Figure 1.1¹⁷.

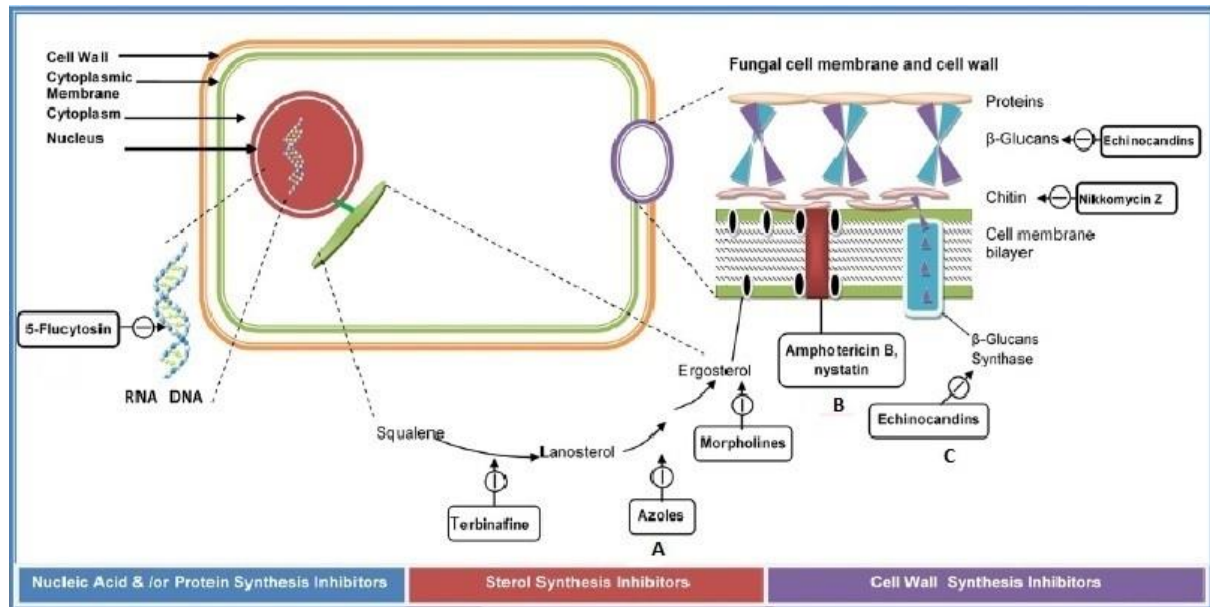


Figure 1.1: Targets of antifungal drugs not present in mammalian cells. A. Azoles inhibits fungal cytochrome P450_{14DM} (14 α -demethylase) which is encoded by *ERG11* and catalyzes a late step in the biosynthesis of ergosterol blocking the production of ergosterol and causing the accumulation of a toxic sterol intermediate¹⁸. B. Polyenes intercalates into ergosterol-containing fungal membranes, thereby forming membrane-spanning channels that lead to the leakage of cellular components and cell death. D. Echinocandins Interferes with fungal cell-wall biosynthesis by inhibiting β -(1,3)-d-glucan synthase¹⁹. The image was altered from Kathiravan et al. 2012²⁰.

Azoles arrived in late 1960s and until now they are still the most used antifungals in the clinic practice²¹. The target of azoles is ergosterol biosynthesis, in specific the cytochrome P450_{14DM} 14 α -demethylase^{22 23}. In *C. glabrata* this enzyme is encoded by the *ERG11* gene. Ergosterol is a major component of fungal cytoplasmic membrane being responsible for the maintenance of membrane fluidity, asymmetry and integrity²⁴. The inhibition of *ERG11* prompted by azoles decrease ergosterol synthesis and lead to a concomitant accumulation of 14 α -methylated sterols that are often highly toxic for the yeast cells by causing significant alterations in the integrity of the plasma membrane structure and perturbing its function as a selective barrier and a matrix for membrane proteins^{22 23 25} (Figure 1.3). There are two types of azoles: i) imidazoles (*e.g.* ketoconazole and miconazole), which contain an imidazole in the ring system, and that are mainly applied topically because of poor water solubility and limited oral bioavailability; and ii) triazoles (including, among others, fluconazole, itraconazole, and voriconazole), which have a triazole ring and that exhibit more amenable properties from the pharmacological point of view.

In Figure 1.2 it is shown the chemical structure of voriconazole and fluconazole, the two azoles more focused on this thesis, as well as of miconazole (an imidazole).



Figure 1.2: Chemical structural of fluconazole, voriconazole and miconazole. Image was modified from Mast et al. 2013²⁶ and Snell et al 2012²⁷.

In several species of *Candida*, alteration of the azole binding site and increased expression due to point-mutations in *ERG11* gene or in its promoter has been highlighted as a key resistance mechanism, however in *C. glabrata* this is not case^{28 29 30}. One of the reasons underlying the higher resilience of *C. glabrata* to azoles results from these cells not accumulating in the plasma membrane the toxic sterol 14 α -methyl 3,6-diol upon azole exposure, but rather accumulates 14- α -methyl sterols, which are non-toxic^{31 32}. Thus, there is no selective pressure for the selection of Erg1 1 variants.

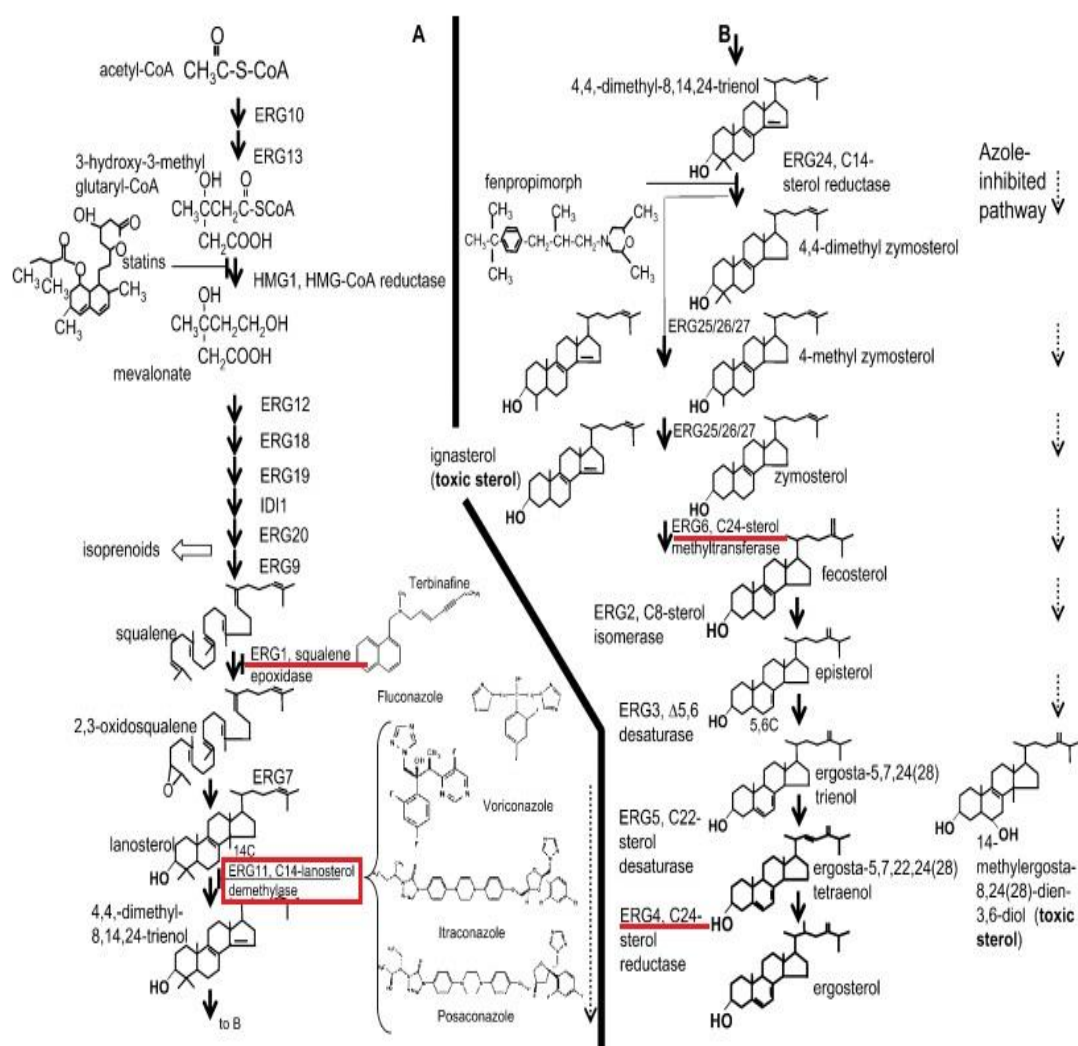


Figure 1.3: Ergosterol biosynthesis pathway. The enzyme Erg11 targeted by azoles is highlighted in the red box. *ERG1*, *ERG4* and *ERG6* genes sites are shown. Deletions of these genes increased susceptibility to azoles in *C. glabrata* showing

that function of these enzymes in the ergosterol biosynthetic pathway is required for maximal tolerance of this yeast species to azoles^{32,33}. Image was modified from Akins, Robert A., 2005³⁴.

The ability of *C. glabrata* to promote the uptake of sterols (cholesterol or ergosterol) from the growth medium is also believed to contribute for the increased resilience of this species to azole stress^{31,32,35}. It is thought that these sterols taken from the growth medium can complement the defect of ergosterol biosynthesis in *C. glabrata* that occurs upon azole stress³². To support this, it has been shown that *CgAUS1* and the mannoprotein *CgTIR3* are highly up-regulated when cellular sterol synthesis is blocked by fluconazole^{36,37,38}. In a different study it was also shown that *CgUPC2A* and *CgUPC2B* genes, encoding two transcriptional regulators, are required for full induction of *CgAUS1* in response to serum and for the growth restoration of fluconazole-inhibited *C. glabrata* cells in response to serum, suggesting a possible cross-regulation between the ergosterol biosynthesis and ergosterol transporters³⁹.

The activity of drug-efflux pumps has also been implicated in the development of the azole-resistance phenotype in *C. glabrata*, as well as in other *Candida* species^{40,41,42,43}. In specific, transporters belonging to the ATP-binding cassette (ABC) Superfamily Cdr1, Cdr2, Phd1 and Snq2 have been found to be over-expressed in azole-resistant *C. glabrata* isolates^{18,29,30,40,41,42,44,45,46,47} (Figure 1.4).

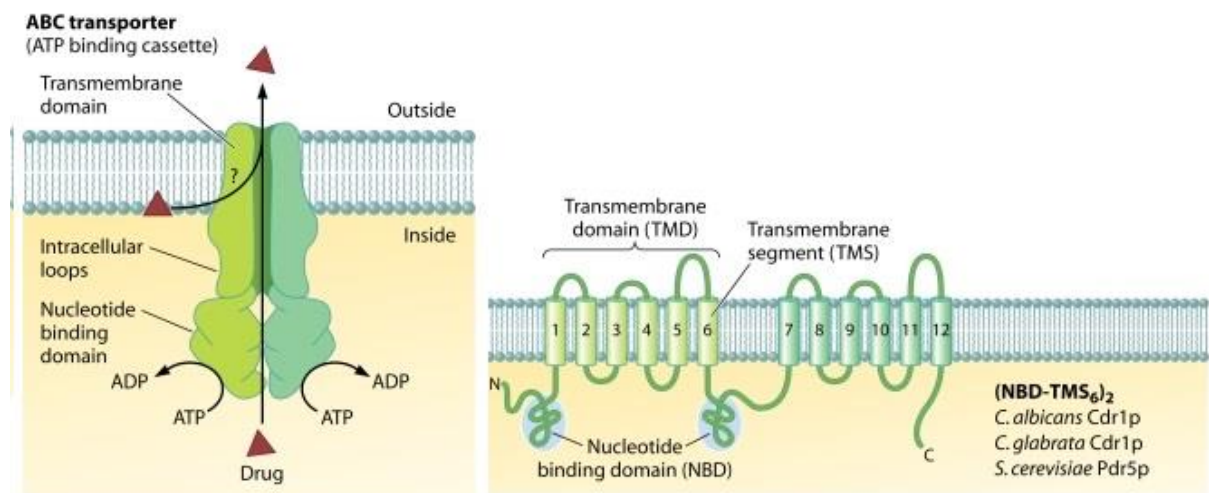


Figure 1.4: Domain arrangement of the ABC transporters and a schematic representation of the predicted topology of the ABC transporter Cdr1p. Image was modified from Cannon D., Richard et al., 2009⁴⁸.

Besides these ABC-MDR transporters, more recently transporters belonging to the Major Facilitator Superfamily have also been found to contribute for azole resistance in *C. glabrata* including, *CgAqr1*, *CgQdr2*, *CgTpo1_1*, *CgTpo1_2* and *CgTpo3*^{49,50,51,52,53} (Figure 1.5). Consistently, the up-regulation of some of these MFS-MDR transporters in azole-resistant clinical isolates has been described to occur⁵⁴.

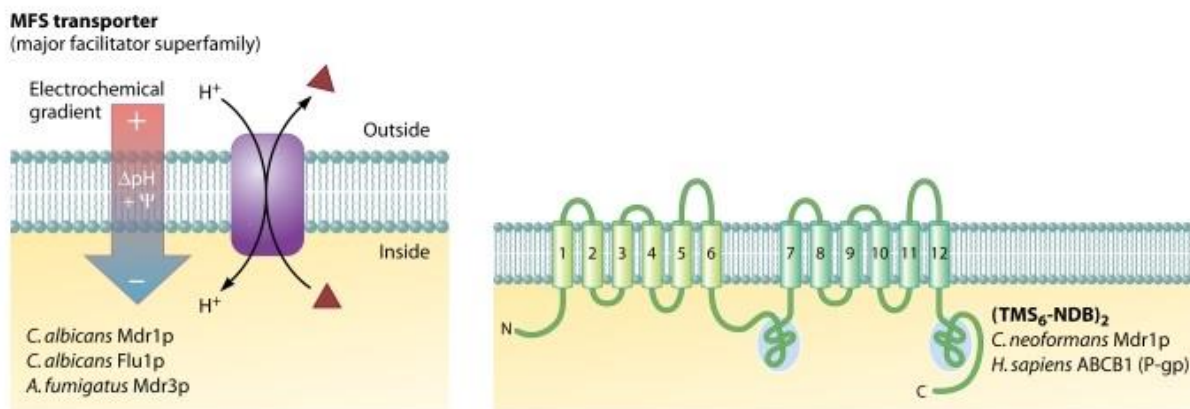


Figure 1.5: Domain arrangement of MFS transporters and a schematic representation of the predicted topology of the MFS transporter Mdr1p. Image was modified from Cannon D., Richard et al., 2009 ⁴⁸.

Recent studies have also shown that defects in DNA repair account for accelerated emergence of various genetic changes responsible for drug resistance. In specific, it has been shown that *C. glabrata* clinical isolates carrying loss-of-function mutations in the mismatch repair (MMR) gene MSH2, led to a hyper-mutator phenotype, resulting in an increase in the emergence of antifungal drug resistance ⁵⁵. Interestingly, the MSH2 partial loss of function genotypes found in the study appear to be geographically dependent, being the difference probably explained by different medical care habits and recommendations ^{56 57}.

1.2.1. The CgPdr1-dependent regulatory network and its role in azole-resistance in *C. glabrata*

The regulation of drug-resistance genes has been well studied in a multitude of organisms, however, in Fungi most of the knowledge has been gathered in *S. cerevisiae* ^{58 59}. Two orthologous transcription factors, ScPdr1 and ScPdr3, were found to mediate pleiotropic drug resistance (PDR) in *S. cerevisiae* by controlling the expression of a panoply of drug-efflux pumps belonging to the ABC (*e.g.* Pdr5p, Snq2p and Yor1p) or MFS Superfamily (*e.g.* Tpo1, Tpo2 and Tpo3) ^{60 61 62 63 64}. A complementary roles for this two transcription factors has been described, since the double mutant $\Delta\text{pdr1}\Delta\text{pdr3}$ increase multidrug sensitivity of *S. cerevisiae* ^{65 66}. Consistently, studies have shown that ScPdr1 and ScPdr3 can act as homo- and heterodimers and can positively or negatively regulate expression of target genes, indicating that additional factor modulate their activity ⁶⁷.

In *C. glabrata*, a homolog of *Saccharomyces cerevisiae* Pdr1/Pdr3 was found to be conserved, designated as CgPdr1. This regulator was demonstrated to play a key regulator in the regulation of the expression of the drug-efflux pumps *CgCDR1*, *CgCDR2* and *CgSNQ2*, among others ^{42 47 68 69}. Besides regulating the expression of drug-efflux pumps, CgPdr1 has also been found to regulate the expression a multitude of genes with other functions including transcription, stress response, adhesion, metabolism of lipids, sterols, and fatty acids ^{69 70 71 72}, as briefly shown in Table 1.1. The involvement of CgPdr1 in the regulations of these genes has been demonstrated in laboratory strains but also in azole-resistant clinical isolates ^{69 70 73 74}.

Table 1.1: Biological class of genes regulated by CgPdr1. Information was retrieved from Claude, K., et al., 2011 ⁷³, Tsai, H., et al., 2010 ⁷⁰, Vermitsky, J., et al., 2006 ⁶⁹ and Ferrari, S., et al., 2011 ⁷⁴.

Class of genes regulated by <i>PDR1</i>	
Group	<i>C. glabrata</i> gene
ABC transporter	<i>CDR1, PDH1, YOR1, SNQ2, YBT1</i>
MFS-transporter	<i>QDR2, TPO3</i>
Mitochondrial porin	CAGL0J09900g
Transcription	<i>PDR1, SUN4, RPN4, MEC3</i>
Response to stress	<i>YMI1, HSP12, RTA1, CAGL0H08844g, CAGL0I05874g, CAGL0M09713g</i>
Lipid, fatty acid and sterol metabolism	<i>ATF2, HFD1, RTA1, ERG4</i>
Biological function Unkown	<i>YJL163C, YIL077C, YNL134C</i>
Virulence	<i>PWP6, EPA1, CAGL0E06600g, EPA8, PUP1</i>
Uncharacterized	CAGL0G01122g, CAGL0M14091g

In *S. cerevisiae* Pdr1 and Pdr3 promote the up-regulation of their target genes by binding to the DNA motif, 5'-TCCGCGGA-3', generally known as PDRE (pleiotropic drug resistance element), present in the promoter region of target genes ⁷⁵. In *C. glabrata*, studies found functional PDRE sequences in the promoters of several genes including the ATP binding cassette (ABC)-transporters *CgCDR1*, *CgCDR2* and *CgSNQ2* ^{70 72 68 76}. Significant contributions for the understanding of the mechanism of activation of *ScPDR1* and *CgPDR1* have been given recently in the field ^{77 78}. In a study was shown that Pdr1p orthologues in *S. cerevisiae* and *C. glabrata* can directly bind to structurally diverse drugs and xenobiotics, resulting in stimulated expression of drug efflux pumps and induction of MDR. This means that drugs can directly trigger *PDR1* activation. It was also shown that Pdr1p interacts physically and functionally with the Gal11p/MED15 subunit of the mediator, a key component of transcriptional machinery. This interaction was interesting as it opened the door to the development of new compounds that could sensitize azole-resistant strains by hampering the Pdr1-Med interaction ⁷⁸.

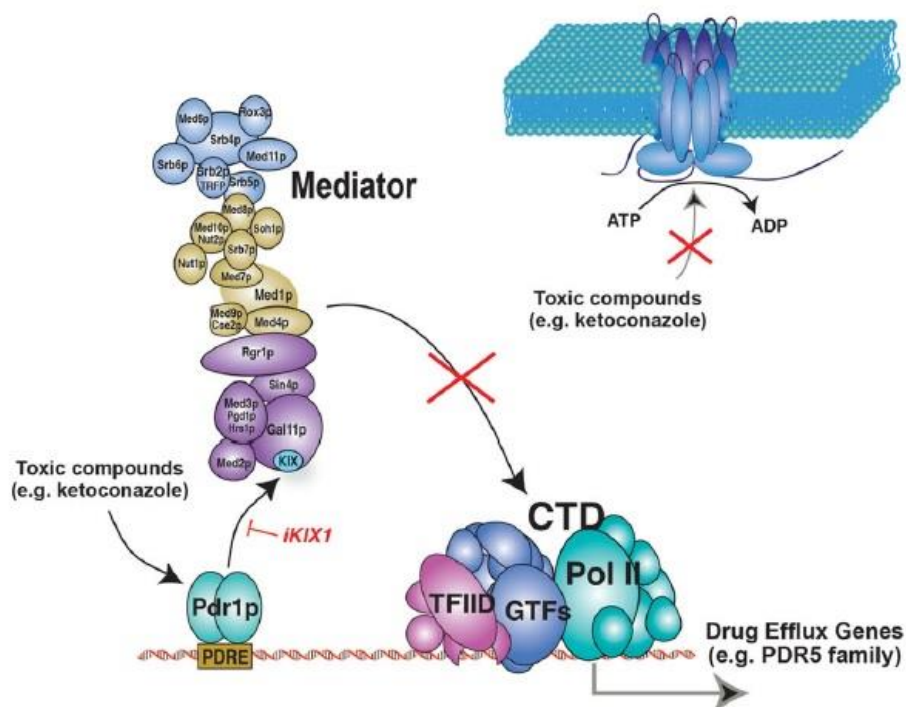


Figure 1.6: Example of a functional model of a new compound (iKIX1) that show to sensitize azole-resistant strains by hampering the Pdr1-Med interaction. The iKIX1 molecule block the azole-induce recruitment of Gal11/Med15-Mediator to Pdr1 target genes upon azole treatment. This blocking prevent the upregulation of Pdr1 target genes, including those which encode drug efflux pumps which result to a restoration of the sensitivity to the azole antifungal. Image was retrieved from Nishikawa, J et al., 2016 ⁷⁸.

It has been shown that the azole-resistance phenotype in clinical isolates often arises from mutations in *CgPDR1* which lead to constitutive activation of the transcription factor and, consequently, to the over-expression of its target genes out of which the drug efflux pumps *Cdr1* and *Cdr2* stand out for their prominent role in azole resistance^{47 68 79 80}. In Figure 1.7 are shown the multitude of point mutations that had already been identified in *CgPDR1* and that have been found to result in hyper-activation of this regulator.

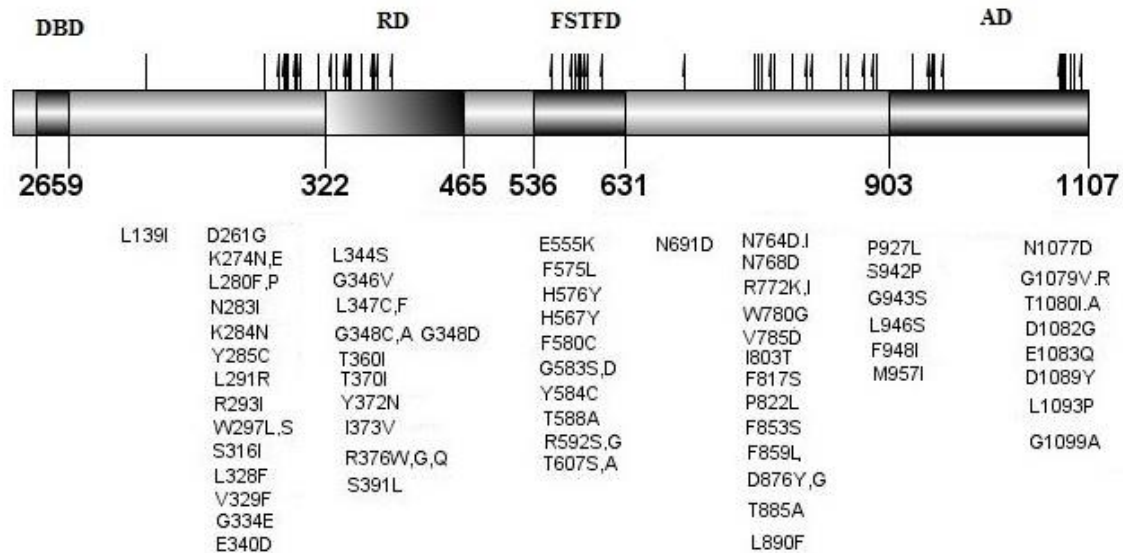


Figure 1.7: Described *C. glabrata* PDR1 gain-of-function mutations. The domains shown were based on the homology between *S. cerevisiae* Pdr1p and *CgPdr1p* retrieved from Tsai, H., et al., 2010⁷⁰. DBD – DNA-binding domain; RD – Regulatory Domain; FSTFD – Fungus-specific Transcription factor Domain; AD – Activation Domain. Mutations described according from the information available in Tsai H., et al.,2006,⁶⁸ Torelli, B., et al.,2008,⁴⁷ Ferrari, S., et al., 2009,⁸⁰ Tsai, H., et al., 2010,⁷⁰ Berila, N. and Subik, J., 2010,⁸¹ Caudle K., et al.,2011,⁷³ Vale-Silva, L., et al.,2015,⁸² Garnaud, C., et al,2015,⁸³ Katiyar, S., et al.,2016,⁸⁴ Healey, K., et al.,2016⁵⁵.

These substitutions are distributed throughout the various domains of the protein being found near the inhibitory domain, in the MHR (Middle homology region) and also in the activation domain⁸⁰. The localization of these mutations along the protein is similar to GOF mutations described in the *S. cerevisiae* homologue Pdr1p⁶⁶. The comparison of the set of genes regulated by different gain-of-function mutations in *CgPDR1* shows an overlap of only two genes, *CgCDR1* and *PUP1*, encoding a mitochondrial protein⁷⁴. These observations suggest that the mechanism by which *CgPdr1* becomes activated could be different depending on the gain-of-function mutation that occurs^{73 80}.

Besides enhancing azole resistance, GOF mutation in *CgPDR1* are also shown to prompt an increase in adherence and virulence in host cells⁸⁵. In specific, Ferrari et al. showed that mutations L280F, R376W, Y584C, T588A and D1082G on *CgPDR1* enhance virulence of *C. glabrata*, this being in part at the result of the up-regulation of *CgCDR1* and *CgPUP1*⁷⁴. It was also shown that gain of function mutation L280F in *CgPDR1* modulate the expression of the adhesin *EPA1* increasing adherence to host tissues⁷¹. It thus seems that the origin of *CgPDR1* GOF mutations results not only in increased resistance to azoles, but also has other outcomes with impact in the context of infections prompted by *C. glabrata*.

1.3. Introduction to the theme of thesis

The emergence of resistance among *C. glabrata* clinical isolates poses a serious challenge to control infections prompted by this pathogenic yeast species. A better understanding of the molecular mechanisms underlying this phenotypic trait is thought to help in the design of more effective antifungal drugs as well as to the development of more rapid strategies for the detection of resistant strains, thereby fastening the application of appropriate treatments to patients. It has to be highlighted that the delay in diagnosis of *Candida* infections as well as of the choice of the more suited antifungal drugs has been found to significantly increase risk of death in infected patients. The present work follows a previous one in which a collection of *C. glabrata* clinical isolates has been phenotyped to search for azole-resistant strains ⁸⁶. In that study a collection of 8 strains were found to be identified as being resistant to fluconazole and voriconazole, as shown by the results presented in Figure 1.8. One of the resistant strains, FFUL887, was found to encode a CgPdr1 gain-of-function mutant exhibiting a point mutation K274Q that had not been previously described ⁸⁶.

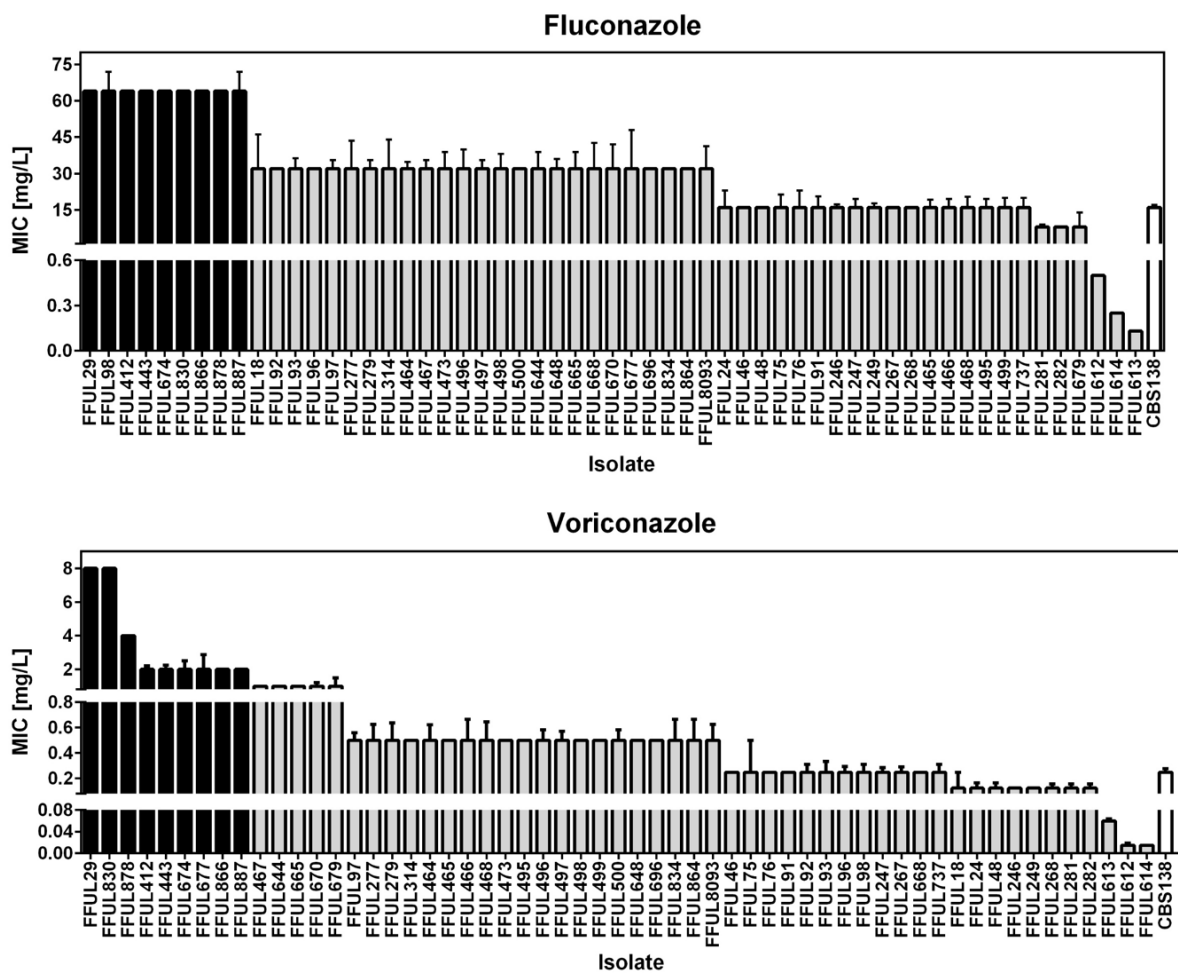


Figure 1.8: Measured MIC values for the antifungals fluconazole, voriconazole of the cohort clinical isolates used in the previous work (Salazar, S., 2015) ⁸⁶ and the reference strains CBS138 (White). Resistant isolates are market in black, while isolates classified as being susceptible or intermediately resistant are market in grey.

In this thesis it were used the isolates FFUL29, FFUL412, FFUL443, FFUL674, FFUL830, FFUL866 and FFUL878 resistant to fluconazole and voriconazole and FFUL677 resistant only to voriconazole. The first task that was performed was the sequencing of the *CgPDR1* in all these strains to search for eventual point mutations. Afterwards several strategies were designed in order to determine on whether or not the *CgPDR1* genes encoded by the above-mentioned clinical isolates indeed encoded gain-of-function mutations. Simultaneously it was examined the efficacy of a set of Ag(I)-camphorimine complexes, recently described to have a good antimicrobial effect against all non-*albicans* *Candida* species^{87 88}, in inhibiting growth of *C. glabrata* including the above-mentioned azole resistant strains (in collaboration with the group of Professor Fernanda Carvalho from CQE at IST). The compounds were obtained using a combination of silver nitrate and camphor derivatives which are two types of compounds with recognized pharmaceutical properties. The usefulness of camphor and silver has long been known in pharmacological uses. (*e.g.* anesthetic, burns, muscular relaxant, nasal decongestant etc^{89 90 91 92}). In recent years, camphor derivative have been explored to inhibit influenza virus^{93 94 95}. Silver nitrate is known to have a potential antimicrobial effect, however, its toxicity severely limits its usefulness^{96 97}. The compounds used in this thesis have the general formula $\{Ag(NO_3)(^YL)\}_n$, in which ^{YL} are the camphorimine compound having the bicyclic structure of camphor (camphor diamine) and used as ligands. To obtain the compounds a reaction was performed using $AgNO_3$ and camphorquinone (designated compound A), mono-camphor (designated compound B) and camphor sulphonilimine (designated compound C) (Figure 1.9).

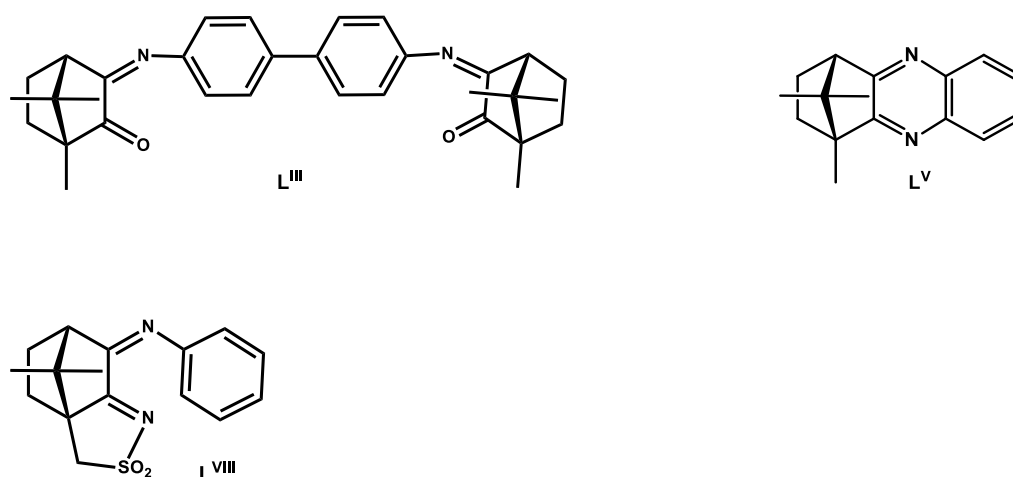


Figure 1.9: Camphorimine compounds used as ligand. L^{III} was used in complex A, L^V in complex B and L^{VIII} in complex C.

Further insights into the mechanisms by which the Ag(I)-camphorimine drugs could interact with *C. glabrata* cells were also further scrutinized in this study, with emphasis on an eventual involvement of CgPdr1 and of CgPdr1-regulated genes.

2. Materials and Methods

2.1. Strains and growth media

A cohort of *C. glabrata* clinical isolates previously described to be resistant to azoles named FFUL29, FFUL412, FFUL443, FFUL674, FFUL830, FFUL866 and FFUL878 resistant to fluconazole and voriconazole and FFUL677 resistant only to voriconazole ⁸⁶ was used. These clinical isolates were recovered from patients attending three major hospitals of the Lisbon area through the years 2000 and 2008 and were kindly provided by Prof. Maria Manuel Lopes, Faculdade de Farmácia da Universidade de Lisboa and Dr. Rosa Barros, Head of the Microbiology Laboratory of “Centro Hospitalar de Lisboa Central”. Besides these clinical isolates, a set of laboratory strains were also used as described in Table 2.1. The deletion strains were kindly provided by Dr. Hiroji Chibana from Chiba University. *Saccharomyces cerevisiae* strain BY4741 (MATa his3Δ1 leu2Δ0 met15Δ0 ura3Δ0; acquired from Euroscarf) and *E. coli* XL1-Blue strain were used as host for molecular biology procedures.

Table 2.1: Description of the group of strains used in this work

Strain	Genotype/Description	Reference
<i>C. glabrata</i> CBS138	<i>C. glabrata</i> laboratory standard strain	CBS-KNAW fungal biodiversity Centre ⁹⁸
<i>C. glabrata</i> KUE100	Parent strain, histidine auxotroph, the recipient enable high efficient gene targeting which <i>yku80</i> is repressed with <i>SAT1</i> flipper	Ueno et al., 2007 ⁹⁹
<i>C. glabrata</i> Δ <i>cdr1</i>	KUE100_Δ <i>cdr1</i>	Prof. Hiroji Chibana, Medical Mycology Research Center, Chiba University, Chiba, Japan
<i>C. glabrata</i> Δ <i>pdr1</i>	KUE100_Δ <i>pdr1</i>	Prof. Hiroji Chibana, Medical Mycology Research Center, Chiba University, Chiba, Japan

C. glabrata cells were batch-cultured at 30 °C, with orbital agitation (250 rpm) in rich growth medium Yeast Peptone Dextrose (YPD) or RPMI (from Roswell Park Memorial Institute Medium). YPD contains, per liter, 20 g glucose (Merck Millipore), 10 g yeast extract (HiMedia Laboratories, Mumbai, India) and 20 g Peptone (HiMedia Laboratories). RPMI, contains, per liter 20.8 g RPMI-1640 synthetic medium (Sigma), 36 g glucose (Merck Millipore), 0.3 g of L-glutamine (Sigma) and 0.165 mol/L of MOPS (3-(N-morpholino) propanesulfonic acid, Sigma). The different *C. glabrata* strains were maintained at -80 °C in YPD medium supplemented with 30 % glycerol (v/v) (Merck). All media were prepared in deionized water. YPD medium was sterilized by autoclave for 15 min at 121 °C and 1 atm. RPMI medium was filtered with a 0.22 μm pore size filter and preserved at 4 °C until further use. Unless otherwise specified the pH of the RPMI growth medium was adjusted to 7 using NaOH as the alkalinizing agent. *E. coli* XL1-Blue strain was maintained and cultivated in LB medium (Sigma) or in this same medium supplemented with 150 mg/L of ampicillin. LB medium contains, per liter, 10 g tryptone, 10 g NaCl and 5 g Yeast extract.

2.2. Preparation of antifungal drugs and of camphorimine-derived chemicals

The stock solution of fluconazole, voriconazole and of camphorimine compounds A, B and C were all prepared from the powder and using DMSO (Dimethyl sulfoxide, Sigma) as the solvent. The concentrations tested ranged from 0.125 mg/L to 64 mg/L for Fluconazole and 0.015 mg/L to 8 mg/L for Voriconazole. The range of concentrations used for each compound in this study were from 1.953 mg/L to 1000 mg/L.

2.3. Genomic DNA extraction

Genomic DNA was extracted from different *C. glabrata/S. cerevisiae* colonies by harvesting three loops of biomass that were afterwards inserted in a 1.5 mL Eppendorf tube. To this mixture it were added approximately 100 μ L of glass beads (0.5 mm) and 200 μ L lysis buffer (Tris 50 mM, EDTA 50 mM, NaCl 250 mM, SDS 0.3 %). The tubes were vortexed for 2 min at maximum speed and then incubated at 65 °C for 1 h. Afterwards, the tubes were put on ice for 2 min and then a second round of vortexing was performed. The obtained disrupted cell suspension was centrifuged at 13000 rpm for 15 min at 4 °C and the supernatant transferred to a clean Eppendorf. After, were added 20 μ L of NaAC 3 M (pH 4.8) and 400 μ L of cold Ethanol to the suspensions to induce DNA precipitation. The samples were left at -20 °C for, at least, 30 min and then centrifuged at 13000 rpm, during 20 min at 4 °C. The pellet obtained was washed with 500 μ L of ethanol 70 %, and then centrifuged at 13000 rpm during 8 min at 4 °C. After, supernatant was discarded and the pellet was dried in speed vacuum and finally resuspended in 30 μ L deionized water.

2.4. PCR reaction and DNA sequencing by Sanger method of *CgPDR1* gene

The sequence of *CgPDR1* gene of the different *C. glabrata* strains was obtained by primer walking. For this 6 rounds of PCR were performed for each strain using specifically primers whose sequence is indicated in Table 2.2.

Table 2.2: Primers sequences used to amplify the selected regions of *CgPDR1* gene of the *C. glabrata* resistant isolates.

Name	Sequence 5' 3'	Primer hybridization position
FW1	CTT CCA TTA CTT CGT ACC C	5'- 120 to 101 -3' - before the beginning of the gene
FW2	GCC TAG TAC AAG AAG AAC AAA AGT TG	5'- 56 to 82 -3'
FW3	TCC ATT GAC GCC ATT GAG TTA CAA C	5'- 721 to 746 -3'
REV3	CAG AGT GCC AAA GTA TGC AGC CTT	5'- 2581 to 2604 -3'
REV2	CGG CGA GGG TAA ATT CAA CTG ATA C	5'- 3023 to 3047 -3'
REV1	GAC AGT GTG CAT AGC CTG	5'- 14 to 32 -3' - after the end of the gene

The PCR amplification was performed using the reaction mixture and the experimental conditions described in Tables 2.3 and 2.4. The sequencing reaction was performed by STABVIDA as a paid service. Clustal Omega was used for sequence alignment establishing as a reference for the comparative analysis the sequence of *CgPDR1* from the reference strain *C. glabrata* CBS138, susceptible to azoles (Figure 1.8.).

Table 2.3: Reaction mixture used for the amplification of the selected regions of *CgPDR1* gene.

Component	Volume per reaction
dNTP's	0.4 μ L
Primer forward	0.4 μ L
Primer reverse	0.4 μ L
Template DNA	2.0 μ L
MgCl ₂	1.2 μ L
Buffer	2.0 μ L
Taq polimerase	0.5 μ L
ddH ₂ O	18.1 μ L
Total	25.0 μL

Table 2.4: Conditions of the PCR cycles for amplification of the selected regions of *CgPDR1* gene.

Time	Temperature	
1 min	94 °C	
30 s	94 °C	x32
1 min	56 °C	
1 min 30 s	72 °C	
10 min	72 °C	
∞	8 °C	

2.5. Cloning of *CgPDR1* gene

To clone gene *CgPDR1* from *C. glabrata* CBS138 or from the resistant clinical isolates FFUL412, FFUL443, FFUL866 and FFUL887 in the pGREG526 plasmid¹⁰⁰ a strategy based on homologous recombination was used. The pGREG526 plasmid was digested with 15 U of Sall (Takara Bio USA, Inc.) at 37 °C during 3 h then the digested product was incubated with 1 U of Calf Intestinal Alkaline Phosphatase (CIAP) (Invitrogen) at 37 °C for 1 h to prevent re-circularization. The *CgPDR1* gene was amplified by PCR using as a template the genomic DNA of the strains with the specific primers listed in Table 2.5. The reaction mixture and the experimental conditions used are also described in Tables 2.6 and 2.7.

Table 2.5: Primers used for the amplification of the *CgPDR1* gene.

Name	Sequence 5' 3'
CgPdr1_rev	GCGTGACATAACTAATTACATGACTCGAGGTCGACGCATCACAAGTAAACATCAG
CgPdr1_fw	GAATTTCGATATCAAGCTTATCGATACCGTTCGACAATGCAAACATTAGAAACTACATC

Table 2.6: Reaction mixture used for the amplification of the *CgPDR1* gene.

Component	Volume per reaction	Volume per reaction
	CBS138	Isolates
HF buffer	5.0 μ L	5.0 μ L
dNTPs	1.0 μ L	1.0 μ L
Primer forward	1.0 μ L	1.0 μ L
Primer reverse	1.0 μ L	1.0 μ L
Template DNA	1.0 μ L	1.0 μ L
MgCl ₂	4.0 μ L	2.0 μ L
DMSO	1.5 μ L	1.5 μ L
Phusion	0.5 μ L	0.5 μ L
ddH ₂ O	35.0 μ L	35.0 μ L
Total	50.0 μL	50.0 μL

Table 2.7: Conditions of the PCR cycles for amplification of the *CgPDR1* gene.

Time	Temperature	
1 min	95 °C	
1 min	95 °C	x32
40 s	54 °C	
3 min 30 s	72 °C	
7 min	72 °C	
∞	4 °C	

The amplified gene and the digested pGREG526 plasmid were used to transform *S. cerevisiae* BY4741 cells using the Alkali-Cation™ Yeast Transformation Kit (MP Biomedicals). For this, the cells were cultivated until mid-exponential phase (OD_{600nm} = 0.4) in 50 mL of YPD and then centrifuged for 5 min at 6000 rpm and 4 °C. The pellet obtained was resuspended in 4.5 mL TE (pH 7.5) and then centrifuged again using the same conditions described above. The pellet was resuspended in 2.5 mL of Lithium/Cesium Acetate Solution and the obtained suspension was then incubated for 30 min at 30 °C with 100 rpm agitation. The cells were centrifuged as described above and finally resuspended in 500 μ L of TE (pH 7.5) to obtain competent cells. Each transformation mixture used 100 μ L of competent cells, 10 μ L of purified promoter fragment, 1 μ L of digested pGREG526 plasmid, 5 μ L of carrier DNA and 5 μ L of histamine solution. The mixtures were incubated at room temperature for 15 min. After this, 0.2 mL of TE/Cation Mix and 0.8 mL of PEG were added to each reaction and these were incubated for another 10 min at 30 °C. Cells were then heat shocked for 10 min at 42 °C and subsequently cooled to 30 °C. The reactions mixtures were centrifuged at 8000 rpm for 3 min and cells were resuspended in 100 μ L of YPD and plated on MMB plates lacking uracil. Confirmation of the integration of the gene in the pGREG526 plasmid was performed by PCR. For this, a Total DNA extraction from each colony obtained in the transformation step was done as described in the subchapter 2.3. Then, 1 μ L of the template DNA were used for the subsequent PCR reaction which was performed using the same conditions described above in Table 2.6 and 2.7. Those colonies in which amplification of a 4400 bp product was observed were considered to be positive candidates.

The plasmid DNA obtained from the positive candidates was inserted in *E. coli* XL1-Blue cells by adding 20 μ L of the purified plasmid DNA to 150 μ L of competent cells plus 50 μ L of TCM solution, 10 mM CaCl₂ 10 mM MgCl₂ 10 mM TrisHCl pH 7.5. After, cells were incubated on ice for 15 min then incubated for 3 min at 42 °C and finally incubated 5 min on ice. After the heat shock, 800 μ L of

liquid LB were added to the cell suspension and this was then incubated for 1 h at 37 °C at 250 rpm to allow recovery of the cells. The culture was then centrifuged at maximum speed in a table-top centrifuge and the pellet obtained was resuspended in LB and finally plated in selective LBA medium. Plasmid DNA was recovered from the *E. coli* transformants using the QIAprep Spin Miniprep Kit (Quiagen). Integration was confirmed by performing the restriction map of the recovered plasmids with the restriction enzyme XhoI.

2.6. Assessment of gene expression based on real time RT-PCR

The expression of *CgCDR1* and *CgPUP1* genes were compared in CBS138 and in 6 resistant isolates, FFUL29, FFUL412, FFUL443, FFUL830, FFUL866 and FFUL878 by real time RT-PCR. For this, the strains were cultivated overnight in 5 mL of YPD at 30 °C with orbital agitation (250 rpm) and then inoculated in 150 mL of RPMI at 30 °C and 250 rpm at an initial OD of 0.025 corresponding to around 1.25×10^5 CFUs/mL which is within the range of 0.5×10^5 – 2.5×10^5 CFUs/mL. When the OD_{600 nm} of the cultures achieved approximately 2, corresponding to mid-exponential phase, cells were harvested by centrifugation (8000 xg, 7 min, 4 °C – Beckman J2.21 Centrifuge, rotor JA.10) and immediately frozen at -80 °C until further use. RNA extraction was performed using the hot-phenol method¹⁰¹. Conversion of total RNA into cDNA was performed using 1 µg of RNA. The reverse-transcription step was performed in a C1000 Thermal Cycler (Bio-Rad, Hercules, USA). The subsequent quantitative PCR step was performed using 2.5 µL of the cDNA and SYBR® Green super mix (BioRad). The sequence of the primers used are listed in Table 2.8. Gene expression was calculated using gene *RDN25* as an internal control.

Table 2.8: Primer sequences used to measure expression of *CgPDR1* gene using real time RT-PCR.

Name	Sequence	
<i>CgPDR1</i>	Forward	5'-GCTTGCCCGCACATTGA-3'
	Reverse	5'- CCTCAGGCAGAGTGTGTTCTTTC-3'
<i>CgPUP1</i>	Forward	5' CACTGGTGCCTGAAAGGTG 3'
	Reverse	5' TGTCCCAGGCTATCTTTGCC 3'

2.7. Quantification of MIC₅₀ using the microdilution method

To determine MIC₅₀, the concentration of each drug that inhibited growth of *C. glabrata* strains by more than 50 % the growth observed in drug-free medium, it was used the microdilution method recommended by EUCAST¹⁰². A schematic representation of the method used is shown in Figure 2.1.

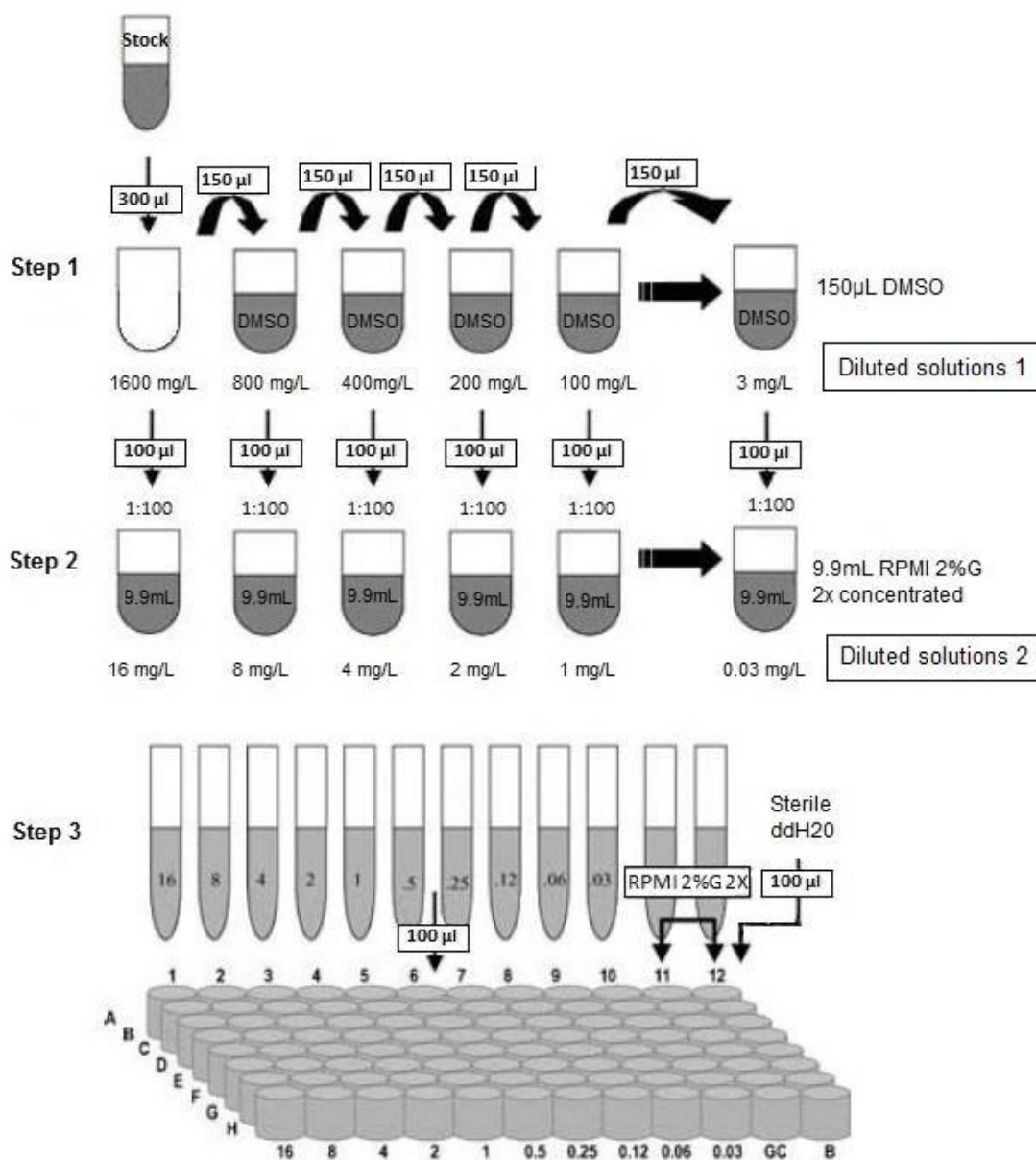


Figure 2.1: Schematic representation of the procedure used to prepare the 96-multiwell plates used to determine MIC of 3 different compounds for the different *C. glabrata* strains. B: blank; GC: control. Image altered from EUCAST discussion document E.Dis 7.1¹⁰². In the case of the compounds the same methodology was applied with the difference that the initial stock concentration was of 1000 mg/L.

To prepare the 96 multiwell-plates required for the microdilution assay, 300 µL of the stock solution of each chemical was transferred for a new tube and 1:2 dilutions (in DMSO) were performed in a final volume of 300 µL, yielding concentrations ranging from 2000 mg/L to 3 mg/L for the compounds. This solution in Figure 2.1 Step 1 is designated as “diluted solutions 1”. Afterwards, 100 µL of “diluted solution 1” was added to 9.9 mL of RPMI medium 2x concentrated yielding what is designated as “diluted solution 2” (Figure 2.1 Step 2). Then, 100 µL of the “diluted solution 2” were used to inoculate the 96-microwell plates. To prepare the final 96-multiwell plates 100 µL of diluted solution 2 were used yielding the range of concentrations desired (1000 mg/L to 1.953 mg/L) for all the com-

pounds (Figure 2.1 Step 3). The cell suspensions used in the assay were prepared from a pre-culture that was cultivated for 18 h in 5 mL of YPD at 30 °C and 250 rpm orbital agitation. The initial OD of the cultures was approximately 0.025 corresponding to around 1.25×10^5 CFUs/mL which is within the range of $0.5 \times 10^5 - 2.5 \times 10^5$ CFU/mL recommended by the EUCAST protocol¹⁰².

In column 11 of the plate the cells were diluted in 100 μ L sterile drug-free medium to assess their growth performance in the absence of the compound (which was used as a control) and in column 12 only the sterile drug-free growth medium was added (diluted 1:2 in sterile water) to serve as blank. After inoculation, the 96-multiwell plates were incubated without agitation at 37 °C for 24 h. After that time, cells were resuspended and the recommended OD_{530 nm} of the cultures was read in a microplate reader. The value of the blank was subtracted from readings of the rest of the wells.

2.8. Growth curves in the presence of camphorimine complexes

Growth of wild-type *C. glabrata* KUE100 and of the corresponding deletion mutants $\Delta cdr1$, $\Delta pdr1$ in RPMI growth medium (pH 7.0) with inhibitory concentrations of different compounds were accompanied during 40 h in 96 multiwell-plates, using a similar setup to the one used for estimation of MIC₅₀. In specific, cells of the different strains were cultivated in YPD until mid-exponential phase (OD_{600 nm} between 0.8 ± 0.05 and 1.0 ± 0.05). After this, the culture suspension with an initial OD_{600nm} of 0.025 was prepared in 5 mL sterile deionized water. Then, 100 μ L of these diluted cell suspensions were used to re-inoculate the 96-multiwell plate containing fresh RPMI growth medium at pH 7.0 supplemented with different compounds in two different concentrations, the breakpoint value and one concentration bellow. Growth of each strain at 30 °C with orbital agitation (250 rpm) in the presence or absence of the different compounds was accompanied based on the increase in OD_{595 nm}.

2.9. Synergy assays between the camphorimine compound and fluconazole

The interaction of fluconazole with camphorimine drugs was tested using a similar setup to the one used to estimate MIC₅₀ of each individual drug. For each strain tested, the following controls were included: control 1 - cells did not receive any different compound or fluconazole. This control group corresponds to the maximum yeast growth and is considered as 100% of growth; control 2 - cells received only an innocuous concentration of each compound; control 3 - cells received only fluconazole. Then cells received a mixture of the two concentrations of compound and fluconazole. After inoculation, the 96-multiwell plates were incubated without agitation at 37 °C for 24 h. After that time, cells were resuspended and the recommended OD_{530 nm} of the cultures was read in a microplate reader. Each set of experiments were made in duplicate.

2.10. [³H]- Fluconazole accumulation assay

To assess the intracellular concentration of fluconazole inside *C. glabrata* cells in response of the synergistic effect between Ag(I)-camphorimine complexes and fluconazole, cells were cultivated in RPMI growth medium (at pH 7.0) at 30 °C with orbital agitation (250 rpm) until mid-exponential phase (OD_{600 nm} = 0.8 ± 0.05), harvested by centrifugation, washed one time with fresh medium and finally resuspended in 5 mL of this same medium to obtain a dense cell suspension (OD_{600 nm} = 0.7 ± 0.05). After this, 4 μ L of [³H]-Fluconazole (Moravek Biochemicals Brea CA USA) were added to the cell suspension as well as 25 μ L of cold Fluconazole in a concentration of 32 mg/L and 75 μ L of the compound in a concentration of 3.91 mg/L. Culture samples were taken after 1, 5, 10, 15, 20, 25 and 30 min of incubation. After, 50 μ L of the supernatant was recovered by centrifugation in a tabletop centrifuge (12000 rpm, 1 min) in order to measure the extracellular radioactive fluconazole and cells were collected from 200 μ L culture sample filtered through pre-wetted glass microfiber filters (Whatman GF/C) and washed with cold water for quantification of intracellular fluconazole. Each sample were added to a 7 mL of scintillation liquid (Beckman) and their radioactivity was measured in a Tri-Carb 2810TR liquid scintillation counter.

3. Results

3.1. Unveiling new gain-of-function mutations in *CgPDR1*

Following the previous work performed in the group which led to the identification of a new gain-of-function (K274Q) mutation in *CgPDR1* from *C. glabrata* (found in the voriconazole- and fluconazole-resistant isolate FFUL887) ⁸⁶ it was hypothesized on whether the remaining isolates identified in the epidemiological study could also encoded *CgPDR1* gain-of-function mutants. As such, the *CgPDR1* gene sequence from isolates FFUL29, FFUL412, FFUL443, FFUL674 FFUL830, FFUL866 and FFUL878, resistant to fluconazole and voriconazole; and FFUL677, only resistant to voriconazole, were obtained by Sanger sequencing. For this, the gene was PCR-amplified using specific primers (Table 2.2) and then sequenced by Sanger. An example of the result of the PCR amplification is shown in Figure 3.1. The alignment of the sequences obtained for the different isolates with the sequence of the azole-susceptible CBS138 strain is shown in annexes and summarized in Table 3.1. The mutations S76P, V91I, L98S, T143P and D243N had been previously described in isolates resistant and susceptible to azoles ⁸⁰ and therefore are not considered putative *CgPDR1* GOFs. Mutations K274Q, E555K and I803T were previously described as GOF mutations ^{80 86} and could therefore underlie the voriconazole and fluconazole-resistance phenotype of the FFUL677, FFUL830 and FFUL878, isolates. Five of the identified mutations E5K, S10T, R35K, I392M and S911C were not previously described. The I392M replacement was found in the *CgPDR1* sequence of the voriconazole- and fluconazole- resistant isolates FFUL412 and FFUL443, which were not found to harbor any other mutation relevant for the azole-resistance phenotype. Similarly, the R35K SNPs was also found in isolate FFUL866, also found to be resistant to voriconazole-and fluconazole. Because the GOF *CgPdr1* phenotype is associated with both fluconazole- and voriconazole- resistance ⁴⁷ we don't favor the idea that the replacement E5K could be a GOF variants of *CgPdr1*. As for S10T, E5K and S911C replacements, because the isolates that harbor these mutations also have others that were previously identified as GOF (Figure 1.7) their role was not further scrutinized. It was also interesting to note that the fluconazole- and voriconazole- resistance phenotype of the FFUL29 isolate could not be linked to any GOF *CgPDR1* mutation since the differences found in the coding sequence of the *CgPDR1* allele encoded by this strain were also found in azole susceptible isolates. On the overall the work performed has suggested that R35K and I392M could be new GOF variants of *CgPdr1*.

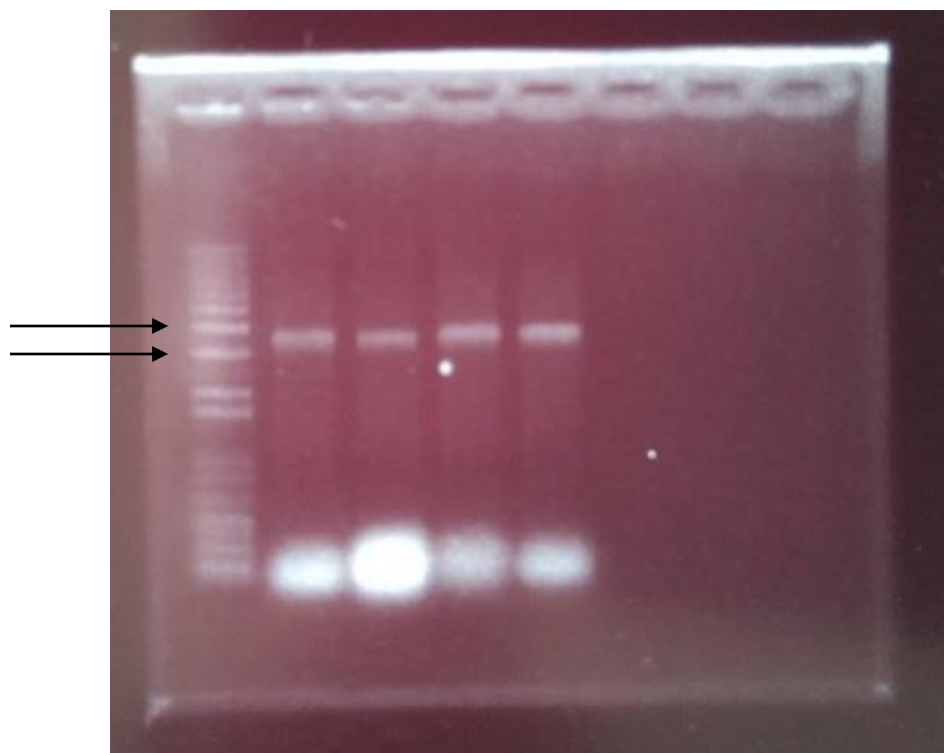


Figure 3.1: Example of the result obtained after amplification of *CgPDR1* gene using primer FW1 and REV1. Lane 1 represents the ladder (1kb plus DNA Ladder) - The black arrows show the 3 kb fragment and the 4 kb fragment.

Resistance to azoles phenotype	Strains	5	10	35	76	91	98	143	173	243	274	392	555	803	911
Susceptible	CBS138	E	S	R	S	V	L	T	D	D	K	I	E	I	S
Voriconazole and Fluconazole	FFUL29					I	S			N					
	FFUL412				P	I	S	P				M*			
	FFUL443				P	I	S	P				M*			
	FFUL674	K				I	S			N					
	FFUL830		T			I				N			K		
	FFUL866			K*		I	S			N					
Voriconazole	FFUL878	K				I	S			N	Q				C
	FFUL677	K				I	S			N				T	

Table 3.1: Alterations in the amino acid sequence of CgPdr1 transcription factor encoded by FFUL29, FFUL412, FFUL443, FFUL674, FFUL677, FFUL830, FFUL866 and FFUL878 when compared to its counter-partners encoded by the CBS138 strain. In green the susceptible mutations and in blue and lighter red the non-described mutations. * Represent the candidates to be new GOF variants of CgPdr1. In red is shown the GOF mutations found in other studies. The described mutations was retrieved from Ferrari, S., et al., 2009⁸⁰ Caudle, K., et al., 2011⁷³ Katiyar, S., et al., 2016⁸⁴ and Salazar, S., 2015⁸⁶

To conclude on whether or not the R35K and I392M replacements indeed corresponded to GOF variants of CgPdr1, the expression of CgPdr1 target genes in isolates FFUL412, FFUL443 and FFUL866 and in the reference strain CBS138 was compared. If the above-mentioned mutations do lead to constitutive activation of CgPdr1 (and are, consequently, GOF variants of this regulator) up-regulation of target genes in these isolates would be expected. Since a recent study has shown that *CgCDR1* and *PUP1* were the sole genes found to be up-regulated in a wide set of GOF CgPdr1 mutants⁷⁴, we focused our attention on these two genes (Figure 3.2).

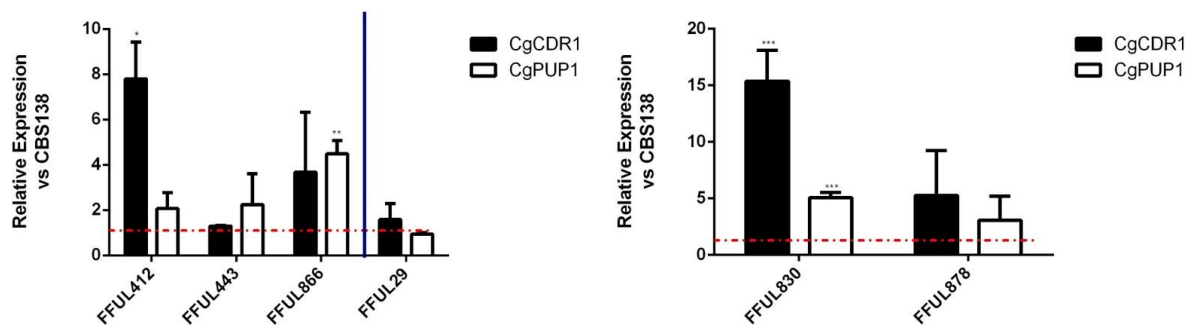


Figure 3.2: Comparison of the transcript levels of *CgCDR1* and *CgPUP1* genes in CBS138, FFUL29, FFUL412, FFUL443, FFUL830, FFUL866 and FFU878. Cells of the different isolates were cultivated in RPMI growth medium until mid-exponential phase after which the expression of *CgCDR1* and *CgPUP1* genes was compared by qRT-PCR. The values represented for the isolates strains are relative to the value obtained for the CBS138 strain, which was considered to be equal to 1. Gene expression was calculated using RDN25 as an internal control. For the statistical analysis the results obtained for the resistant isolates strains were compared with those gathered for CBS138. * p-value below 0.05, ** p-value below 0.001, *** p-value below 0.0001.

The results obtained confirm the expected up-regulation of *CgCDR1* and *CgPUP1* in isolates FFUL878 and FFUL830 which are known to harbor described *CgPdr1* GOF variants (K274Q, E555K). Concerning isolates FFUL412 and FFUL443, which harbor the I392M variation, the results obtained are not fully clear since it is observed up-regulation of *CgCDR1* in FFUL412, but not in FFUL443. In both cases up-regulation of *CgPUP1* is observed, although this is slight (around 2-fold). As for FFUL866, which harbor the R35K variant, it is observed a significant up-regulation of *CgPUP1* and *CgCDR1*. It was interesting to note that for isolate FFUL29, found to be resistant to both antifungal drugs, the expression of both genes are not significant and it is possible to suggest that the resistance phenotype of this isolate could be the result of another molecular mechanism of resistance.

3.1.1. Cloning of *CgPDR1* gene of the reference strain and of the resistant clinical isolates FFUL412, FFUL443 and FFUL866

To further clarify on whether or not the replacements R35K and I392M correspond to GOF variants of *CgPdr1* it was decided to express these genes ectopically from a plasmid in the background of an azole-susceptible *C. glabrata* strain. In case this hypothesis is confirmed the expression of the *CgPDR1* gene coming from the resistant isolates FFUL412, FFUL443 and FFUL866 would result in fluconazole and voriconazole resistance of the susceptible strain. As a negative control, it was planned to express the *CgPDR1* allele coming from the azole-susceptible strain CBS138. As a positive control, it was chosen to express the *CgPDR1* gene from FFUL887, already known to correspond to a GOF variant⁸⁶. All the *CgPDR1* alleles would be expressed in the pGREG526 cloning vector, from the Drag&Drop collection¹⁰⁰, which allows expression of target genes in an inducible manner simultaneously allowing the C-terminal tagging of the protein with an histidine tag. The strategy used is schematically represented in Figure 3.3. *S. cerevisiae* was used as a host for the cloning procedure considering the high efficacy by which this yeast species is able to perform homologous recombination.

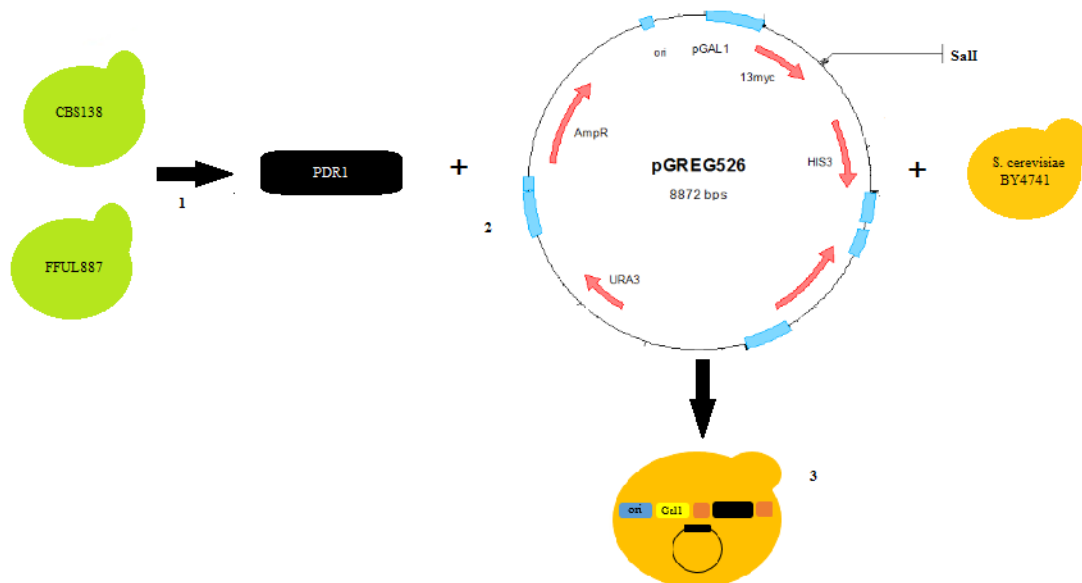


Figure 3.3: Genetic engineering strategy scheme used to clone *CgPDR1* gene encoded by the CBS138 and FFUL887. 1 – Amplification of *CgPDR1* by PCR; 2 – Digestion of plasmid with *SalI*; 3 – Homologous recombination in *S. cerevisiae* (representation of linearized plasmid after insertion of the *CgPDR1*: black rectangle refers to *CgPDR1*)

Briefly, the procedure consisted in amplification of the *CgPDR1* gene (confirmed by agarose gel, as shown in Figure 3.4 and subsequent transformation to the *SalI*-digested pGREG526 vector. After transformation and plating in a growth medium depleted of uracil (the strain used is auxotrophic for uracil this being complemented by the *URA3* marker present in pGREG526), about 30 to 80 *S. cerevisiae* colonies were obtained. To confirm if indeed these candidates do had the different *CgPDR1* alleles cloned in the pGREG526 vector, colony PCR was performed aiming to obtain a fragment with approximately 4467 bp (the size of the *CgPDR1* gene 3324 bp plus 1143 bp which consist of the distance between the hybridization region of the confirmation primer until the beginning of the inserted gene). Two positive candidates, coming from the FFUL887 and the reference strain CBS138 were obtained for each strain (Figure 3.5). For isolates FFUL412, FFUL443 and FFUL866 until now it was not possible to obtain positive candidates in *S. cerevisiae*. After recovery of the plasmid DNA of the positive yeast candidates, a subsequent transformation to *E. coli* was performed. Unfortunately, up to now it was not possible to obtain a bacterial clone of that was confirmed to have the expected pGREG-*CgPDR1* allele for the isolate FFUL887 and the reference strain CBS138.

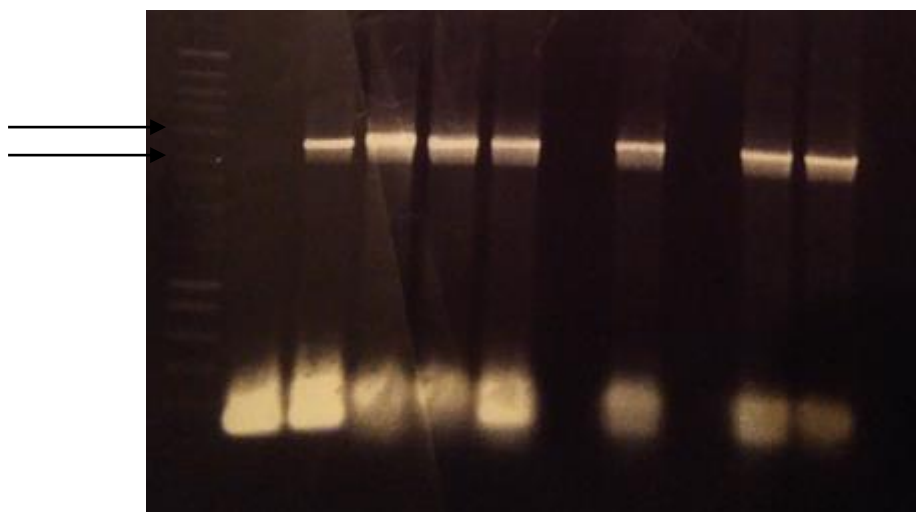


Figure 3.4: PCR products fragments expected after amplification of *CgPDR1* and separated by an agarose gel electrophoresis. The amplification of *CgPDR1* gene was done using the genomic DNA of the CBS138 (lane 3), FFUL412 (lane 4), FFUL443 (lane 5), FFUL866 (lane 8) and FFUL887 (lane10). Lane 1 represents the ladder (Nzy Ladder III) – The black arrows show the 3 kb fragment and the 4 kb fragment.

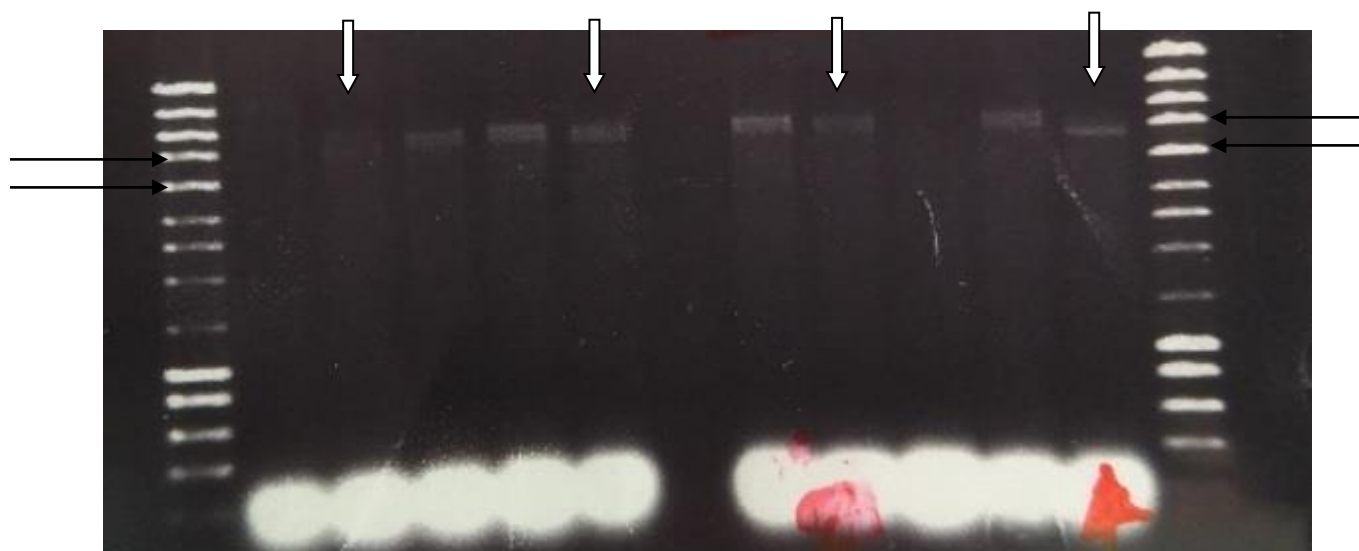


Figure 3.5: PCR colony of potential candidates of CBS138 and FFUL887. Lane 1 and 13 represents the ladder (Nzy Ladder III). Lanes 2 to 6 represents CBS138 candidates and lanes 8 to 12 FFUL887 candidates. The expect fragment should be approximately 4500bp. Black arrows show the 4 kb fragment and the 5 kb fragment.

3.2. Study on the antimicrobial effect against *C. glabrata* of Ag(I) camphorimine complexes

A previous study has demonstrated the potential of several Ag(I) camphorimine complexes against species of the *Candida* genus, the highest effect being obtained against *C. parapsilosis* and *C. tropicalis*, while for *C. glabrata* it was registered a mild effect⁸⁷. However, in this previous study the experiments were performed in an acidic growth medium (pH ~5) considering that some niches where *Candida* species thrive are indeed acidic (*e.g.* the vaginal tract). However, in other infection sites (such as the bloodstream, for example) the pH is higher (close to 7) which prompted the examination of the effect of Ag(I)-camphorimine chemicals against *C. glabrata* under these conditions. For such, a microdilution assay¹⁰² was performed to assess the MIC₅₀ of three Ag(I)-camphorimine complexes (A, B and C), against the reference strain CBS138. Two experimental setups were used concerning the pH of the growth medium, pH 5.38 (obtained without adjusting the pH after preparation of the RPMI

medium; identical to the previously published study) and pH 7 (by adjusting the pH of the growth medium to 7 using NaOH as the alkalizing agent). MIC₅₀ was defined as the lowest concentration of a compound that inhibited to a 50% of the growth of the strain, when compared with the growth registered in the absence of the drug. The results obtained confirmed the previously published results concerning the mild effect obtained in acidic growth medium, however, in the near-neutral pH a much stronger effect was obtained with the MIC₅₀ in the range of 15.63 mg/L and 31.25 mg/L. (Figure 3.6a and table 3.2). To check that there were no other variable responsible for the observed pH-dependent effect, the same experiment was performed using buffering agent (Tris base instead of MOPS) or not adding any buffering agent at all and solely adjusting the pH of the medium using NaOH or HCl. The result obtained in all cases was identical, thus confirming the potent effect of Ag(I)-camphorimine complexes against *C. glabrata* in near-neutral conditions. (Figure 3.6)

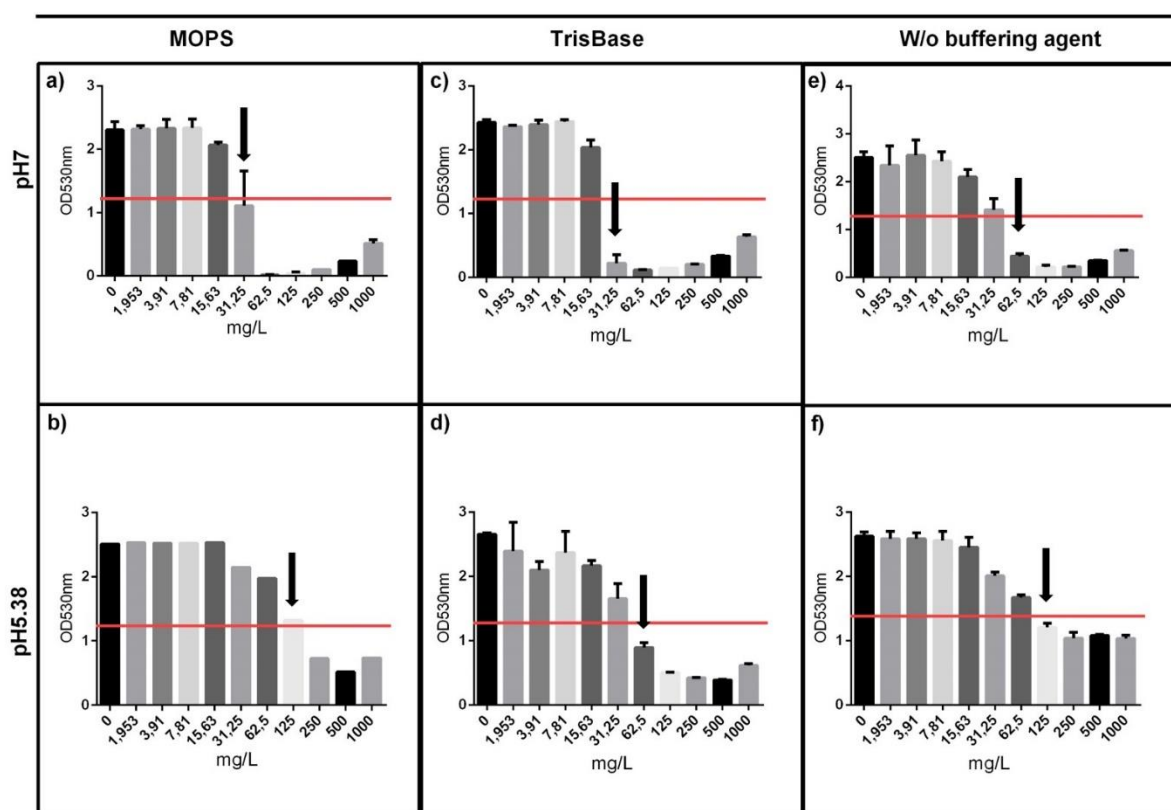


Figure 3.6: Microdilution assay performed in several condition of the growth medium RPMI supplemented with compound A against the reference strain CBS138. a) Growth medium RPMI (pH 7) prepared as recommended by EUCAST (for more information see materials and methods), b) RPMI (pH 5.38) prepared as recommended by EUCAST, c) RPMI (pH 7) with TrisBase instead of MOPS, d) RPMI (pH 5,38) with TrisBase instead of MOPS, e) RPMI (pH 7) without MOPS buffer, f) RPMI (pH 5.38) without MOPS buffer. The MIC₅₀ was determined comparing the values of the different isolates in the supplemented medium with chemical and the one registered in control conditions after 24 h of cultivation at 37 °C in RPMI growth medium (pH 7), as described in materials and methods. The MIC₅₀ value in indicated by a black arrows and the 50 % reduction of the growth registered in the absence of the chemicals is indicated by the red line.

3.2.1. Assessment of the activity of compound A, B and C against *C. glabrata* azole-resistant clinical isolates

The high inhibitory activity of compounds A, B and C against the reference strain *C. glabrata* CBS138, prompted the examination of a similar effect in the azole-resistant strains FFUL29, FFUL674, FFUL830, FFUL866, FFUL878 and FFUL887.

A microdilution method similar to the one described above (using the pH 7) was used to assess MIC₅₀ in these strains, the results obtained being summarized in Table 3.2 and shown in full in Annexes I, J and K. Significantly, the three compounds inhibited growth of the azole-resistant isolates in a similar extent to the one observed for the reference strain CBS138.

Isolates	Compound		
	A	B	C
CBS138	31.25	15.63	15.63
FFUL29	62.5	31.25	31.25
FFUL674	62.5	31.25	15.63
FFUL830	31.25	15.63	31.25
FFUL866	31.25	15.63	15.63
FFUL878	31.25	15.63	15.63
FFUL887	31.25	15.63	31.25

Table 3.2: MIC₅₀ values (mg/L) for Ag(I) camphorimine complexes A, B and C against the azoles resistant isolates FFUL29, FFUL674, FFUL830, FFUL866, FFUL878 and FFUL887 and reference strain CBS138 based on the EU-CAST microdilution method.

The fact that the Ag(I)-camphorimine complexes showed activity against the azole-resistant strains suggest that this drug may inhibit *C. glabrata* through a mechanism different from the one used by these cells to respond to azole stress. To confirm that hypothesis it was examined the effect of deleting *CgPDR1* or the drug-efflux pump *CgCDR1* in tolerance of *C. glabrata* to the Ag(I)-camphorimine complexes. For this, the cells of the three strains (wild-type, $\Delta cdr1$, $\Delta pdr1$) were cultivated under the same experimental conditions as those used in the microdilution test, but in this case the absorbance values were measured hourly for approximately 40 h. Two concentrations were used, one corresponding to the MIC value obtained for each compound on the CBS138 strain (related to the genetic background of the KUE100 strain), 31.25 mg/L for compound A and 15.63 mg/L for compounds B and C and a concentration below the MIC value obtained for the three compounds (7.81 mg/L) (Figure 3.7). The results obtained show a similar growth curve of the wild-type and of the two deletion mutant strains in all the conditions tested, thereby demonstrating that indeed *CgPDR1* and *CgCDR1* are dispensable for *C. glabrata* tolerance to Ag(I)-camphorimine complexes.

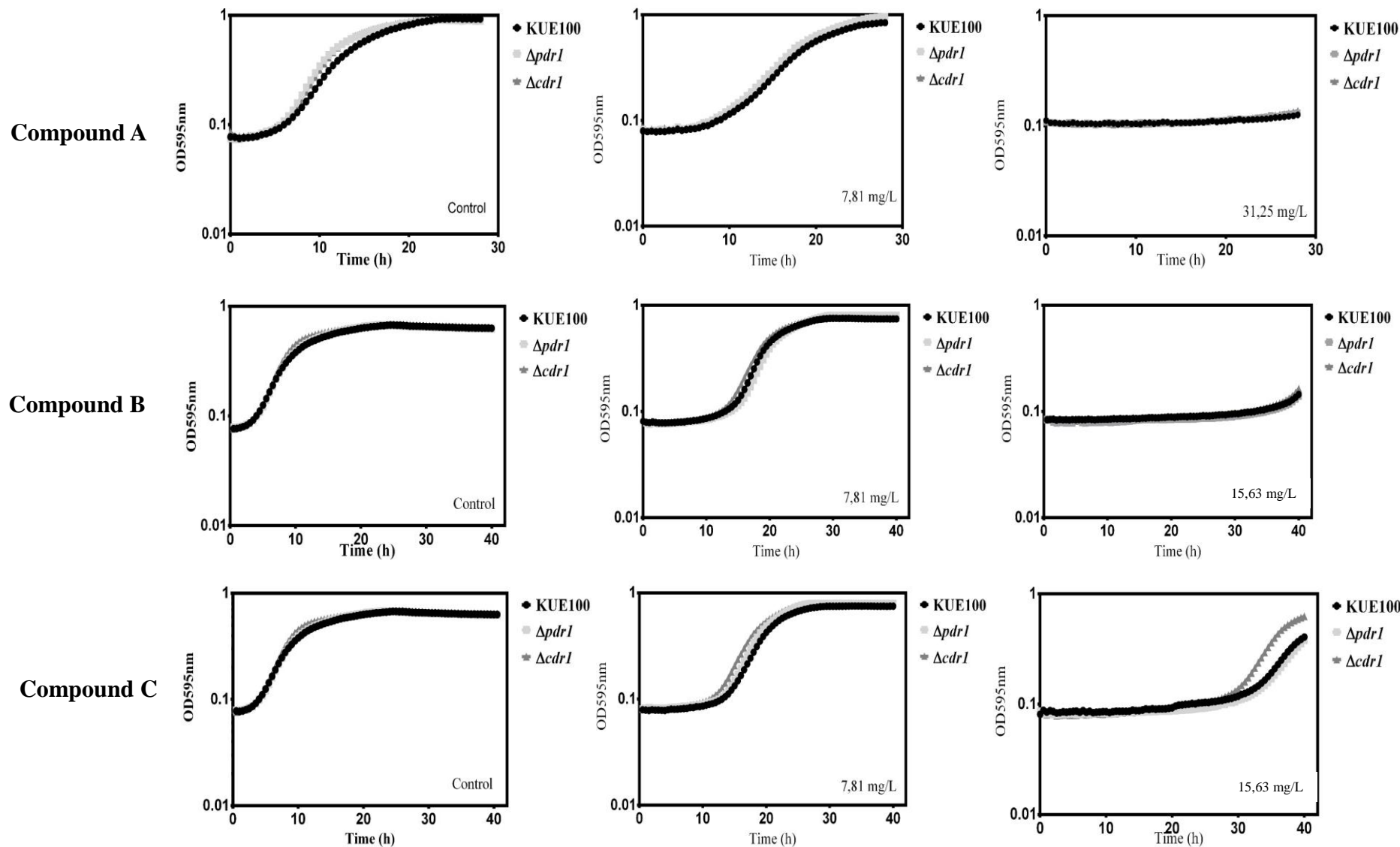


Figure 3.7: Growth curves of KUE100 (●), $\Delta pdr1$ (■) and $\Delta cdr1$ (▲) in growth medium RPMI (pH 7), or with the same medium supplemented with compound A (7.81 mg/L and 31.25 mg/L), B and C (7.81 mg/L and 15.63 mg/L). The growth was followed during approximately 40 h and the absorbance of the growth increasing was measured in OD595 nm.

3.2.2. Synergistic effect of Ag(I)-camphorimine complexes with fluconazole

Fluconazole is one of the most used antifungal drugs in the clinical practice and an interesting strategy to improve susceptibility of *Candida* cells to this drug could be through its application in synergism with other sensitizing chemicals. In that sense we have reasoned on the possibility of a synergistic effect between the Ag(I)-camphorimine compounds with fluconazole. To test that, *C. glabrata* cells were exposed to three non-inhibitory concentrations of the camphorimine complexes (A, B and C) in combination with 64 mg/L of fluconazole (the breakpoint resistance concentration) or 32 mg/L. The results obtained showed, as expected, no inhibition in growth prompted by the presence of the Ag(I)-camphorimine complexes, while exposure to the selected concentrations of fluconazole led to a slight inhibition in growth. Combination of the two drugs had, however, a much more potent effect, being observed a marked inhibitory effect preventing growth of almost all the strains tested. It is important to note that this effect was observed either for the reference strain CBS138 but also for the azole-resistant clinical isolates. In Figure 3.8 are represented the heatmaps obtained in the synergism assay of the reference strain CBS138 and isolate FFUL887. The remaining isolates are in Annex M.

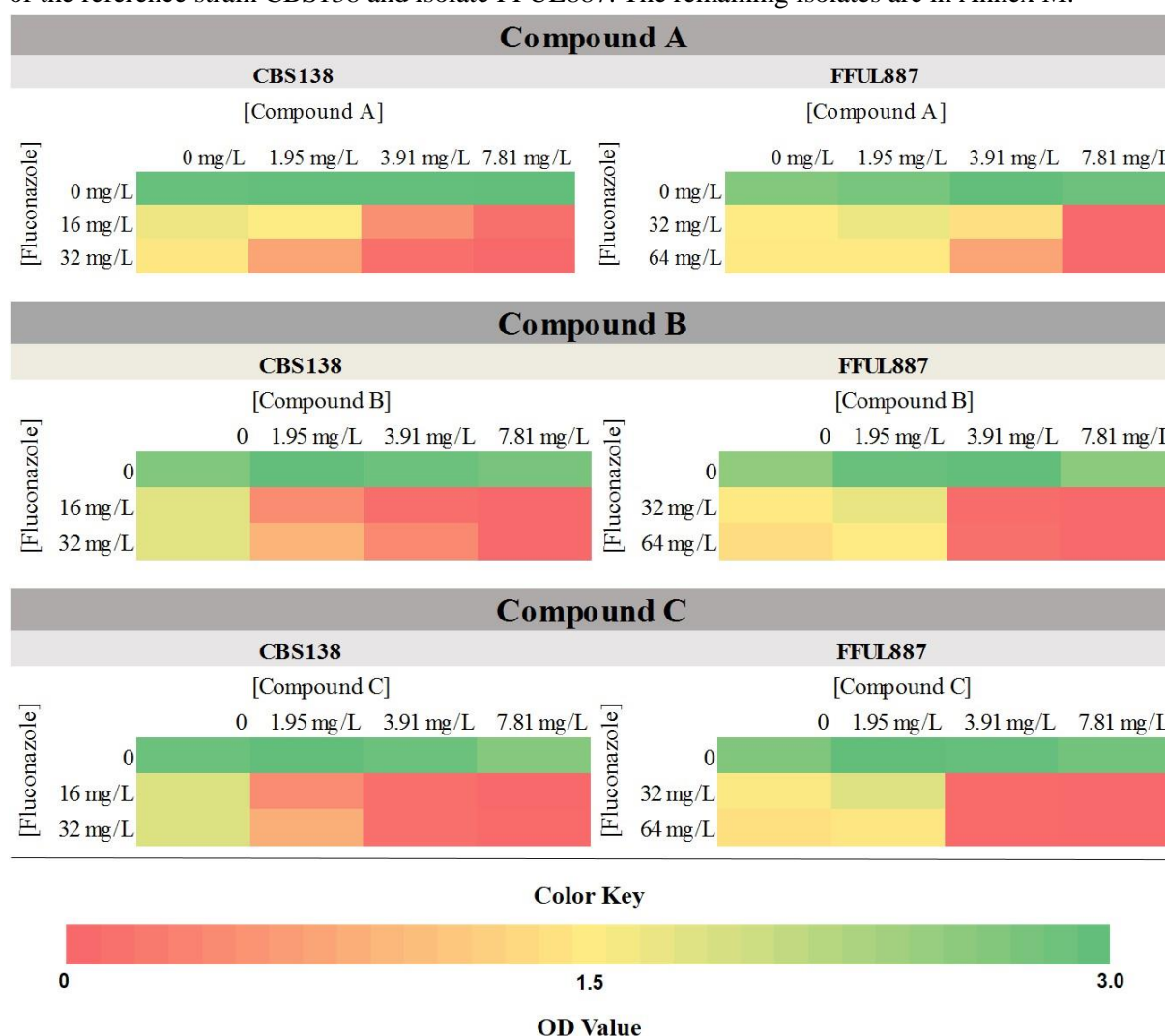


Figure 3.8: Heatmaps obtained in the synergism assay used to assess the potential of the synergistic effect of fluconazole and camphorimine compound A, B and C. Darker green means a larger growth and red a greater inhibition.

To have a clearer view of the data obtained that shows the synergistic effect of the compounds, in Figure 3.9, Figure 3.10 and Figure 3.11 are shown the results obtained after 24 h of growth in the different conditions, that is, in the presence of compound only, in the presence of fluconazole only in two different concentration or in the presence of the two drugs together.

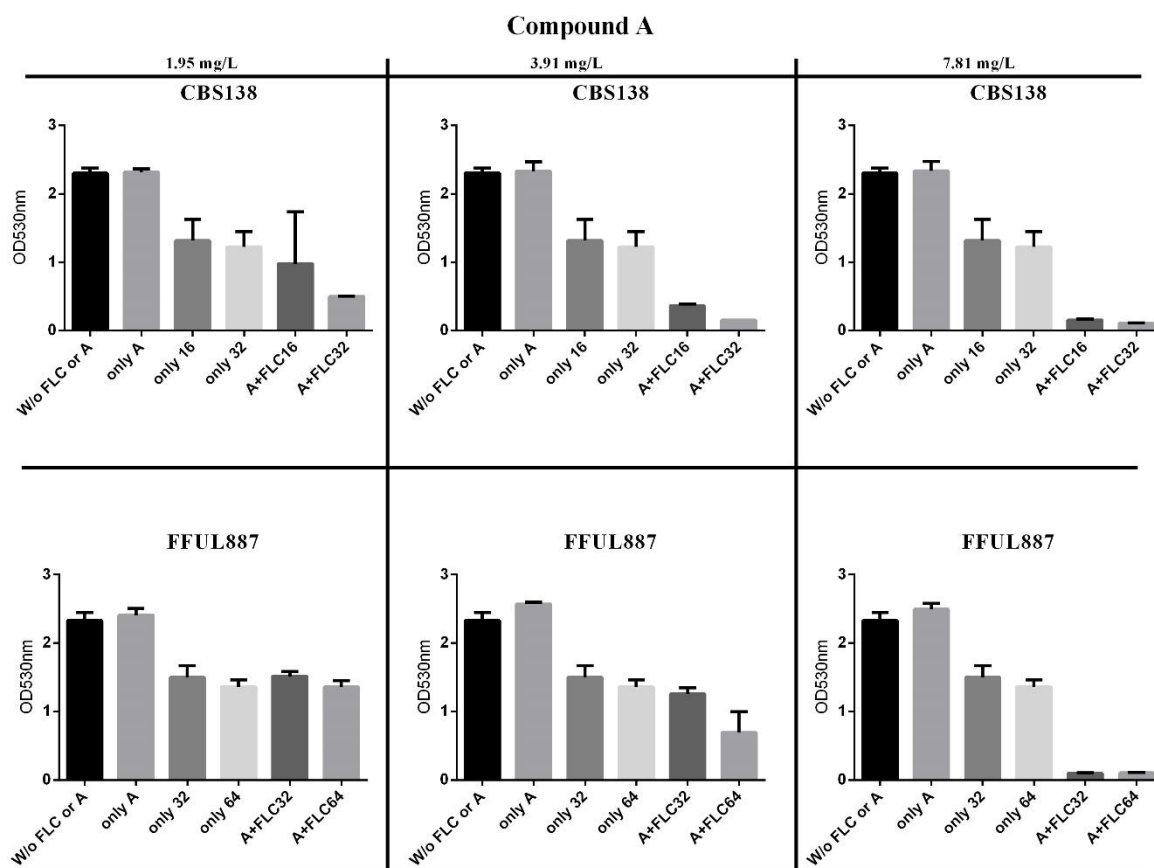


Figure 3.9: Graphic representation of the ODs obtained in the assays to assess the effects of the potential synergistic combination of compound A and fluconazole against *C. glabrata* strains. In the graphic is represented a control column (w/o FLC or A) with the growth medium without stress, or the medium supplemented only with compound A (only A), or with the concentration of the breakpoint value (32 mg/L for CBS138 (only 32) and 64 mg/L for the resistant isolates (only 64)), and one concentration below (16 mg/L for CBS138 (only 16) and 32 mg/L for the resistant isolates (only 32)) and at last a combination of the compound plus each one of the concentrations of fluconazole. Three non-inhibitory concentrations of the compound was used, 1.95 mg/L, 3.91 mg/L and 7.81 mg/L.

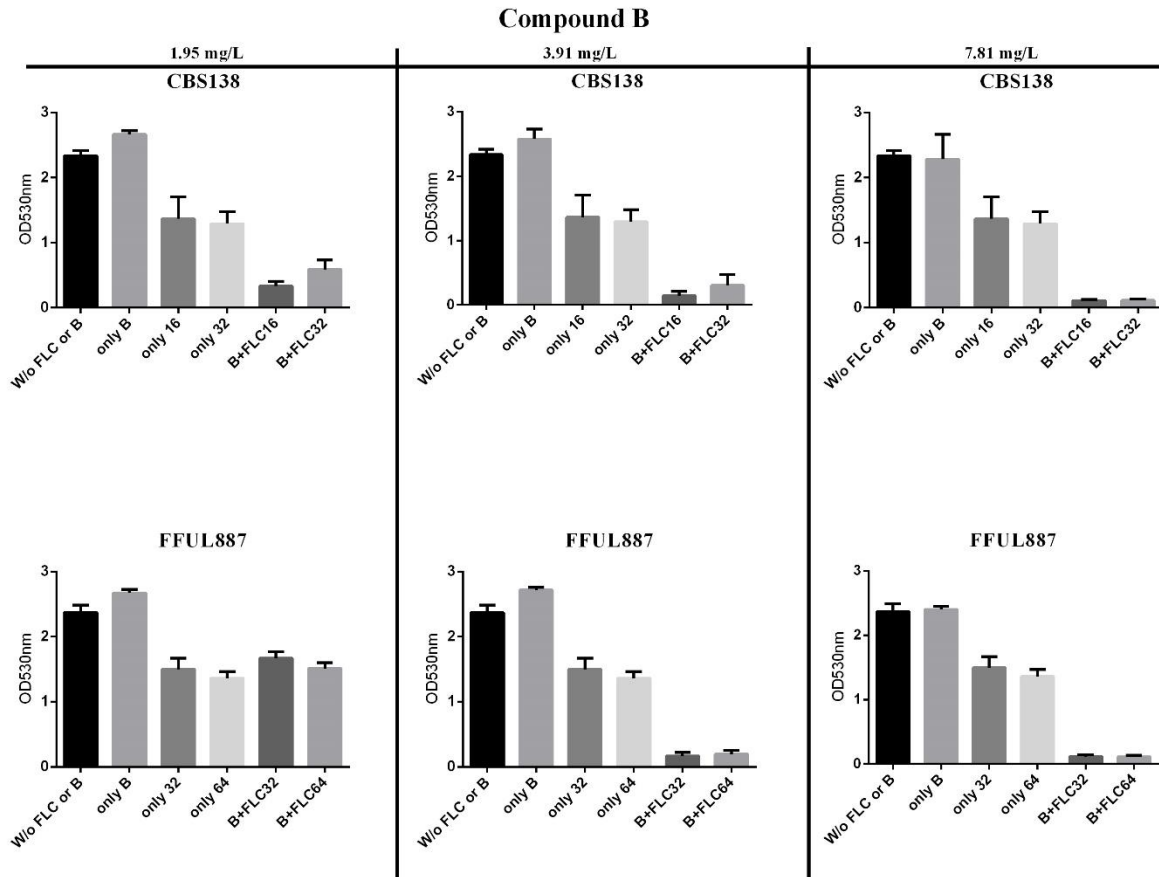


Figure 3.10: Graphic representation of the ODs obtained in the assays to assess the effects of the potential synergistic combination of compound B and fluconazole against *C. glabrata* strains. In the graphic is represented a control column (w/o FLC or B) with the growth medium without stress, or the medium supplemented only with compound B (only B), or with the concentration of the breakpoint value (32 mg/L for CBS138 (only 32) and 64 mg/L for the resistant isolate (only 64)), and one concentration below (16 mg/L for CBS138 (only 16) and 32 mg/L for the resistant isolate (only 32)) and at last a combination of the compound plus each one of the concentrations of fluconazole. Three non-inhibitory concentrations of the compound was used, 7.81 mg/L, 3.91 mg/L and 1.95 mg/L.

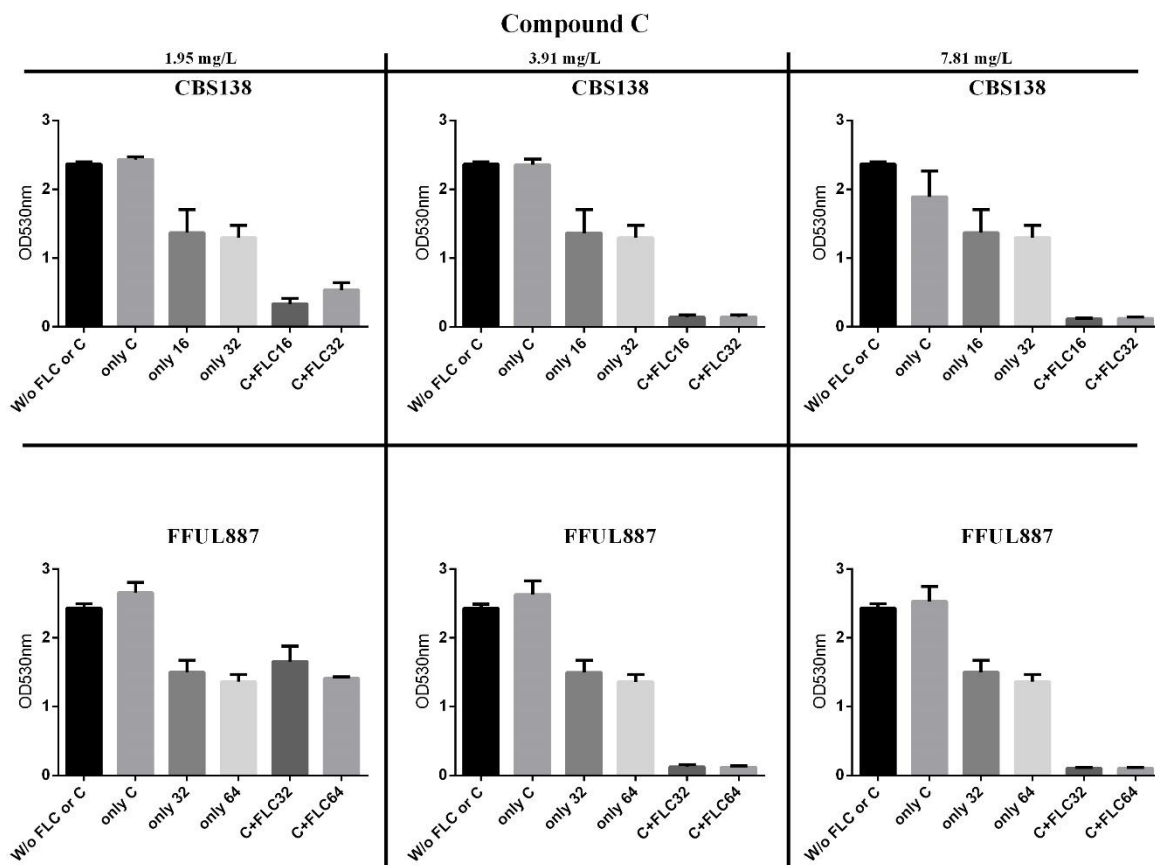


Figure 3.11: Graphic representation of the ODs obtained in the assays to assess the effects of the potential synergistic combination of compound C and fluconazole against *C. glabrata* strains. In the graphic is represented a control column (w/o FLC or C) with the growth medium without stress, or the medium supplemented only with compound C (only C), or with the concentration of the breakpoint value (32 mg/L for CBS138 (only 32) and 64 mg/L for the resistant isolate (only 64)), and one concentration below (16 mg/L for CBS138 (only 16) and 32 mg/L for the resistant isolate (only 32)) and at last a combination of the compound plus each one of the concentrations of fluconazole. Three non-inhibitory concentrations of the compound was used, 7.81 mg/L, 3.91 mg/L and 1.95 mg/L.

3.2.3. The synergistic effect between Ag(I)-camphorimine complexes and fluconazole does not result from increased accumulation of the azole inside *C. glabrata* cells

One possible reason underlying the synergistic combination of Ag(I)-camphorimines and fluconazole against *C. glabrata* could result from increased intracellular concentration of fluconazole inside the cells potentiated by the Ag(I)-based drugs. To test that, the internal concentration of [^3H]-fluconazole was monitored when *C. glabrata* CBS138 cells were cultivated in the presence of cold fluconazole (32 mg/L) and of a selected concentration (3.91 mg/L, a concentration at which the existence of a synergistic effect was already observed, Figure 3.9) of chemical A. The cells used to perform this assay were cultivated in RPMI growth medium (at pH 7.0) until mid-exponential phase ($\text{OD}_{600 \text{ nm}} = 0.8 \pm 0.05$).

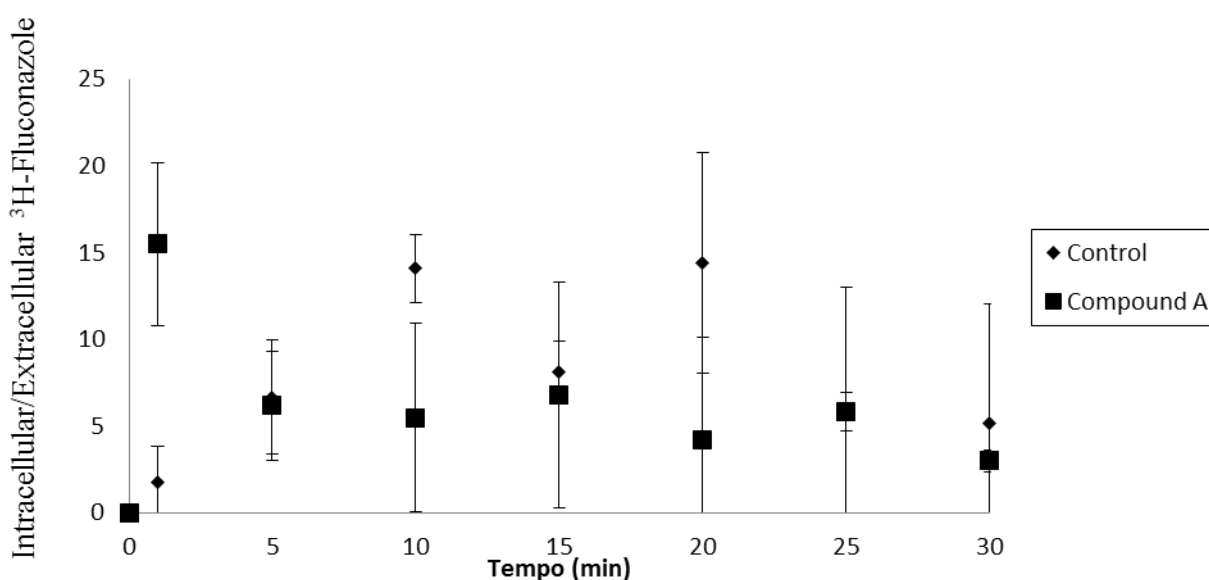


Figure 3.12: Intracellular accumulation of fluconazole inside *Candida glabrata* cells potentiated by the Ag(I)-based drugs. *Candida glabrata* cells don't accumulate more fluconazole intracellular with the RPMI supplemented with camphorimine compound than cells without the supplementation. The results obtained were representative of, at least, three independent experiments.

4. Discussion and Future Perspectives

In this work it was examined in detail the *CgPDR1* alleles encoded by various *C. glabrata* clinical isolates exhibiting increased resistance to fluconazole and voriconazole aiming to identify new GOF variants. A multitude of point mutations have been shown to result in CgPdr1 GOF variants, leading to the constitutive activation of this transcriptional regulator and, consequently, to azole resistance. The identification of these point mutations that result in *CgPDR1* hyperactivity is essential for a rapid diagnostic of patients undergoing at risk of developing an azole-resistant infection prompted by *C. glabrata*. The point substitutions identified in *CgPDR1* until so far were observed to occur throughout various domains of the protein including near the inhibitory domain, in the FSTFD (Fungus-specific transcription factor Domain) and also in the activation domain (Figure 4.1A). The result of the comparison of the sequence of *CgPDR1* in the different isolates resulted in the identification of two substitutions that emerged as prominent candidates to be new GOF variants of CgPdr1, R35K and I392M, the first located in the DNA-binding Domain of the protein (located between residues 26 – 59) while the second is located in the regulatory domain (located between residues 322 – 465) (Figure 4.1B).

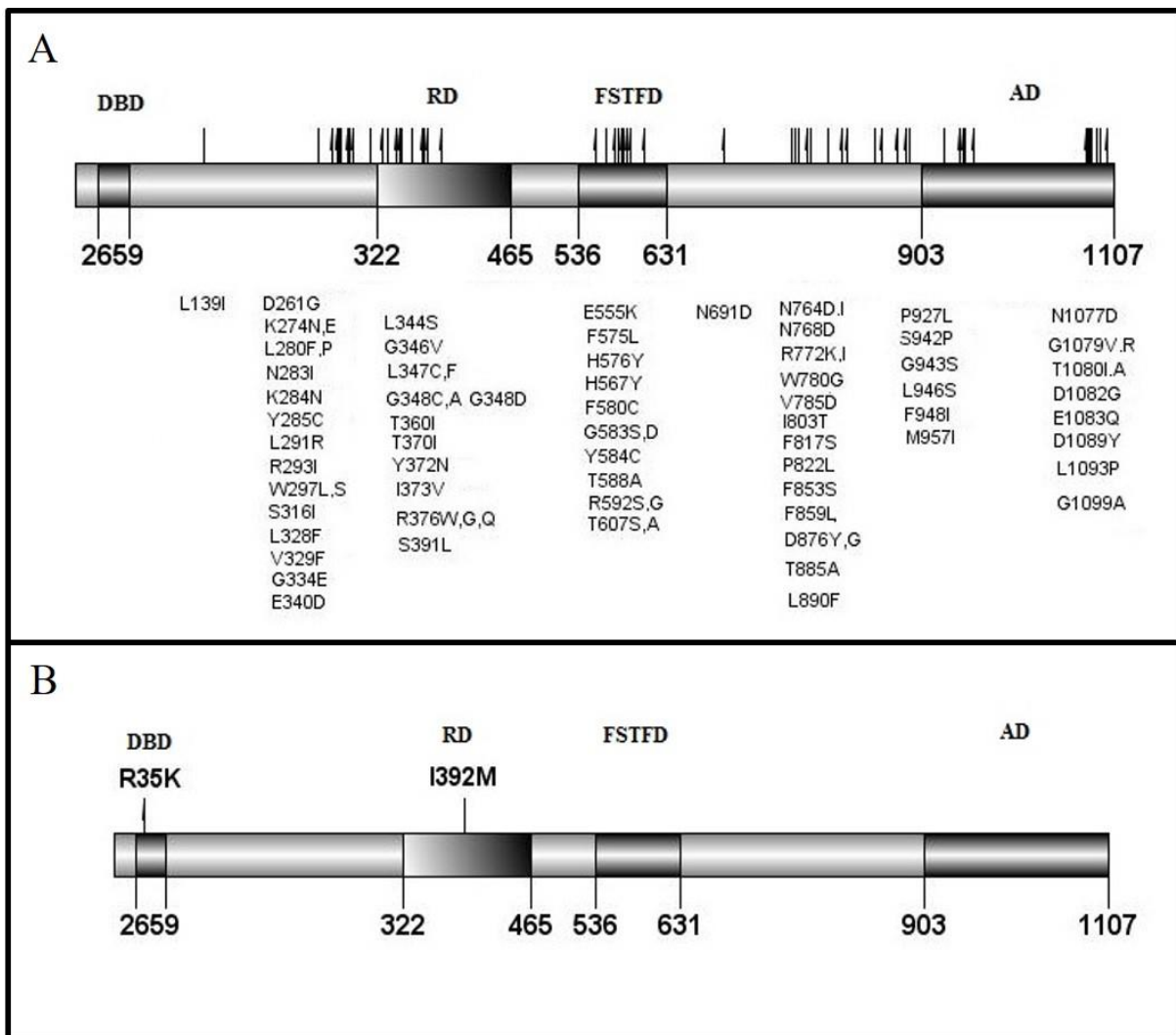


Figure 4.1: Described GOF mutations and two aminoacid substitutions candidates to be new GOF variants of CgPdr1. A - Location of the described *C. glabrata* PDR1 GOF mutations B – Location of the R35K and I392M replacement

candidates to be new GOF variants of CgPdr1. The domains shown were based on the homology between *S. cerevisiae* Pdr1p and CgPdr1p retrieved from Tsai, H., et al., 2010⁷⁰. DBD – DNA-binding domain; RD – Regulatory Domain; FSTFD – Fungus-specific Transcription factor Domain; AD – Activation Domain.

In ScPdr1 the regulatory domain inhibits activity of the regulator¹⁰³ and it was also found to include the xenobiotic binding domain, which is responsible for activation of the protein upon drug-binding⁷⁷. Alterations in this regulatory domain of CgPdr1 can result in gain-of-function mutations by counteracting the negative action of the regulatory domain or by altering the binding of the drugs to the protein, eventually bypassing the need of drug-binding to promote activation. The results obtained with the profiling of the expression of *CgPUP1* and *CgCDR1* in the isolates harboring the *CgPDR1* I392M allele (FFUL412 and FFUL443) show up-regulation of these two genes, supporting the idea that indeed this could correspond to a new gain-of-function CgPdr1 variant. Nevertheless, the result obtained is not totally clear since the up-regulation of *CgPUP1* was mild and below the one registered in isolates FFUL830 and FFUL878, which encode already described CgPdr1 GOF variants. In this sense, it will be relevant to extend the analysis of the expression of other CgPdr1 targets in isolates FFUL412 and FFUL443 as well as to conclude the cloning experiments performed to fully determine the relevance of the I392M replacement in constitutively activating *CgPDR1*. As for the R35K substitution, the results of the transcript profiling of genes *CgCDR1* and *CgPUP1* in isolate FFUL866 show a prominent and significant up-regulation of *CgPUP1*, while in the case of *CgCDR1* it was observed a consistent up-regulation of the gene in all the replicas performed albeit the registered level of variation showed a significant variation (resulting in a large standard deviation). Either way, the consistent up-regulation of the two genes points to the R35K indeed corresponding to a GOF mutation, something that needs to be further confirmed with the planned expression of this variant in an azole-susceptible strain. The R35K replacement occurs in the DNA-binding Domain of CgPdr1 which is responsible for binding of the regulator to the DNA motif PDRE found in the promoter region of target genes⁷⁵. It is not clear how an alteration in the DNA binding domain of CgPdr1 could promote constitutive activation of this regulator since up to now all described GOF mutations were located outside this domain. Further studies are required to better understand how this replacement may affect binding of CgPdr1 to its target sequence and the interaction with the transcriptional machinery.

In this work it was also deepened the study concerning the activity of Ag(I) camphorimine compounds against *C. glabrata*, by demonstrating the potential of these compounds in inhibiting growth of this pathogenic yeast specially in near-neutral conditions⁸⁷. Interestingly, it was observed a much stronger effect of these Ag(I)-based compounds in neutral growth medium than in mild acidic (pH~5) conditions. The evidences gathered in this work show that this effect cannot be attributable to an artifact caused by the type of buffering agent used as the same profile was obtained using different buffers and even when the pH of the medium was adjusted using strong acids or bases. It therefore seems that a more neutral pH favors the toxic action of the drug. One hypothesis that could explain these results is the higher capability of the drug to enter the yeast cells since in a higher pH the compound is expected to be more lipophilic as the result of the smaller protonation of nitrogens. A better understand on the mechanistic action of how Ag(I)-based chemicals affect the overall *C. glabrata* physiology will shed light into this matter. Of notice was the fact that these chemicals were able to sensitize azole-resistant strains (including those harboring CgPdr1 variants) and synergize with fluconazole, two results that may have a strong impact in the treatment of patients infected with azole-resistant strains. These two results and also the fact that *CgPDR1* and its regulated target gene, *CgCDR1*, are dispensable for *C. glabrata* tolerance to Ag(I)-based chemicals, strongly suggest that the mechanism of action of these compounds and of azoles are largely different. In particular, it is relevant the demonstration that the drug-efflux pump CgCdr1, that demonstrate to catalyze the extrusion of a number of structurally unrelated chemicals, plays no role in protecting *C. glabrata* cells against Ag(I)-based chemicals. Up to now the deleterious effects of Ag(I) or of Ag(I)-derived chemicals in *C. glabrata* have been poorly studied and were mostly performed addressing the use of nanoparticles. For AgNPs it was demonstrat-

ed their potent effect in inhibiting hyphae formation, changing cell surface by leading to the formation of “pits” or pores on the cell surface and/or affecting cell wall structure ^{87 104 105}. Additional studies have to be performed to better understand how Ag(I)-camphorimine complexes interact with *C. glabrata* in order to foster the implementation of these chemicals as a possible treatment of candidiasis. It will also be required to obtain information on the toxicity of these chemicals against mammals, both at local and systemic level.

The increasing emergence of azole-resistance among *C. glabrata* demands the development of more rapid diagnostic tools able to identify, in a fast and high-throughput manner, patients that could be colonized by azole-resistant strains and therefore require other therapeutics. Furthermore, it is also required the development of new antifungals focused on biological targets other than those that are targeted by azoles. The work presented in this thesis provides a contribution in both these two fields, either by expanding the knowledge on the panoply of CgPdr1 variants, as well as by providing evidences on the efficacy of Ag(I)-camphorimine complexes as anti-*Candida* agents (either alone or in combination with fluconazole). Considering that delayed diagnosis of drug-resistant strains and subsequent fine-tuning of the treatment is one of the factors with a stronger impact in determining the death rate of patients infected with candidiasis, the knowledge gathered is therefore of significance to improve the success of current strategies used in the treatment of candidiasis.

References

1. Fidel, P. L., Vazquez, J. A. & Sobel, J. D. *Candida glabrata*: Review of epidemiology, pathogenesis, and clinical disease with comparison to *C. albicans*. *Clin. Microbiol. Rev.* **12**, 80–96 (1999).
2. Brunke, S. & Hube, B. Two unlike cousins: *Candida albicans* and *Candida glabrata* infection strategies. *Cell. Microbiol.* **15**, 701–708 (2013).
3. Emri, T., Majoros, L., Tóth, V. & Pócsi, I. Echinocandins: production and applications. *Appl. Microbiol. Biotechnol.* **97**, 3267–3284 (2013).
4. Wisplinghoff, H., Bischoff, T., Tallent, S., Seifert, H., Wenzel, R. & Edmond M. Nosocomial bloodstream infections in US hospitals: Analysis of 24,179 cases from a prospective nationwide surveillance study. *Clin. Infect. Dis.* **39**, 309–17 (2004).
5. Costa-De-Oliveira, S., Pina-Vaz, C., Mendonça, D. & Rodrigues, A. A first Portuguese epidemiological survey of fungaemia in a university hospital. *Eur. J. Clin. Microbiol. Infect. Dis.* **27**, 365–374 (2008).
6. Shorr, F., Gupta, V., Sun, X., Johannes, R., Spalding, J. & Tabak, Y. Burden of early-onset candidemia: Analysis of culture-positive bloodstream infections from a large U.S. database. *Crit. Care Med.* **37**, 2519–2526; (2009).
7. Sofair, A., Lyon, G., Huie-White, S., Reiss, E., Harrison, L., Sanza, L., Arthington-Skaggs, B. & Fridkin, S. Epidemiology of Community-Onset Candidemia in Connecticut and Maryland. *Clin. Infect. Dis.* **43**, 32–9 (2006).
8. Castanheira, M., Messer, S. A., Jones, R. N., Farrell, D. J. & Pfaller, M. A. Activity of echinocandins and triazoles against a contemporary (2012) worldwide collection of yeast and moulds collected from invasive infections. *Int. J. Antimicrob. Agents* **44**, 320–326 (2014).
9. Paulo, C., Mourão, C., Veiga, P., Marques, J., Rocha, G., Alves, A., Querol, A., Meliço-Silvestre, A., Gonçalves, I., Flores, O., Clemente, C. & Gonçalves, T. Retrospective analysis of clinical yeast isolates in a hospital in the centre of Portugal: spectrum and revision of the identification procedures. *Med. Mycol.* **47**, 836–844 (2009).
10. Moran, C., Grussemeyer, A. Spalding, J. R., Benjamin, D. K. & Reed, S. D. Comparison of Costs, Length of stay, and Mortality Associated with *Candida glabrata* and *Candida albicans* Bloodstream Infections. *Am J Infect Control* **38**, 78–80 (2010).
11. Klevay, M., Ernst, E., Hollanbaugh J., Miller, J., Pfaller, M. & Diekema, D. Therapy and outcome of *Candida glabrata* versus *Candida albicans* bloodstream infection. *Diagn. Microbiol. Infect. Dis.* **60**, 273–277 (2008).
12. Faria-Ramos, I., Tavares, P. R., Farinha, S., Neves-Maia, J., Miranda, I. M., Silva, R. M., Estevinho, L. M., Pina-Vaz, C. & Rodrigues, A. G. Environmental azole fungicide, prochloraz, can induce cross-resistance to medical triazoles in *Candida glabrata*. *FEMS Yeast Res.* **14**, 1119–1123 (2014).
13. Pfaller, M. A., Messer, S. A., Woosley, L. N., Jones, R. N. & Castanheira, M. Echinocandin and triazole antifungal susceptibility profiles for clinical opportunistic yeast and mold isolates collected from 2010 to 2011: Application of new CLSI clinical breakpoints and epidemiological cutoff values for characterization of geographic. *J. Clin. Microbiol.* **51**, 2571–2581 (2013).
14. Borst, A., Raimer, M. T., Warnock, D. W., Morrison, C. J. & Arthington-Skaggs, B. A. Rapid acquisition of stable azole resistance by *Candida glabrata* isolates obtained before the clinical introduction of fluconazole. *Antimicrob. Agents Chemother.* **49**, 783–787 (2005).
15. Arendrup, M. C. *Candida* and Candidaemia: Susceptibility and epidemiology. *Danish Medical Journal* **60**, (2013).
16. Pfaller, M., Boyken, L., Hollis, R., Kroeger, J., Messer, S., Tendolkar, S. & Diekema, D. Use

- of epidemiological cutoff values to examine 9-year trends in susceptibility of *Candida* species to anidulafungin, caspofungin, and micafungin. *J. Clin. Microbiol.* **49**, 624–629 (2011).
17. Sharma, P., Kumar, D., Mahajan, G. & Mintoo, M. J. Complete update on antifungal therapy. *Int. J. Pharmacol. Pharm. Sci.* **3**, 1–9 (2016).
 18. Lupetti, A., Danesi, R., Campa, M., Tacca, M. D. & Kelly, S. Molecular basis of resistance to azole antifungals. *Trends Mol. Med.* **8**, 76–81 (2002).
 19. Cowen, L. E. The evolution of fungal drug resistance: modulating the trajectory from genotype to phenotype. *Nat. Rev. Microbiol.* **6**, 187–198 (2008).
 20. Kathiravan, M. K. Salake, A. B., Chothe, A. S., Dudhe, P. B., Watode, R. P., Mukta, M. S. & Gadhwane, S. The biology and chemistry of antifungal agents: A review. *Bioorganic Med. Chem.* **20**, 5678–5698 (2012).
 21. Odds, F. C., Brown, A. J. P. & Gow, N. A. R. Antifungal agents: Mechanisms of action. *Trends Microbiol.* **11**, 272–279 (2003).
 22. Bosscheff, H. V., Koymans, L. & Moereels, H. P450 Inhibitors of use in medical treatment: Focus on mechanisms of action. *Pharmac. Ther.* **67**, 79–100 (1995).
 23. Kelly, S. L., Lamb, D. C., Kelly, D. E., Manning, N. J., Loeffler, J., Hebart, H., Schumacher, U. & Einsele, H. Resistance to fluconazole and cross-resistance to amphotericin B in *Candida albicans* from AIDS patients caused by defective sterol $\Delta 5,6$ -desaturation. *FEBS Lett.* **400**, 80–82 (1997).
 24. White, T. C., Marr, K. A. & Bowden, R. A. Clinical, cellular, and molecular factors that contribute to antifungal drug resistance. *Clin. Microbiol. Rev.* **11**, 382–402 (1998).
 25. Beule, K. D. & Gestel, J. V. Pharmacology of itraconazole. *Drugs* **61 Suppl 1**, 27–37 (2001).
 26. Mast, N., Zheng, W., Stout, C. D. & Pikuleva, I. A. Antifungal Azoles: Structural insights into undesired tight binding to cholesterol-metabolizing CYP46A1. *Mol. Pharmacol.* **84**, 86–94 (2013).
 27. Snell, S. B., Foster, T. H. & Haidaris, C. G. Miconazole induces fungistasis and increases killing of *Candida albicans* subjected to photodynamic Therapy. *Photochem Photobiol.* **88**, 596–603 (2012).
 28. Whaley, S. G. & Rogers, P. D. Azole Resistance in *Candida glabrata*. *Curr. Infect. Dis. Rep.* **18**, 19–21 (2016).
 29. Sanguinetti, M., Posteraro, B., Fiori, B., Ranno, S., Torelli, R. & Fadda, G. Mechanisms of azole resistance in clinical isolates of *Candida glabrata* collected during a hospital survey of antifungal resistance. *Antimicrob. Agents Chemother.* **49**, 668–679 (2005).
 30. Szweda, P., Gucwa, K., Romanowska, E., Dzierzanowska-Fangrat, K., Naumiuk, L., Brilowaska-Dabrowaska, A., Wojciechowaska-Koszko, I. & Milewaski, Stawomir. Mechanisms of azole resistance among clinical isolates of *Candida glabrata* in Poland. *J. Med. Microbiol.* **64**, 610–619 (2015).
 31. Hull, C. M., Parker, J. E., Bader, O., Weig, M., Gross, U., Warrilow, A. G. S., Kelly, D. E. & Kelly, S. L. Facultative sterol uptake in an ergosterol-deficient clinical isolate of *Candida glabrata* harboring a missense mutation in ERG11 and exhibiting cross-resistance to azoles and amphotericin B. *Antimicrob. Agents Chemother.* **56**, 4223–4232 (2012).
 32. Nakayama, H., Izuta, M., Nakayama, N., Arisawa, M. & Aoki, Y. Depletion of the squalene synthase (ERG9) gene does not impair growth of *Candida glabrata* in mice. *Antimicrob. Agents Chemother.* **44**, 2411–2418 (2000).
 33. Henry, K. W., Nickels, J. T. & Edlind, T. D. Upregulation of ERG genes in *Candida* species by azoles and other sterol biosynthesis inhibitors. *Antimicrob. Agents Chemother.* **44**, 2693–2700 (2000).
 34. Akins, R. A. An update on antifungal targets and mechanisms of resistance in *Candida albicans*. *Med. Mycol.* **43**, 285–318 (2005).
 35. Bard, M., Sturm, A. M., Pierson, C. A., Brown, S., Rogers, K. M., Nabinger, S., Eckstein, J.,

- Barbuch, R., Lees, N. D., Howell, S. A. & Hazen, K. C. Sterol uptake in *Candida glabrata*: Rescue of sterol auxotrophic strains. *Diagn. Microbiol. Infect. Dis.* **52**, 285–293 (2005).
36. Nakayama, H., Tanabe, K., Bard, M., Hodgson, W., Wu, S., Takemori, D., Aoyama, T., Kumaraswami, S. N., Metzler, L., Takano, Y., Chibana, H. & Niimi, M. The *Candida glabrata* putative sterol transporter gene CgAUS1 protects cells against azoles in the presence of serum. *J. Antimicrob. Chemother.* **60**, 1264–1272 (2007).
 37. Nagi, M., Tanabe, K., Nakayama, H., Yamagoe, S., Umeyama, T., Oura, T., Ohno, H., Kajiwara, S. & Miyazaki, Y. Serum cholesterol promotes the growth of *Candida glabrata* in the presence of fluconazole. *J. Infect. Chemother.* **19**, 138–143 (2013).
 38. Inukai, T., Nagi, M., Morita, A., Tanabe, K., Aoyama, T., Miyazaki, Y., Bard, M. & Nakayama, H. The mannoprotein TIR3 (CAGL0C03872g) is required for sterol uptake in *Candida glabrata*. *Biochim. Biophys. Acta - Mol. Cell Biol. Lipids* **1851**, 141–151 (2015).
 39. Nagi, M., Nakayama, H., Tanabe, K., Bard, M., Aoyama, T., Okano, M., Higashi, S., Ueno, K., Chibana, H., Niimi, M., Yamagoe, S., Umeyama, T., Kajiwara, S., Ohno, H. & Miyazaki, Y. Transcription factors CgUPC2A and CgUPC2B regulate ergosterol biosynthetic genes in *Candida glabrata*. *Genes to Cells* **16**, 80–89 (2011).
 40. Lyons, C. N. & White, T. C. Transcriptional analyses of antifungal drug resistance in *Candida albicans*. *Antimicrob. Agents Chemother.* **44**, 2296–2303 (2000).
 41. Sanglard, D., Ischer, F., Calabrese, D., Majcherczyk, P. a & Bille, J. The ATP binding cassette transporter gene CgCDR1 from *Candida glabrata* is involved in the resistance of clinical isolates to azole antifungal agents. *Antimicrob. Agents Chemother.* **43**, 2753–2765 (1999).
 42. Vermitsky, J. P. & Edlind, T. D. Azole Resistance in *Candida glabrata*: Coordinate upregulation of multidrug transporters and evidence for a Pdr1-Like transcription factor. *Am. Soc. Microbiol.* **48**, 3773–3781 (2004).
 43. Neji, S., Hadrich, I., Trabelsi, H., Abbes, S., Cheikhrouhou, F., Sellami, H., Makni, F. & Ayadi, A. Virulence factors, antifungal susceptibility and molecular mechanisms of azole resistance among *Candida parapsilosis* complex isolates recovered from clinical specimens. *Journal Biomed. Sci.* **24**, 1–16 (2017).
 44. Sanglard, D., Kuchler, K., Ischer, F., Pagani, J. L., Monod, M. & Bille, J. Mechanisms of resistance to azole antifungal agents in *Candida albicans* isolates from AIDS patients involve specific multidrug transporters. *Antimicrob. Agents Chemother.* **39**, 2378–2386 (1995).
 45. Zhang, J. Y., Liu, J. H., Liu, F. D., Xia, Y. H., Wang, J., Liu, X., Zhang, Z. Q., Zhu, N. Y., Ying, Y. & Huang, X. T. Vulvovaginal candidiasis: Species distribution, fluconazole resistance and drug efflux pump gene overexpression. *Mycoses* **57**, 584–591 (2014).
 46. Izumikawa, K., Kakeya, H., Tsai, H. F., Grimberg, B. & Bennett, J. E. Function of *Candida glabrata* ABC transporter gene, PDH1. *Yeast* **20**, 249–261 (2003).
 47. Torelli, R., Posteraro, B., Ferrari, S., Sorda, M., Fadda, G., Sanglard, D. & Sanguinetti, M. The ATP-binding cassette transporter-encoding gene CgSNQ2 is contributing to the CgPDR1-dependent azole resistance of *Candida glabrata*. *Mol. Microbiol.* **68**, 186–201 (2008).
 48. Cannon, R. D., Lamping, E., Holmes, A. R., Niimi, K., Baret, P. V., Keniya, M. V., Tanabe, K., Niimi, M., Goffeau, A. & Monk, B. C. Efflux-Mediated Antifungal Drug Resistance. *Clin. Microbiol. Rev.* **22**, 291–321 (2009).
 49. Costa, C., Pires, C., Cabrito, T. R., Renaudin, A., Ohno, M., Chibana, H., Sá-Correia, I. & Teixeira, M. C. *Candida glabrata* drug: H⁺ antiporter CgQdr2 confers imidazole drug resistance, being activated by transcription factor CgPdr1. *Antimicrob. Agents Chemother.* **57**, 3159–3167 (2013).
 50. Costa, C., Henriques, A., Pires, C., Nunes, J., Ohno, M., Chibana, H., Sá-Correia, I. & Teixeira, M. C. The dual role of *Candida glabrata* drug: H⁺ antiporter CgAqr1 (ORF CAGL0J09944g) in antifungal drug and acetic acid resistance. *Front. Microbiol.* **4**, 1–13 (2013).

51. Costa, C., Dias, P. J., Sá-correia, I. & Teixeira, M. C. MFS multidrug transporters in pathogenic fungi: do they have real clinical impact? *Front. Microbiol.* **5**, 1–8 (2014).
52. Pais, P., Costa, C., Pires, C., Shimizu, K., Chibana, H. & Teixeira, M. C. Membrane Proteome-Wide Response to the Antifungal Drug Clotrimazole in *Candida glabrata*: Role of the Transcription Factor CgPdr1 and the Drug: H⁺ Antiporters CgTpo1_1 and CgTpo1_2. *Mol. Cell. Proteomics* **15**(1), 57–72 (2015).
53. Costa, C., Nunes, J., Henriques, A., Mira, N. P., Nakayama, H., Chibana, H. & Teixeira, M. C. *Candida glabrata* drug: H⁺ antiporter CgTpo3 (ORF CAGL0I10384g): role in azole drug resistance and polyamine homeostasis. *Journal Antimicrob. Chemother.* **69**, 1767–1776 (2014).
54. Costa, C., Ribeiro, J. M., Miranda, I., Silva-Dias, A., Cavalheiro, M., Costa-de-oliveira, S., Rodrigues, A. G., Teixeira, M. C. Clotrimazole drug resistance in *Candida glabrata* clinical isolates correlates with increased expression of the drug: H⁺ antiporters CgAqr1, CgTpo1_1, CgTpo3, and CgQdr2. *Front. Microbiol.* **7**, 1–11 (2016).
55. Healey, K. R., Zhao, Y., Perez, W. B., Lockhart, S. R., Sobel, J. D., Farmakiotis, D., Kontoyiannis, D. P., Sanglard, D., Taj-Aldeen, S. J., Alexander, B. D., Jimenez-Ortigosa, C., Shor, E. & Perlin, D. S. Prevalent mutator genotype identified in fungal pathogen *Candida glabrata* promotes multi-drug resistance. *Nat. Commun.* **7**, 1–10 (2016).
56. Dellière, S., Healey, K., Gits-muselli, M., Carrara, B., Barbaro, A., Guigue, N., Lecefel, C., Touratier, S., Desnos-ollivier, M., Perlin, D. S., Bretagne, S. & Alanio, A. Fluconazole and echinocandin resistance of *Candida glabrata* correlates better with antifungal drug exposure rather than with MSH2 mutator genotype in a French cohort of patients harboring low rates of resistance. *Front. Microbiol.* **7**, 1–9 (2016).
57. Healey, K. R., Ortigosa, C. J., Shor, E. & Perlin, D. S. Genetic drivers of multidrug resistance in *Candida glabrata*. *Front. Microbiol.* **7**, 1–9 (2016).
58. Balzi, E., Chen, W., Ulaszewski, S., Capieaux, E. & Goffeau, A. The multidrug resistance gene PDR1 from *Saccharomyces cerevisiae*. *J. Biol. Chem.* **262**, 16871–16879 (1987).
59. Katzmann, D. J., Hallstrom, T. C., Mahe, Y. & Moye-rowley, W. S. Multiple Pdr1p/Pdr3p binding sites are essential for normal expression of the ATP binding cassette transporter protein-encoding gene *PDR5*. *J. Biol. Chem.* **271**, 23049–23054 (1996).
60. Adelaide, M., Jonniaux, J., Balzi, E., Goffeau, A. & Hazel, B. Van Den. Novel target genes of the yeast regulator Pdr1p: a contribution of the *TPO1* gene in resistance to quinidine and other drugs. *Gene* **272**, 111–119 (2001).
61. Fernandes, A. R., Mira, N. P., Vargas, R. C., Canelhas, I. & Sá-Correia, I. *Saccharomyces cerevisiae* adaptation to weak acids involves the transcription factor Haa1p and Haa1p-regulated genes. *Biochem. Biophys. Res. Commun.* **337**, 95–103 (2005).
62. Katzmann, D. J., Burnett, P. E., Golin, J., Mahé, Y. & Moye-Rowley, W. S. Transcriptional control of the yeast *PDR5* gene by the *PDR3* gene product. *Mol. Cell. Biol.* **14**, 4653–4661 (1994).
63. Servos, J., Haase, E. & Brendel, M. Gene SNQ2 of *Saccharomyces cerevisiae*, which confers resistance to 4-nitroquinoline-N-oxide and other chemicals, encodes a 169 kDa protein homologous to ATP-dependent permeases. *Mol. Gen. Genet.* **236**, 214–218 (1993).
64. Katzmann, D. J., Hallstrom, T. C., Voet, M., Wysock, W., Golin, J., Volckaert, G. & Moye-rowley, W. S. Expression of an ATP-binding cassette transporter-encoding gene (*YOR1*) is required for oligomycin resistance in *Saccharomyces cerevisiae*. *Mol. Cell. Biol.* **15**, 6875–6883 (1995).
65. Rogers, B., Decottignies, A., Kolaczowski, M. & Carvajal, E., Balzi, E. Goffeau, A. The pleiotropic drug ABC transporters from *Saccharomyces cerevisiae*. *Journal Mol. Microbiol. Biotechnol.* **3**, 207–214 (2001).
66. Delaveau, T., Delahodde, A., Carvajal, E., Subik, J. & Jacq, C. PDR3, a new yeast regulatory gene, is homologous to PDR1 and controls the multidrug resistance phenomenon. *Mol. Gen.*

- Genet.* **244**, 501–511 (1994).
67. Mamnun, Y. M., Pandjaitan, R., Mahé, Y., Delahodde, A. & Kuchler, K. The yeast zinc finger regulators Pdr1p and Pdr3p control pleiotropic drug resistance (PDR) as homo- and heterodimers in vivo. *Mol. Microbiol.* **46**, 1429–1440 (2002).
 68. Tsai, H., Krol, A. A., Sarti, K. E. & Bennett, J. E. *Candida glabrata* PDR1, a transcriptional regulator of a pleiotropic drug resistance network, mediates azole resistance in clinical isolates and petite mutants. *Antimicrob. Agents Chemother.* **50**, 1384–1392 (2006).
 69. Vermitsky, J., Earhart, K. D., Smith, W. L., Homayouni, R., Edlind, T. D. & Rogers, P. D. Pdr1 regulates multidrug resistance in *Candida glabrata*: gene disruption and genome-wide expression studies. *Mol. Microbiol.* **61**, 704–722 (2006).
 70. Tsai, H. F., Sammons, L. R., Zhang, X., Suffis, S. D., Su, Q., Myers, T. G., Marr, K. A. & Bennett, J. E. Microarray and molecular analyses of the azole resistance mechanism in *Candida glabrata* oropharyngeal isolates. *Antimicrob. Agents Chemother.* **54**, 3308–3317 (2010).
 71. Vale-silva, L. A., Moeckli, B., Torelli, R., Posteraro, B., Sanguinetti M. & Sanglard, D. Upregulation of the adhesin gene *EPA1* mediated by *PDR1* in *Candida glabrata* leads to enhanced host colonization. *mSphere* **1**, 1–16 (2016).
 72. Paul, S., Bair, T. B. & Moye-Rowley, W. S. Identification of genomic binding sites for *Candida glabrata* Pdr1 transcription factor in Wild-Type and p0 cells. *Antimicrob. Agents Chemother.* **58**, 6904–6912 (2014).
 73. Caudle, K. E., Barker, K. S., Wiederhold, N. P., Xu, L., Homayouni, R. & Rogers, P. D. Genomewide expression profile analysis of the *Candida glabrata* Pdr1 regulon. *Eukaryot. Cell* **10**, 373–383 (2011).
 74. Ferrari, S., Sanguinetti, M., Torelli, R., Posteraro, B. & Sanglard, D. Contribution of CgPDR1-regulated genes in enhanced virulence of azole-resistant *Candida glabrata*. *PLoS One* **6**, 1–16 (2011).
 75. MacPherson, S., Larochele, M. & Turcotte, B. A Fungal family of transcriptional regulators: the zinc cluster proteins. *Microbiol. Mol. Biol. Rev.* **70**, 583–604 (2006).
 76. Paul, S., Schmidt, J. A. & Moye-rowley, W. S. Regulation of the CgPdr1 transcription factor from the pathogen *Candida glabrata*. *Eukaryot. Cell* **10**, 187–197 (2011).
 77. Thakur, J. K., Arthanari, H., Yang, F., Pan, S., Fan, X., Breger, J., Frueh, D. P., Gulshan, K., Li, D. K., Mylonakis, E., Struhl, K., Moye-Rowley, W. S., Cormack, B. P., Wagner, G. & Näär, Anders M. A nuclear receptor-like pathway regulating multidrug resistance in fungi. *Nature* **452**, 604–609 (2008).
 78. Nishikawa, J. L., Boeszoermyeni, A., Vale-Silva, L. A., Torelli, R., Posteraro, B., Sohn, Y. Ji, F., Gelev, V., Sanglard, D., Sanguinetti, M., Sadreyev, R. I., Mukherjee, G., Bhyravabhotla, J., Buhrlage, S. J., Gray, N. S., Wagner, G., Näär, A. M. & Arthanari, H. Inhibiting fungal multidrug resistance by disrupting an activator-mediator interaction. *Nature* **530**, 485–489 (2016).
 79. Berila, N., Borecka, S., Dzugasova, V., Bojnansky, J. & Subik, J. Mutations in the CgPDR1 and CgERG11 genes in azole-resistant *Candida glabrata* clinical isolates from Slovakia. *Int. J. Antimicrob. Agents* **33**, 574–578 (2009).
 80. Ferrari, S., Ischer, F., Calabrese, D., Posteraro, B., Sanguinetti, M., Fadda, G., Rohde, B., Bauser, C., Bader, O. & Sanglard, D. Gain of function mutations in *CgPDR1* of *Candida glabrata* not only mediate antifungal resistance but also enhance virulence. *PLoS Pathog.* **5**, 1–17 (2009).
 81. Berila, N. & Subik, J. Molecular analysis of *Candida glabrata* clinical isolates. *Mycopathologia* **170**, 99–105 (2010).
 82. Vale-Silva, L. A. & Sanglard, D. Tipping the balance both ways: Drug resistance and virulence in *Candida glabrata*. *FEMS Yeast Res.* **15**, 1–8 (2015).

83. Garnaud, C., Botterel, F., Sertour, N., Bougnoux, M., Dannaoui, E., Larrat, S., Hennequin, C., Guinea, J., Cornet, M. & Maubon, D. Next-generation sequencing offers new insights into the resistance of *Candida* spp. to echinocandins and azoles. *J. Antimicrob. Chemother.* **70**, 2556–2565 (2015).
84. Katiyar, S., Shiffrin, E., Shelton, C., Healey, K., Vermitsky, J. & Edlind, T. Evaluation of polymorphic locus sequence typing for *Candida glabrata* epidemiology. *J. Clin. Microbiol.* **54**, 1042–1050 (2016).
85. Vale-Silva, L., Ischer, F., Leibundgut-Landmann, S. & Sanglard, D. Gain-of-function mutations in *PDR1*, a regulator of antifungal drug resistance in *Candida glabrata*, control adherence to host cells. *Infect. Immun.* **81**, 1709–1720 (2013).
86. Salazar, S. B. Genomic analysis of a *Candida glabrata* clinical isolate resistant to antifungals unveils novel features of drug resistance in this pathogenic yeast. MSc in Biotechnology. Instituto Superior Técnico (2015).
87. Cardoso, J. M. S., Guerreiro, S. I., Lourenço, A., Alves, M. M., Montemor, F., Mira, N. P., Leitão, J. H. & Carvalho, M. F. N. N. Ag(I) camphorimine complexes with antimicrobial activity towards clinically important bacteria and species of the *Candida* genus. *PLoS One* **12**, 1–15 (2017).
88. Cardoso, J. M. S., Galvão, A. M., Guerreiro, S. I., Leitão, J. H., Suarez, A. C., Carvalho, M. F. N. N. Antibacterial activity of silver camphorimine coordination polymers. *Dalt. Trans.* **45**, 7114–7123 (2016).
89. Klasen, H. J. A historical review of the use of silver in the treatment of burn. *Burns* **26**, 131–138 (2000).
90. Burrow, A., Eccles, R. & Jones, A. S. The effects of camphor, eucalyptus and menthol vapour on nasal resistance to airflow and nasal sensation. **96**, 157–161 (1983).
91. Chen, W., Vermaak, I. & Viljoen, A. Camphor-A fumigant during the black death and a coveted fragrant wood in ancient egypt and babylon-A review. *Molecules* **18**, 5434–5454 (2013).
92. Xu, H., Blair, N. T. & Clapham, D. E. Camphor activates and strongly desensitizes the transient receptor potential vanilloid subtype 1 channel in a vanilloid-independent mechanism. *J. Neurosci.* **25**, 8924–8937 (2005).
93. Sokolova, A. S., Yarovaya, O. I., Shernyukov, A. V., Gatilov, Y. V., Razumova, Y. V., Zarubaev, V. V., Tretiak, T. S., Pokrovsky, A. G., Kiselev, O. I. & Salakhutdinov, N. F. Discovery of a new class of antiviral compounds: Camphor imine derivatives. *Eur. J. Med. Chem.* **105**, 263–273 (2015).
94. Zarubaev, V. V., Garshinina, A. V., Tretiak, T. S., Fedorova, V. A., Shtro, A. A., Sokolova, A. S., Yarovaya, O. I. & Salakhutdinov, N. F. Broad range of inhibiting action of novel camphor-based compound with anti-hemagglutinin activity against influenza viruses in vitro and in vivo. *Antiviral Res.* **120**, 126–133 (2015).
95. Sokolova, A. S., Yarovaya, O. I., Korchagina, D. V., Zarubaev, V. V., Tretiak, T. S., Anfimov, P. M., Kiselev, O. I. & Salakhutdinov, N. F. Camphor-based symmetric diimines as inhibitors of influenza virus reproduction. *Bioorganic Med. Chem.* **22**, 2141–2148 (2014).
96. McRee, A. E. Therapeutic Review: Silver. *J. Exot. Pet Med.* **24**, 240–244 (2015).
97. Drake, P. L. & Hazelwood, K. J. Exposure-related health effects of silver and silver compounds: A review. *Ann. Occup. Hyg.* **49**, 575–585 (2005).
98. Dujon, B., Sherman, D., Fischer, G., Durrens, P., Casaregola, S., Lafontaine, I., Montigny, J., Marck, C., Blanchin, S., Beckerich, J., Beyne, E., Bleykasten, C., Babour, A., Boyer, J., Cattolico, L., Confanioleri, F., Daruvar, A., Despons, L., Fabre, E., Scarpelli, C., Gaillardin, C., Weissenbach, J., Wincker, P. & Souciet, J. Genome evolution in yeasts. *Nature* **430**, 35–44 (2004).
99. Ueno, K., Uno, J., Nakayama, H., Sasamoto, K., Mikami, Y. & Chibana, H. Development of a

- highly efficient gene targeting system induced by transient repression of YKU80 expression in *Candida glabrata*. *Eukaryot. Cell* **6**, 1239–1247 (2007).
100. Jansen, G., Wu, C., Schade, B., Thomas, D. Y. & Whiteway, M. Drag&Drop cloning in yeast. *Gene* **344**, 43–51 (2005).
 101. Köhrer, K. & Domdey, H. Preparation of high molecular weight RNA. *Methods Enzymol.* **194**, 398–405 (1991).
 102. Rodríguez-Tudela, J. L., Barchiesi, F., Bille, J., Chryssanthou, E., Cuenca-Estrella, M., Denning, D., Donnelly, J.P., Dupont, B., Fegeler, W., Moore, C., Richardson, M. & Verweij, P.E. Method for the determination of minimum inhibitory concentration (MIC) by broth dilution of fermentative yeasts. *Clin. Microbiol. Infect.* **9**, i–viii (2003).
 103. Kolaczowska, A., Kolaczowski, M., Delahodde, A. & Goffeau, A. Functional dissection of Pdr1p, a regulator of multidrug resistance in *Saccharomyces cerevisiae*. *Mol Genet Genomics* **267**, 96–106 (2002).
 104. Keuk-jun, K., Sung, W. S., Suh, B. K., Moon, S., Choi, J., Kim, J. G., Lee, D. G. Antifungal activity and mode of action of silver nano-particles on *Candida albicans*. *Biometals* **22**, 235–242 (2009).
 105. Kudrinskiy, A. A., Ivanov, A. Y., Kulakovskaya, E. V., Klimov, A. I., Zherebin, P. M., Khodarev, D. V., Le, A., Tam, L. T., Lisichkin, G. V. & Krutyakov, Y. A. The mode of action of silver and silver halides nanoparticles against *Saccharomyces cerevisiae* cells. *J. Nanoparticles* **2014**, 1–7 (2014).

Annex A

Alignment of the sequence of *CgPDR1* from isolate FFUL29 obtained with the sequence of the CBS138 reference strain. The sequencing reaction was performed by STABVIDA as a paid service and Clustal Omega was used for sequence alignment. Aminoacids substitutions are represented by a black rectangle.

CAGL0A00451g PDR1 FFUL29	MQTLETTSKSNPGEVKAQKPSTRRTKVGKACDSCRRRKIKCNGLKPCPSCTIYGCECTYT MQTLETTSKSNPGEVKAQKPSTRRTKVGKACDSCRRRKIKCNGLKPCPSCTIYGCECTYT *****	60 60
CAGL0A00451g PDR1 FFUL29	DAKSTKNLKSNDAGKSKPTGRVSKNKETTRIDKDIRHLEQQYVPIANIHVGRFPSENI DAKSTKNLKSNDAGKSKPTGRVSKNKETTRIDKDIRHLEQQYVPIANIHVGRFPSENI *****	120 120
CAGL0A00451g PDR1 FFUL29	LNGYPQCGAPQNNVVGNIPLAVNTQCHRGLSETPMSSTFKESNLRDDRLQSSDQDDMRNG LNGYPQCGAPQNNVVGNIPLAVNTQCHRGLSETPMSSTFKESNLRDDRLQSSDQDDMRNG *****	180 180
CAGL0A00451g PDR1 FFUL29	DSEERDLKGSSENVKSKDNKSDPLIIYKDDTHIESTVNLKQAVNELKSLQNPSSIKS DSEERDLKGSSENVKSKDNKSDPLIIYKDDTHIESTVNLKQAVNELKSLQNPSSIKS *****	240 240
CAGL0A00451g PDR1 FFUL29	SDIAIELQLRNILDNWKPEVDFEKAKINESATTKSLETNLLRNKYTNHVHLTRFRIWIDY SDIAIELQLRNILDNWKPEVDFEKAKINESATTKSLETNLLRNKYTNHVHLTRFRIWIDY *****	300 300
CAGL0A00451g PDR1 FFUL29	KNANKNNHFMGECGFSLAESFFASNQPLVDELFGLYSQVEAFSLQGLGYCVHLYEPYMKT KNANKNNHFMGECGFSLAESFFASNQPLVDELFGLYSQVEAFSLQGLGYCVHLYEPYMKT *****	360 360
CAGL0A00451g PDR1 FFUL29	EEAIKLMKETLYIILRFIDICVHHINEESISIANPLETYLRKKHLMPTPTPRSSYGSQ EEAIKLMKETLYIILRFIDICVHHINEESISIANPLETYLRKKHLMPTPTPRSSYGSQ *****	420 420
CAGL0A00451g PDR1 FFUL29	SASTKSLVSKIIERIPQPFIESVTNVSSLQLDLRDDSEKMFGLTLLNMCKSIRRKFD SVM SASTKSLVSKIIERIPQPFIESVTNVSSLQLDLRDDSEKMFGLTLLNMCKSIRRKFD SVM *****	480 480
CAGL0A00451g PDR1 FFUL29	SDYDSIVTEKSEGEQNDGKVTVAEFTSLCEAEEMLLALCYNYNLTLYSFFEFGTNIEYM SDYDSIVTEKSEGEQNDGKVTVAEFTSLCEAEEMLLALCYNYNLTLYSFFEFGTNIEYM *****	540 540
CAGL0A00451g PDR1 FFUL29	EHLLEELQALDEYYGFEKVLNVAVANAKMGFHRWEFYVGYEESTAEKRRLLWVKLY EHLLEELQALDEYYGFEKVLNVAVANAKMGFHRWEFYVGYEESTAEKRRLLWVKLY *****	600 600
CAGL0A00451g PDR1 FFUL29	NYEKASTMKKGFSSVIDDATVNCLLPKIFRNFGLDRVEFLENIQKPMDSLVSFSDVPISV NYEKASTMKKGFSSVIDDATVNCLLPKIFRNFGLDRVEFLENIQKPMDSLVSFSDVPISV *****	660 660
CAGL0A00451g PDR1 FFUL29	LCKYELALTIVTSEFHEKFLYADRYTSIRNSAKPPTLKNQLIKEIVDGIAYTETSYEAI LCKYELALTIVTSEFHEKFLYADRYTSIRNSAKPPTLKNQLIKEIVDGIAYTETSYEAI *****	720 720
CAGL0A00451g PDR1 FFUL29	RKQTAKLWDIALGKVTKDKINKEDTAAASKFTLSYEHYRFRLINMADNLIARLMVKPKSD RKQTAKLWDIALGKVTKDKINKEDTAAASKFTLSYEHYRFRLINMADNLIARLMVKPKSD *****	780 780
CAGL0A00451g PDR1 FFUL29	WLISVMKGHLNRLYEHKVMNEIILSMDNDYSIATTFEYAPSCCLATQTFLIVRNMEM WLISVMKGHLNRLYEHKVMNEIILSMDNDYSIATTFEYAPSCCLATQTFLIVRNMEM *****	840 840
CAGL0A00451g PDR1 FFUL29	DDVKMMVAVYKRFNLGMFLQSAKVCSLADSHFRDFSRSFSFIIISRLMIEFMQIKE DDVKMMVAVYKRFNLGMFLQSAKVCSLADSHFRDFSRSFSFIIISRLMIEFMQIKE *****	900 900
CAGL0A00451g PDR1 FFUL29	LTKVEFIEKFSEVCPDLADLPMLLDPNSCLYFSLQIQKSGFTLSFKKILEDARMDF LTKVEFIEKFSEVCPDLADLPMLLDPNSCLYFSLQIQKSGFTLSFKKILEDARMDF *****	960 960
CAGL0A00451g PDR1 FFUL29	NYDRNLDEAIKKNCGEFSKMPSCNTVSDTTAVSDNSAKKASMGARVNSTDTLTAS NYDRNLDEAIKKNCGEFSKMPSCNTVSDTTAVSDNSAKKASMGARVNSTDTLTAS *****	1020 1020
CAGL0A00451g PDR1 FFUL29	PLSGLRNQTLQDSKDSVPSLEAYTPIDSVSDVPTGEINVPFPVYVYQNGLDQQTYYNLGT PLSGLRNQTLQDSKDSVPSLEAYTPIDSVSDVPTGEINVPFPVYVYQNGLDQQTYYNLGT *****	1080 1080
CAGL0A00451g PDR1 FFUL29	LDEFVNGDNLNLYNSLWGLFSDVYL* 1107 LDEFVNGDNLNLYNSLWGLFSDVYL* 1107 *****	

Annex B

Alignment of the sequence of *CgPDR1* from isolate FFUL412 obtained with the sequence of the CBS138 reference strain. The sequencing reaction was performed by STABVIDA as a paid service and Clustal Omega was used for sequence alignment. Aminoacids substitutions are represented by a black rectangle.

CAGL0A00451g PDR1 FFUL412	MQTLETTKSNPGEVKAQKPSRRRTKVGKACDSCRRRKIKCNGLKPCPSTIYGCECTYT MQTLETTKSNPGEVKAQKPSRRRTKVGKACDSCRRRKIKCNGLKPCPSTIYGCECTYT *****	60 60
CAGL0A00451g PDR1 FFUL412	DAKSTKNLKSNDAGKSKPTGRVSKNKETTRV[K]DKIRKLEQQYVPIANAIHVGRFPSENI DAKSTKNLKSNDAGKSKPTGRVSKNKETTRV[K]DKIRKLEQQYVPIANAIHVGRFPSENI *****	120 120
CAGL0A00451g PDR1 FFUL412	LNGYPQCGAPQNNVVGNP[LV]AVITDCHRG[LS]ETPM[S]STFKESNLRD[R]LLQSSD[TD]DMRNG LNGYPQCGAPQNNVVGNP[LV]AVITDCHRG[LS]ETPM[S]STFKESNLRD[R]LLQSSD[TD]DMRNG *****	180 180
CAGL0A00451g PDR1 FFUL412	DSEERDLKGS[DS]ENVKSKDNKSDPLIIYKDDTHIESTVNKLQAVNELKSLQNA[P]SSIKS DSEERDLKGS[DS]ENVKSKDNKSDPLIIYKDDTHIESTVNKLQAVNELKSLQNA[P]SSIKS *****	240 240
CAGL0A00451g PDR1 FFUL412	SIDAIELQLRNILDNWKPEVDFEKAKINESATTKSLETNLLRNKYTNHVHLTRFR[IN]IDY SIDAIELQLRNILDNWKPEVDFEKAKINESATTKSLETNLLRNKYTNHVHLTRFR[IN]IDY *****	300 300
CAGL0A00451g PDR1 FFUL412	KNANKNNHFMGECGFSLAESFFASNQPLVDELFGLYSQVEAFSLQGLGVCVHLYEPYMKT KNANKNNHFMGECGFSLAESFFASNQPLVDELFGLYSQVEAFSLQGLGVCVHLYEPYMKT *****	360 360
CAGL0A00451g PDR1 FFUL412	EEAIKLMKETLYIILRFIDICVHHINEESIS[IA]NPLETYLRKKHLM[PM]TPTPRSSY[GS]PQ EEAIKLMKETLYIILRFIDICVHHINEESIS[IA]NPLETYLRKKHLM[PM]TPTPRSSY[GS]PQ *****	420 420
CAGL0A00451g PDR1 FFUL412	SASTKSLVSKIIERIPQPFIESVTNVSSLQLDLRDESKMFGTLLNMCKSIRRKFD[SV]M SASTKSLVSKIIERIPQPFIESVTNVSSLQLDLRDESKMFGTLLNMCKSIRRKFD[SV]M *****	480 480
CAGL0A00451g PDR1 FFUL412	SDYDSIVTEKSEGEQNDGKVTVAEFTSLCEAEEMLLALCYNYYNLTLYSFFEF[GT]NIEYM SDYDSIVTEKSEGEQNDGKVTVAEFTSLCEAEEMLLALCYNYYNLTLYSFFEF[GT]NIEYM *****	540 540
CAGL0A00451g PDR1 FFUL412	EHL[LL]LEEQLALDEYYGFEKVLNVAVANAKM[GF]HRNEFYVGYEESTAEKR[RL]LW[K]LY EHL[LL]LEEQLALDEYYGFEKVLNVAVANAKM[GF]HRNEFYVGYEESTAEKR[RL]LW[K]LY *****	600 600
CAGL0A00451g PDR1 FFUL412	NYEKASTMKKGF[FS]VIDDATVNCLLPKIFRNF[GY]LDRVEFLENIQK[PM]DL[SV]FSDV[PI]SV NYEKASTMKKGF[FS]VIDDATVNCLLPKIFRNF[GY]LDRVEFLENIQK[PM]DL[SV]FSDV[PI]SV *****	660 660
CAGL0A00451g PDR1 FFUL412	LCKY[GE]LALTI[VT]SEFHEKFLYADRYTSIRNSAKPPTLKNQ[LI]KEIVDGIAYTETS[YE]AI LCKY[GE]LALTI[VT]SEFHEKFLYADRYTSIRNSAKPPTLKNQ[LI]KEIVDGIAYTETS[YE]AI *****	720 720
CAGL0A00451g PDR1 FFUL412	RKQTA[KL]NDIALGKVT[KD]KINKEDTAAASKFTLSYEYHRFRLINMADNLIARLMV[KP]KSD RKQTA[KL]NDIALGKVT[KD]KINKEDTAAASKFTLSYEYHRFRLINMADNLIARLMV[KP]KSD *****	780 780
CAGL0A00451g PDR1 FFUL412	WLISVMK[GH]LNRLYEH[KV]MNEIILSMDNDYSIATTFEY[AP]SCLCLATQTF[LI]VRNMEM WLISVMK[GH]LNRLYEH[KV]MNEIILSMDNDYSIATTFEY[AP]SCLCLATQTF[LI]VRNMEM *****	840 840
CAGL0A00451g PDR1 FFUL412	DDVKM[V]VAVYKRFNLGMFLQSAKVC[SL]ADSHTRDFRS[SF]ITIIISRLMIEFMQI[KE] DDVKM[V]VAVYKRFNLGMFLQSAKVC[SL]ADSHTRDFRS[SF]ITIIISRLMIEFMQI[KE] *****	900 900
CAGL0A00451g PDR1 FFUL412	LTKVEFIEK[FS]EVC[PD]LADLPPMLLDPNSCLYFSL[LL]QIKKSGFTLSFKKILE[DA]R[M]MDF LTKVEFIEK[FS]EVC[PD]LADLPPMLLDPNSCLYFSL[LL]QIKKSGFTLSFKKILE[DA]R[M]MDF *****	960 960
CAGL0A00451g PDR1 FFUL412	NYDRNLDSEAIKKN[CG]EFSKSMPSCTNVSDTTAVSDNSAKKASMG[SAR]VNSTDTLTAS NYDRNLDSEAIKKN[CG]EFSKSMPSCTNVSDTTAVSDNSAKKASMG[SAR]VNSTDTLTAS *****	1020 1020
CAGL0A00451g PDR1 FFUL412	PLSGLRNQ[TL]DSDKDSVPSLEAYTPIDSVSDVPTGEINVPFP[VY]NQGLDQ[QT]TYNLGT PLSGLRNQ[TL]DSDKDSVPSLEAYTPIDSVSDVPTGEINVPFP[VY]NQGLDQ[QT]TYNLGT *****	1080 1080
CAGL0A00451g PDR1 FFUL412	LDEFV[NK]GDLNELYNSLWGD[LF]SDVYL* 1107 LDEFV[NK]GDLNELYNSLWGD[LF]SDVYL* 1107 *****	

Annex C

Alignment of the sequence of *CgPDR1* from isolate FFUL443 obtained with the sequence of the CBS138 reference strain. The sequencing reaction was performed by STABVIDA as a paid service and Clustal Omega was used for sequence alignment. Aminoacids substitutions are represented by a black rectangle.

CAGL0A00451g PDR1 FFUL443	MQTLETTSKSNPGEVKAQKPSTRRTKVGKACDSCRRIKICNGLKPCPSCTIYGCECTYT MQTLETTSKSNPGEVKAQKPSTRRTKVGKACDSCRRIKICNGLKPCPSCTIYGCECTYT *****	60 60
CAGL0A00451g PDR1 FFUL443	DAKSTKNLKSNDAGK[PTGRVSKNKETTRV]DKDIRK[EQYV]PINANIHVGRPFPSENI DAKSTKNLKSNDAGK[PTGRVSKNKETTRV]DKDIRK[EQYV]PINANIHVGRPFPSENI *****	120 120
CAGL0A00451g PDR1 FFUL443	LNGYPQCGAPQNNVVGNIPLAVN[PC]HRGLSETPMSSTFKESNLRDDRLQSSDODDMRNG LNGYPQCGAPQNNVVGNIPLAVN[PC]HRGLSETPMSSTFKESNLRDDRLQSSDODDMRNG *****	180 180
CAGL0A00451g PDR1 FFUL443	DSEERDLKGSDESNVSKDNKSDPLIYKDDTHIESTVNKLTQAVNELKSLQNPSSIKS DSEERDLKGSDESNVSKDNKSDPLIYKDDTHIESTVNKLTQAVNELKSLQNPSSIKS *****	240 240
CAGL0A00451g PDR1 FFUL443	SIDAIELQLRNILDNWKPEVDFEKAKINESATTKSLETNLLRNKYTNHVHLTRFRINIDY SIDAIELQLRNILDNWKPEVDFEKAKINESATTKSLETNLLRNKYTNHVHLTRFRINIDY *****	300 300
CAGL0A00451g PDR1 FFUL443	KNANKNNHFMGECGFLAESFFASNQPLVDELFGLYSQVEAFSLQGLGYCVHLYEPYMKT KNANKNNHFMGECGFLAESFFASNQPLVDELFGLYSQVEAFSLQGLGYCVHLYEPYMKT *****	360 360
CAGL0A00451g PDR1 FFUL443	EEAIKLMKETLYIILRFIDICVHHINEESIS[AN]PLETYLRKKHLMPTPTPRSSYGSPO EEAIKLMKETLYIILRFIDICVHHINEESIS[AN]PLETYLRKKHLMPTPTPRSSYGSPO *****	420 420
CAGL0A00451g PDR1 FFUL443	SASTKSLVSKIIERIPQPFIESVTNVSSLQLLDLRDESKMFGTLLMCKSIRKRFDSVM SASTKSLVSKIIERIPQPFIESVTNVSSLQLLDLRDESKMFGTLLMCKSIRKRFDSVM *****	480 480
CAGL0A00451g PDR1 FFUL443	SDYDSIVTEKSEGEQNDGKVTVAEFTSLCEAEMLLALCYNYYNLTLYSFFEFGTNIEYM SDYDSIVTEKSEGEQNDGKVTVAEFTSLCEAEMLLALCYNYYNLTLYSFFEFGTNIEYM *****	540 540
CAGL0A00451g PDR1 FFUL443	EHLLEELQALDEYYGFEKVLNVAVANAKMGFHRNEFYVGYEESTAEKRRLWIKLY EHLLEELQALDEYYGFEKVLNVAVANAKMGFHRNEFYVGYEESTAEKRRLWIKLY *****	600 600
CAGL0A00451g PDR1 FFUL443	NYEKASTMKKGFSSVIDDATVNCLLPKIFRNFGYLDLDRVEFLENIQKPMDSLVSFSDVPISV NYEKASTMKKGFSSVIDDATVNCLLPKIFRNFGYLDLDRVEFLENIQKPMDSLVSFSDVPISV *****	660 660
CAGL0A00451g PDR1 FFUL443	LCKYGEALITVTEFHEKFLYADRYTSIRNSAKPPTLKNQLIKEIVDGIAYTETSIEAI LCKYGEALITVTEFHEKFLYADRYTSIRNSAKPPTLKNQLIKEIVDGIAYTETSIEAI *****	720 720
CAGL0A00451g PDR1 FFUL443	RKQTAKLWIDIALGKVTDKINKEDTAAASKFTLSYEHYRFRLINMADNLIARLMVVKPKSD RKQTAKLWIDIALGKVTDKINKEDTAAASKFTLSYEHYRFRLINMADNLIARLMVVKPKSD *****	780 780
CAGL0A00451g PDR1 FFUL443	WLISVMKGLNRLYEHWKVMNEIILSMDNDYSIATTFEYAPSCLCLATQTFLIVRNMEM WLISVMKGLNRLYEHWKVMNEIILSMDNDYSIATTFEYAPSCLCLATQTFLIVRNMEM *****	840 840
CAGL0A00451g PDR1 FFUL443	DOVKMVAVYKRFNLGMFLQSAKVCSLADSHTRFDRSRSFSFIIISRLMIEFMIQIE DOVKMVAVYKRFNLGMFLQSAKVCSLADSHTRFDRSRSFSFIIISRLMIEFMIQIE *****	900 900
CAGL0A00451g PDR1 FFUL443	LTKVEFIEKFSEVCPDLADLPPMLLDPNCLYFSLQIQIKKSGFTLSFKKILEDARMMDF LTKVEFIEKFSEVCPDLADLPPMLLDPNCLYFSLQIQIKKSGFTLSFKKILEDARMMDF *****	960 960
CAGL0A00451g PDR1 FFUL443	NYDRNLDESAIKKCNGEFSKMPSCNTNVSODTTTAVSDNSAKKASMGARSVNSTDLTAS NYDRNLDESAIKKCNGEFSKMPSCNTNVSODTTTAVSDNSAKKASMGARSVNSTDLTAS *****	1020 1020
CAGL0A00451g PDR1 FFUL443	PLSGLRNQTLQDSKDSVPSLEAYTPIDSVSDVPTGEINVPFPVYVQNGLDQQTYYNLGT PLSGLRNQTLQDSKDSVPSLEAYTPIDSVSDVPTGEINVPFPVYVQNGLDQQTYYNLGT *****	1080 1080
CAGL0A00451g PDR1 FFUL443	LDEFVNGDLNELYNSLWGLFSDVYL* 1107 LDEFVNGDLNELYNSLWGLFSDVYL* 1107 *****	

Annex D

Alignment of the sequence of *CgPDR1* from isolate FFUL674 obtained with the sequence of the CBS138 reference strain. The sequencing reaction was performed by STABVIDA as a paid service and Clustal Omega was used for sequence alignment. Aminoacids substitutions are represented by a black rectangle.

CAGL0A00451g PDR1 FFUL674	MQTLETTSKSNPGEVKAQKPSTRRTKVGKACDSCRRRKIKCNGLKPCPSCTIYGCECTYT MQLKTTTSKSNPGEVKAQKPSTRRTKVGKACDSCRRRKIKCNGLKPCPSCTIYGCECTYT *****	60 60
CAGL0A00451g PDR1 FFUL674	DAKSTKNLKSNDAGKSKPTGRVSKNKETTAVKDIRKLEQQYVPIANIHVGRPRFSENI DAKSTKNLKSNDAGKSKPTGRVSKNKETTAVKDIRKLEQQYVPIANIHVGRPRFSENI *****	120 120
CAGL0A00451g PDR1 FFUL674	LNGYQCGAPQNNVVGNIPLAVNTQCHRGLETSPMSSTFKESNLRDDRLQSSDQDDMRNG LNGYQCGAPQNNVVGNIPLAVNTQCHRGLETSPMSSTFKESNLRDDRLQSSDQDDMRNG *****	180 180
CAGL0A00451g PDR1 FFUL674	DSEERDLKGSDSENVKSKDNKSDPLIYKDDTHIESTVNKLTQAVNELKSLQAPSSIKS DSEERDLKGSDSENVKSKDNKSDPLIYKDDTHIESTVNKLTQAVNELKSLQAPSSIKS *****	240 240
CAGL0A00451g PDR1 FFUL674	SDIAIELQLRNILDNWKPEVDFEKAKINESATTKSLETNLRNKYTNHVLTRFRIWIDY SDIAIELQLRNILDNWKPEVDFEKAKINESATTKSLETNLRNKYTNHVLTRFRIWIDY *****	300 300
CAGL0A00451g PDR1 FFUL674	KNANKNNHFMGECGFLAESFFASNQPLVDFLGLYSQVEAFSLQGLGYCVHLYEPYMKT KNANKNNHFMGECGFLAESFFASNQPLVDFLGLYSQVEAFSLQGLGYCVHLYEPYMKT *****	360 360
CAGL0A00451g PDR1 FFUL674	EEAIKLMKETLYIILRFIDICVHHINEESISIANPLETYLRKKHLMPTPTPRSSYGSPO EEAIKLMKETLYIILRFIDICVHHINEESISIANPLETYLRKKHLMPTPTPRSSYGSPO *****	420 420
CAGL0A00451g PDR1 FFUL674	SASTKSLVSKIIERIPQPFIESVTNVSSLQLDLRDESKMFGTLNLMCKSIRKFD SVM SASTKSLVSKIIERIPQPFIESVTNVSSLQLDLRDESKMFGTLNLMCKSIRKFD SVM *****	480 480
CAGL0A00451g PDR1 FFUL674	SOYDSIVTEKSEGEQNDGKVTVAEFTSLCEAEMLLALCYNYNLTLYSFFFGTNI EYM SOYDSIVTEKSEGEQNDGKVTVAEFTSLCEAEMLLALCYNYNLTLYSFFFGTNI EYM *****	540 540
CAGL0A00451g PDR1 FFUL674	EHLLEELQALDEYGFVKLVNVAVANAKMGFHRNEFYVGYEESTAEKRRLWVKLY EHLLEELQALDEYGFVKLVNVAVANAKMGFHRNEFYVGYEESTAEKRRLWVKLY *****	600 600
CAGL0A00451g PDR1 FFUL674	NYEKASTMKGGFFSVIDDATVNCLLPKIFRNFYGLDRVEFLENIQKPMDSLVSFSDVPISV NYEKASTMKGGFFSVIDDATVNCLLPKIFRNFYGLDRVEFLENIQKPMDSLVSFSDVPISV *****	660 660
CAGL0A00451g PDR1 FFUL674	LCKYGEALTIVTSEFHEKFLYADRYTSIRNSAKPPTLKNQLIKEIVDGIAYTETS YEAI LCKYGEALTIVTSEFHEKFLYADRYTSIRNSAKPPTLKNQLIKEIVDGIAYTETS YEAI *****	720 720
CAGL0A00451g PDR1 FFUL674	RKQTAKLNDIALGKVTKDKINKEDTAAASKFTLSYEYHRFRLINMADNLIARLMVKPKSD RKQTAKLNDIALGKVTKDKINKEDTAAASKFTLSYEYHRFRLINMADNLIARLMVKPKSD *****	780 780
CAGL0A00451g PDR1 FFUL674	WLISVMKGHLNRLYEHMKVMNEIILSMNDYSIATTFEYAPSCLC LATQTF LIVRNMEM WLISVMKGHLNRLYEHMKVMNEIILSMNDYSIATTFEYAPSCLC LATQTF LIVRNMEM *****	840 840
CAGL0A00451g PDR1 FFUL674	DOVKMMVAVYKRFNLGMFLQSAKVCSLADSHTRDFRSRFSFIIISRLMIEFMIQIKE DOVKMMVAVYKRFNLGMFLQSAKVCSLADSHTRDFRSRFSFIIISRLMIEFMIQIKE *****	900 900
CAGL0A00451g PDR1 FFUL674	LTKVEFIEKFSEVCPDLADLPMLLDPNLSCLYFSLQIQKSGFTLSFKKILEDARMMDF LTKVEFIEKFSEVCPDLADLPMLLDPNLSCLYFSLQIQKSGFTLSFKKILEDARMMDF *****	960 960
CAGL0A00451g PDR1 FFUL674	NYDRNLDEAIIKKNGEFSKSMPSCTNVSOTTTAVSDNSAKKASMG SARVNSTDLTAS NYDRNLDEAIIKKNGEFSKSMPSCTNVSOTTTAVSDNSAKKASMG SARVNSTDLTAS *****	1020 1020
CAGL0A00451g PDR1 FFUL674	PLSGLRNQTQLDSKDSVPSLEAYTPIDSVSDVPTGEINWPFPPVYNQNGLDQQTTYNLGT PLSGLRNQTQLDSKDSVPSLEAYTPIDSVSDVPTGEINWPFPPVYNQNGLDQQTTYNLGT *****	1080 1080
CAGL0A00451g PDR1 FFUL674	LDEFVNGDLNELYNSLWGLFSDVYL* 1107 LDEFVNGDLNELYNSLWGLFSDVYL* 1107 *****	

Annex E

Alignment of the sequence of *CgPDR1* from isolate FFUL677 obtained with the sequence of the CBS138 reference strain. The sequencing reaction was performed by STABVIDA as a paid service and Clustal Omega was used for sequence alignment. Aminoacids substitutions are represented by a black rectangle.

CAGL0A00451g PDR1 FFUL677	MQTLETTSKSNPGEVKAQKPTRRTRKVGKACDSCRRRKIKCNGLKPCPSCIYGCCTY MQLKTTSKSNPGEVKAQKPTRRTRKVGKACDSCRRRKIKCNGLKPCPSCIYGCCTY *****	60 60
CAGL0A00451g PDR1 FFUL677	DAKSTKNLKSNDAGKSKPTGRVSKNKETT[REDACTED]KDIRNLEQQVYPINANIHVGRPFPS DAKSTKNLKSNDAGKSKPTGRVSKNKETT[REDACTED]KDIRNLEQQVYPINANIHVGRPFPS *****	120 120
CAGL0A00451g PDR1 FFUL677	LNGYPQCGAPQNNVVGNP[REDACTED]LAVNTQCHRGLSETPMSSTFKESNLRDDRLQSSD LNGYPQCGAPQNNVVGNP[REDACTED]LAVNTQCHRGLSETPMSSTFKESNLRDDRLQSSD *****	180 180
CAGL0A00451g PDR1 FFUL677	DSEERDLKGSDESNVSKDNKSDPLIYKDDTHIESTVWKLQAVNELKSLQ[NAPSSIKS DSEERDLKGSDESNVSKDNKSDPLIYKDDTHIESTVWKLQAVNELKSLQ[NAPSSIKS *****	240 240
CAGL0A00451g PDR1 FFUL677	SDAIEIQLRNLIDNWKPEVDFEKAKINESATTKSLETNLLRNKYTNHVHLTRFRWIDY SDAIEIQLRNLIDNWKPEVDFEKAKINESATTKSLETNLLRNKYTNHVHLTRFRWIDY *****	300 300
CAGL0A00451g PDR1 FFUL677	KNANKNNHFMGECGFLAESFFASNQPLVDELFGLYSQVEAFSLQGLGVCVHLYEPYMK KNANKNNHFMGECGFLAESFFASNQPLVDELFGLYSQVEAFSLQGLGVCVHLYEPYMK *****	360 360
CAGL0A00451g PDR1 FFUL677	EEAIKLMKETLYIILRFIDICVHHINEESISIANPLETYLRKKHLMPTPTPRSSYGS EEAIKLMKETLYIILRFIDICVHHINEESISIANPLETYLRKKHLMPTPTPRSSYGS *****	420 420
CAGL0A00451g PDR1 FFUL677	SASTKSLVSKIIERIPQPFIESVTNVSSLQLDLRDESKMFGTLLNMCKSIRRFDSV SASTKSLVSKIIERIPQPFIESVTNVSSLQLDLRDESKMFGTLLNMCKSIRRFDSV *****	480 480
CAGL0A00451g PDR1 FFUL677	SDYDSIVTEKSEGEQNDGKVTVAEFTSLCEAEMLLALCYNNYNTLYSFFEFGTNIEY SDYDSIVTEKSEGEQNDGKVTVAEFTSLCEAEMLLALCYNNYNTLYSFFEFGTNIEY *****	540 540
CAGL0A00451g PDR1 FFUL677	EHL[REDACTED]LLEQLALDEYGFYFEKVLNVAVANAKMGFHRNEFYVGYEESTAEKRLLM EHL[REDACTED]LLEQLALDEYGFYFEKVLNVAVANAKMGFHRNEFYVGYEESTAEKRLLM *****	600 600
CAGL0A00451g PDR1 FFUL677	NYEKASTMKKGF[REDACTED]SVIDDATVNCLLPKIFRNFYGLDRVEFLNIQKPM[REDACTED]SVFSDVPI NYEKASTMKKGF[REDACTED]SVIDDATVNCLLPKIFRNFYGLDRVEFLNIQKPM[REDACTED]SVFSDVPI *****	660 660
CAGL0A00451g PDR1 FFUL677	LCKY[REDACTED]GELALTI[REDACTED]VTEFHEKFLYADRYTSIRNSAKPPTLKNQLIKEIVDGIAYTETS LCKY[REDACTED]GELALTI[REDACTED]VTEFHEKFLYADRYTSIRNSAKPPTLKNQLIKEIVDGIAYTETS *****	720 720
CAGL0A00451g PDR1 FFUL677	RKQTAKLNDIALGKVT[KDINKEDTAAASKFTLSYEHYRFLINMADNLIARLMVKPKSD RKQTAKLNDIALGKVT[KDINKEDTAAASKFTLSYEHYRFLINMADNLIARLMVKPKSD *****	780 780
CAGL0A00451g PDR1 FFUL677	WLISVMK[REDACTED]GHLNRLYEHWKVMNEITLLSMDNDYSIATTFEYAPSCCLATQTF WLISVMK[REDACTED]GHLNRLYEHWKVMNEITLLSMDNDYSIATTFEYAPSCCLATQTF *****	840 840
CAGL0A00451g PDR1 FFUL677	DDVKMMVAVYKRFNLGMFLQSAKVC[REDACTED]LADSHFRD[REDACTED]SRSFSFIIISRLMIEFMQI DDVKMMVAVYKRFNLGMFLQSAKVC[REDACTED]LADSHFRD[REDACTED]SRSFSFIIISRLMIEFMQI *****	900 900
CAGL0A00451g PDR1 FFUL677	LTKVEFIEKFSEVCPDLADLPPMLLDPNSCLYFSL[REDACTED]LQIKKSGFTLSFKKILEARMDF LTKVEFIEKFSEVCPDLADLPPMLLDPNSCLYFSL[REDACTED]LQIKKSGFTLSFKKILEARMDF *****	960 960
CAGL0A00451g PDR1 FFUL677	NYDRNL[REDACTED]DSEAIKKCN[REDACTED]GFEFSKSMPSCTNVSDTTTAVSDNSAKKASMG[SARVNSTDLTAS NYDRNL[REDACTED]DSEAIKKCN[REDACTED]GFEFSKSMPSCTNVSDTTTAVSDNSAKKASMG[SARVNSTDLTAS *****	1020 1020
CAGL0A00451g PDR1 FFUL677	PLSGLRNQTLQDSKDSVPSLEAYTPIDSVSDVPTGEINVPFPVYVYVQNGLDQQT[REDACTED]TYNLGT PLSGLRNQTLQDSKDSVPSLEAYTPIDSVSDVPTGEINVPFPVYVYVQNGLDQQT[REDACTED]TYNLGT *****	1080 1080
CAGL0A00451g PDR1 FFUL677	LDEFV[REDACTED]KGD[REDACTED]LNELYN[REDACTED]SLWGLDFSDVYL* 1107 LDEFV[REDACTED]KGD[REDACTED]LNELYN[REDACTED]SLWGLDFSDVYL* 1107 *****	

Annex F

Alignment of the sequence of *CgPDR1* from isolate FFUL830 obtained with the sequence of the CBS138 reference strain. The sequencing reaction was performed by STABVIDA as a paid service and Clustal Omega was used for sequence alignment. Aminoacids substitutions are represented by a black rectangle.

CAGL0A00451g PDR1 FFUL830	MQTLETTSKSNPGEVKAQKPSTRRTKVGKACDSCRRIKICNGLKPCPSCTIYGCECTYT MQTLETTSKTNPGEVKAQKPSTRRTKVGKACDSCRRIKICNGLKPCPSCTIYGCECTYT *****	60 60
CAGL0A00451g PDR1 FFUL830	DAKSTKNLKSNDAGKSKPTGRVSKNKETTRVDKDIRKLEQQYVPIANIHVGRFPFSENI DAKSTKNLKSNDAGKSKPTGRVSKNKETTRVDKDIRKLEQQYVPIANIHVGRFPFSENI *****	120 120
CAGL0A00451g PDR1 FFUL830	LNGYPQCGAPQNNVGNPLAVNTQCHRGLSETPMSSTFKESNLRDDRLQSSDODDMRNG LNGYPQCGAPQNNVGNPLAVNTQCHRGLSETPMSSTFKESNLRDDRLQSSDODDMRNG *****	180 180
CAGL0A00451g PDR1 FFUL830	DSEERDLKGSSENVKSKDNKSDPLIYKDDTHIESTVNKLTQAVNELKSLQNAAPSSIKS DSEERDLKGSSENVKSKDNKSDPLIYKDDTHIESTVNKLTQAVNELKSLQNAAPSSIKS *****	240 240
CAGL0A00451g PDR1 FFUL830	SIDAIELQLRNILDNWKPEVDFEKAKINESATTKSLETNLLRNKYTNHVHLTRFRIWIDY SIDAIELQLRNILDNWKPEVDFEKAKINESATTKSLETNLLRNKYTNHVHLTRFRIWIDY *****	300 300
CAGL0A00451g PDR1 FFUL830	KNANKNNHFMGECGFLAESFFASNQPLVDELFGLYSQVEAFSLQGLGVCVHLYEPYMKT KNANKNNHFMGECGFLAESFFASNQPLVDELFGLYSQVEAFSLQGLGVCVHLYEPYMKT *****	360 360
CAGL0A00451g PDR1 FFUL830	EEAIKMKETLYIILRFIDICVHINEESISIANPLETYLRKKHLMPTPTPRSSYGSQP EEAIKMKETLYIILRFIDICVHINEESISIANPLETYLRKKHLMPTPTPRSSYGSQP *****	420 420
CAGL0A00451g PDR1 FFUL830	SASTKSLVSKIIERIPQPFIESVTNVSSLQLDLRDDKSMFGTLLNMCKSIRKFDVSM SASTKSLVSKIIERIPQPFIESVTNVSSLQLDLRDDKSMFGTLLNMCKSIRKFDVSM *****	480 480
CAGL0A00451g PDR1 FFUL830	SDYDSIVTEKSEGEQNDGKVTVAEFTSLCEAEEMLLALCYNNYNTLYSFFFGTNIIEYM SDYDSIVTEKSEGEQNDGKVTVAEFTSLCEAEEMLLALCYNNYNTLYSFFFGTNIIEYM *****	540 540
CAGL0A00451g PDR1 FFUL830	EHLLEELQALDQKYYGFEKVLNVAVANAKMGFHRWEFYVGYEESTAEKRLLWVKLY EHLLEELQALDQKYYGFEKVLNVAVANAKMGFHRWEFYVGYEESTAEKRLLWVKLY *****	600 600
CAGL0A00451g PDR1 FFUL830	NYEKASTMKGGFFSVIDDATVNCLLPKIFRNFGLDRVEFLENIQKPMDLVSVSDVPISV NYEKASTMKGGFFSVIDDATVNCLLPKIFRNFGLDRVEFLENIQKPMDLVSVSDVPISV *****	660 660
CAGL0A00451g PDR1 FFUL830	LCKYGEALTIIVTSEFHEKFLYADRYTSIRNSAKPPTLKNQLIKEIVDGIAYTETSYEAI LCKYGEALTIIVTSEFHEKFLYADRYTSIRNSAKPPTLKNQLIKEIVDGIAYTETSYEAI *****	720 720
CAGL0A00451g PDR1 FFUL830	RKQTAKLWIDIALGKVTKDKINKEDTAAASKFTLSYEHYRFRLINMADNLIARLMVKPKSD RKQTAKLWIDIALGKVTKDKINKEDTAAASKFTLSYEHYRFRLINMADNLIARLMVKPKSD *****	780 780
CAGL0A00451g PDR1 FFUL830	WLISVMKGHLNRLYEHWKVMNEIILSMNDYSIATTFEYAPSCCLATQTFLIVRNMEM WLISVMKGHLNRLYEHWKVMNEIILSMNDYSIATTFEYAPSCCLATQTFLIVRNMEM *****	840 840
CAGL0A00451g PDR1 FFUL830	DDVKMMVAVYKRFNLGMFLQSAKVCSLADSHTRDFRSFSFITIIISRLMIEFMQIKE DDVKMMVAVYKRFNLGMFLQSAKVCSLADSHTRDFRSFSFITIIISRLMIEFMQIKE *****	900 900
CAGL0A00451g PDR1 FFUL830	LTKVEFIEKFSEVCPDLADLPMLLDPNCLYFSLQIKKSGFTLSFKKILEDARMMDF LTKVEFIEKFSEVCPDLADLPMLLDPNCLYFSLQIKKSGFTLSFKKILEDARMMDF *****	960 960
CAGL0A00451g PDR1 FFUL830	NYDRNLDSEAIKKCNGEFSKSMPSCTNVSDDTTAVSDNSAKKASMGARSVNSTDLTAS NYDRNLDSEAIKKCNGEFSKSMPSCTNVSDDTTAVSDNSAKKASMGARSVNSTDLTAS *****	1020 1020
CAGL0A00451g PDR1 FFUL830	PLSGLRNQTLQDSKDSVPSLEAYTPIDSVDVPTGEINWPPVYVYQNGLDQQTYYNLGT PLSGLRNQTLQDSKDSVPSLEAYTPIDSVDVPTGEINWPPVYVYQNGLDQQTYYNLGT *****	1080 1080
CAGL0A00451g PDR1 FFUL830	LDFVNGDNLNELYNLWGLFSDVYL* LDFVNGDNLNELYNLWGLFSDVYL* *****	1107 1107

Annex G

Alignment of the sequence of *CgPDR1* from isolate FFUL866 obtained with the sequence of the CBS138 reference strain. The sequencing reaction was performed by STABVIDA as a paid service and Clustal Omega was used for sequence alignment. Aminoacids substitutions are represented by a black rectangle.

CAGL0A00451g PDR1 FFUL866	MQTLETTSKSNPGEVKAQKPSTRRTKVGKACDSRRRRIKIKCNGLKPCPSCTIYGCECTYT MQTLETTSKSNPGEVKAQKPSTRRTKVGKACDSRRRRIKIKCNGLKPCPSCTIYGCECTYT *****	60 60
CAGL0A00451g PDR1 FFUL866	DAKSTKNLKSNDAGKSKPTGRVSKNKETTRVKKDIRKLEQQYVPINANIHVGRFPFSENI DAKSTKNLKSNDAGKSKPTGRVSKNKETTRVKKDIRKLEQQYVPINANIHVGRFPFSENI *****	120 120
CAGL0A00451g PDR1 FFUL866	LNGYPQCGAPQNNVVGNIPLAVNTQCHRGLSETPMSSTFKESNLRDDRLQSSDTPDMRNG LNGYPQCGAPQNNVVGNIPLAVNTQCHRGLSETPMSSTFKESNLRDDRLQSSDTPDMRNG *****	180 180
CAGL0A00451g PDR1 FFUL866	DSEERDLKGSDESNVSKDNKSDPLIYKDDTHIESTVNKLTAQAVNELKSLQMAPSSIKS DSEERDLKGSDESNVSKDNKSDPLIYKDDTHIESTVNKLTAQAVNELKSLQMAPSSIKS *****	240 240
CAGL0A00451g PDR1 FFUL866	SIDAIELQLRNILDNWKPEVDFEKAKINESATTKSLETNLLRNKYTNHVHLTRFRIWIDY SIDAIELQLRNILDNWKPEVDFEKAKINESATTKSLETNLLRNKYTNHVHLTRFRIWIDY *****	300 300
CAGL0A00451g PDR1 FFUL866	KNANKNNHFMGECGFSLAESFFASNQPLVDELFGLYSQVEAFSLQGLGYCVHLYEPYMKT KNANKNNHFMGECGFSLAESFFASNQPLVDELFGLYSQVEAFSLQGLGYCVHLYEPYMKT *****	360 360
CAGL0A00451g PDR1 FFUL866	EEAIKLMKETLYIILRFIDICVHHINEESISIANPLETYLRKKHLMPTPTPRSSYGSQ EEAIKLMKETLYIILRFIDICVHHINEESISIANPLETYLRKKHLMPTPTPRSSYGSQ *****	420 420
CAGL0A00451g PDR1 FFUL866	SASTKSLVSKIIERIPQPFIESVTNVSSLQLDLRDESKMFGTLLNMCKSIRRKFD SVM SASTKSLVSKIIERIPQPFIESVTNVSSLQLDLRDESKMFGTLLNMCKSIRRKFD SVM *****	480 480
CAGL0A00451g PDR1 FFUL866	SDYDSIVTEKSEGEQNDGKVTVAEFTSLCEAEEMLLALCYNYNLTLYSFFEFGTNIEYM SDYDSIVTEKSEGEQNDGKVTVAEFTSLCEAEEMLLALCYNYNLTLYSFFEFGTNIEYM *****	540 540
CAGL0A00451g PDR1 FFUL866	EHLLEELQALDEYYGFEKVLNVAVANAKMGFHRNEFYVGYEESTAEKRRLLWVKLY EHLLEELQALDEYYGFEKVLNVAVANAKMGFHRNEFYVGYEESTAEKRRLLWVKLY *****	600 600
CAGL0A00451g PDR1 FFUL866	NYEKASTMKKGFSSVIDDATVNCLLPKIFRNFGYLD RVEFLENIQKPMDL SVFSDVPISV NYEKASTMKKGFSSVIDDATVNCLLPKIFRNFGYLD RVEFLENIQKPMDL SVFSDVPISV *****	660 660
CAGL0A00451g PDR1 FFUL866	LCKYGEALATIVTSEFHEKFLYADRYTSIRNSAKPPTLKNQLIKEIVDGIAYTETS YEAI LCKYGEALATIVTSEFHEKFLYADRYTSIRNSAKPPTLKNQLIKEIVDGIAYTETS YEAI *****	720 720
CAGL0A00451g PDR1 FFUL866	RKQTAKLWDIALGKVTDKINKEDTAAASKFTLSYEHFRFLINMADNLIARLWVKPKSD RKQTAKLWDIALGKVTDKINKEDTAAASKFTLSYEHFRFLINMADNLIARLWVKPKSD *****	780 780
CAGL0A00451g PDR1 FFUL866	WLISVMKGLNRLYEHKVMNEIILSMDNDYSIATTFEYAPSCCLATQTF LIVRNMEM WLISVMKGLNRLYEHKVMNEIILSMDNDYSIATTFEYAPSCCLATQTF LIVRNMEM *****	840 840
CAGL0A00451g PDR1 FFUL866	DDVKMMVAVYKRFNLNLMFLQSAKVCSLADSHTRDFRSFSFITIISRLMIEFMQIKE DDVKMMVAVYKRFNLNLMFLQSAKVCSLADSHTRDFRSFSFITIISRLMIEFMQIKE *****	900 900
CAGL0A00451g PDR1 FFUL866	LTKVEFIEKFSEVCPDLADLPMLLDPNSCLYFSLQIQKSGFTLSFKKILEDARMMDF LTKVEFIEKFSEVCPDLADLPMLLDPNSCLYFSLQIQKSGFTLSFKKILEDARMMDF *****	960 960
CAGL0A00451g PDR1 FFUL866	NYDRNLDSEAIKKNCGEFSKSMPSCTNVSDTTTAVSDNSAKKASMG SARVNSTDTLTAS NYDRNLDSEAIKKNCGEFSKSMPSCTNVSDTTTAVSDNSAKKASMG SARVNSTDTLTAS *****	1020 1020
CAGL0A00451g PDR1 FFUL866	PLSGLRNQQLDSKDSVPSLEAYTPIDSVDVPTGEINVPFPVYVQNGLDQQTYYNLGT PLSGLRNQQLDSKDSVPSLEAYTPIDSVDVPTGEINVPFPVYVQNGLDQQTYYNLGT *****	1080 1080
CAGL0A00451g PDR1 FFUL866	LDEFVVKGDLNELYNSLWGLFSDVYL* 1107 LDEFVVKGDLNELYNSLWGLFSDVYL* 1107 *****	

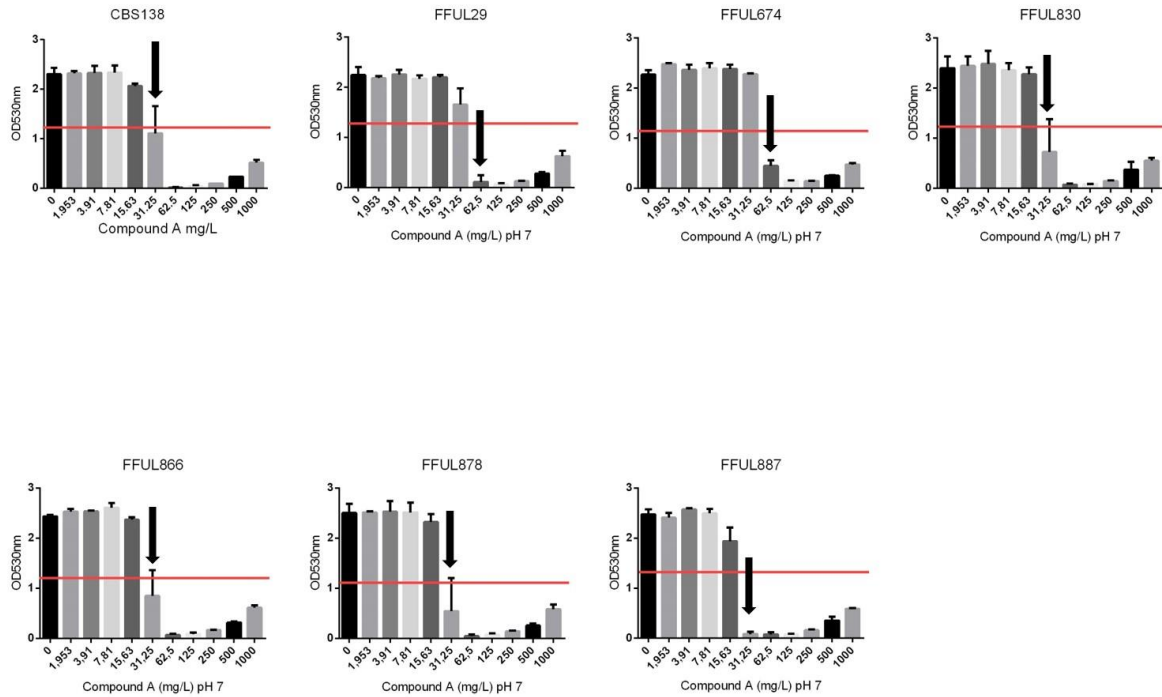
Annex H

Alignment of the sequence of *CgPDR1* from isolate FFUL878 obtained with the sequence of the CBS138 reference strain. The sequencing reaction was performed by STABVIDA as a paid service and Clustal Omega was used for sequence alignment. Aminoacids substitutions are represented by a black rectangle.

CAGL0A00451g PDR1 FFUL878	MQT[E]TSKSNPGEVKAQKPSTRRTKVGKACDSCRRIKICNGLKPCPSCTIYGCECTYT MQLK[T]TSKSNPGEVKAQKPSTRRTKVGKACDSCRRIKICNGLKPCPSCTIYGCECTYT *****	60 60
CAGL0A00451g PDR1 FFUL878	DAKSTKNLKSNDAGKSKPTGRVSKNKETTRV[K]DKIRK[LE]QQYVPINANIHVGRFRPSENI DAKSTKNLKSNDAGKSKPTGRVSKNKETTRV[K]DKIRK[SE]QQYVPINANIHVGRFRPSENI *****	120 120
CAGL0A00451g PDR1 FFUL878	LNGYPQCGAPQNNVVGNIPLAVNTQCHRGLSETPMSSTFKESNLRDDRLQSSDODDMRNG LNGYPQCGAPQNNVVGNIPLAVNTQCHRGLSETPMSSTFKESNLRDDRLQSSDODDMRNG *****	180 180
CAGL0A00451g PDR1 FFUL878	DSEERDLKGSDESNVSKDNKSDPLIIYKDDTHIESTVNKLQAVNELKSLQNAAPSSIKS DSEERDLKGSDESNVSKDNKSDPLIIYKDDTHIESTVNKLQAVNELKSLQNAAPSSIKS *****	240 240
CAGL0A00451g PDR1 FFUL878	SID[AI]ELQLRNLIDNMKPEVDFEKAKINESATT[K]LETNLLRNKYTNHVLTRFRIWIDY SIN[AI]ELQLRNLIDNMKPEVDFEKAKINESATT[K]LETNLLRNKYTNHVLTRFRIWIDY *****	300 300
CAGL0A00451g PDR1 FFUL878	KNANKNNHFMGECGFLAESFFASNQPLVDELFGLYSQVEAFSLQGLGYCVHLYEPYMKT KNANKNNHFMGECGFLAESFFASNQPLVDELFGLYSQVEAFSLQGLGYCVHLYEPYMKT *****	360 360
CAGL0A00451g PDR1 FFUL878	EEAIKLMKETLYIILRFIDICVHHINEESISIANPLETYLRKKHLMPTPTPRSSYGSPO EEAIKLMKETLYIILRFIDICVHHINEESISIANPLETYLRKKHLMPTPTPRSSYGSPO *****	420 420
CAGL0A00451g PDR1 FFUL878	SASTKSLVSKIIERIPQPFIESVTNVSSLQLDLRDESKMFGTLLNMCKSIIRKFD SVM SASTKSLVSKIIERIPQPFIESVTNVSSLQLDLRDESKMFGTLLNMCKSIIRKFD SVM *****	480 480
CAGL0A00451g PDR1 FFUL878	SDYDSIVTEKSEGEQNDGKVTVAEFTSLCEAEMLLALCYNYNLTLYSFFEFGTNIEYM SDYDSIVTEKSEGEQNDGKVTVAEFTSLCEAEMLLALCYNYNLTLYSFFEFGTNIEYM *****	540 540
CAGL0A00451g PDR1 FFUL878	EHLLEELQALDEYYGFEKVLNVAVANAKMGFHRNEFYVGYEESTAEKRLLWVKLY EHLLEELQALDEYYGFEKVLNVAVANAKMGFHRNEFYVGYEESTAEKRLLWVKLY *****	600 600
CAGL0A00451g PDR1 FFUL878	NYEKASTMKKGFSSVIDDATVNCLLPKIFRNFYGLDRVEFLENIQKPMDSLVSFSDVPISV NYEKASTMKKGFSSVIDDATVNCLLPKIFRNFYGLDRVEFLENIQKPMDSLVSFSDVPISV *****	660 660
CAGL0A00451g PDR1 FFUL878	LCKYGEALTIIVTSEFHEKFLYADRYTSIRNSAKPPTLKNQLIKEIVDGIAYTETS YEAI LCKYGEALTIIVTSEFHEKFLYADRYTSIRNSAKPPTLKNQLIKEIVDGIAYTETS YEAI *****	720 720
CAGL0A00451g PDR1 FFUL878	RKQTAKLWDIALGKVTOKINKEDTAAASKFTLSYEHYRFRLINMADNLIARLMVKPKSD RKQTAKLWDIALGKVTOKINKEDTAAASKFTLSYEHYRFRLINMADNLIARLMVKPKSD *****	780 780
CAGL0A00451g PDR1 FFUL878	WLISVMKGHNLRLYEHWKVMNEIILSMDNDYSIATTFEYAPSCLCLATQTF LIVRNMEM WLISVMKGHNLRLYEHWKVMNEIILSMDNDYSIATTFEYAPSCLCLATQTF LIVRNMEM *****	840 840
CAGL0A00451g PDR1 FFUL878	DDVKMMVAVYKRFNLNLMFLQSAKVCSLADSHTRDFSRFSFIIISRLMIEFMQIKE DDVKMMVAVYKRFNLNLMFLQSAKVCSLADSHTRDFSRFSFIIISRLMIEFMQIKE *****	900 900
CAGL0A00451g PDR1 FFUL878	LTKVEFIEK[FC]VCPDLADLPPMLLDPNSCLYFSLQKIKKSGFTLSFKKILEDARMDF LTKVEFIEK[FC]VCPDLADLPPMLLDPNSCLYFSLQKIKKSGFTLSFKKILEDARMDF *****	960 960
CAGL0A00451g PDR1 FFUL878	NYDRNLDESAIKKCNGEFSSKMPSCITNVSDDTTAVSDNSAKKASMG SARVNSTDLTAS NYDRNLDESAIKKCNGEFSSKMPSCITNVSDDTTAVSDNSAKKASMG SARVNSTDLTAS *****	1020 1020
CAGL0A00451g PDR1 FFUL878	PLSGLRNQTLQDSKDSVPSLEAYTIDSVSDVPTGEINWPFPPVYNQGLDQQTTYNLGT PLSGLRNQTLQDSKDSVPSLEAYTIDSVSDVPTGEINWPFPPVYNQGLDQQTTYNLGT *****	1080 1080
CAGL0A00451g PDR1 FFUL878	LDEFVNGDLNELYNSLWGLFSDVYL* 1107 LDEFVNGDLNELYNSLWGLFSDVYL* 1107 *****	

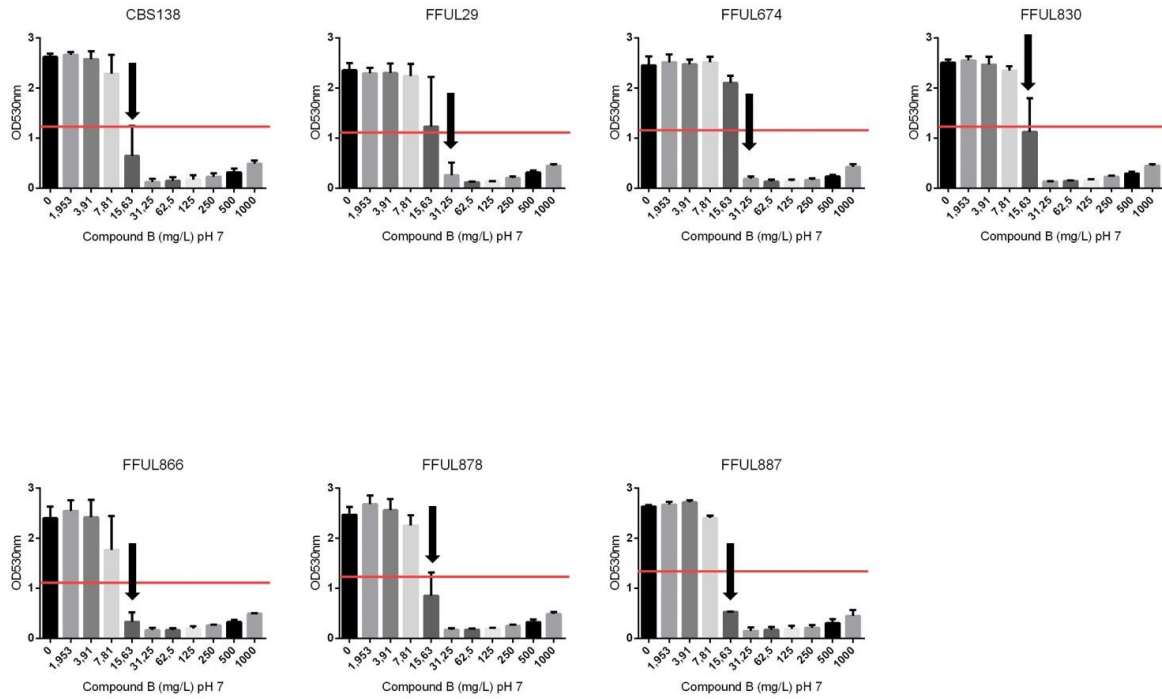
Annex I

Antifungal activity of compound A against the resistant clinical isolates, FFUL29, FFUL674, FFUL830, FFUL866, FFUL878, FFLU887 and the reference strain CBS138. The MIC₅₀ was determined comparing the values of the different isolates in the supplemented medium with chemical and the one registered in control conditions after 24 h of cultivation at 37 °C in RPMI growth medium (pH 7), as described in materials and methods. The MIC₅₀ value is indicated by a black arrows and the 50 % reduction of the growth registered in the absence of the chemicals is indicated by the red line.



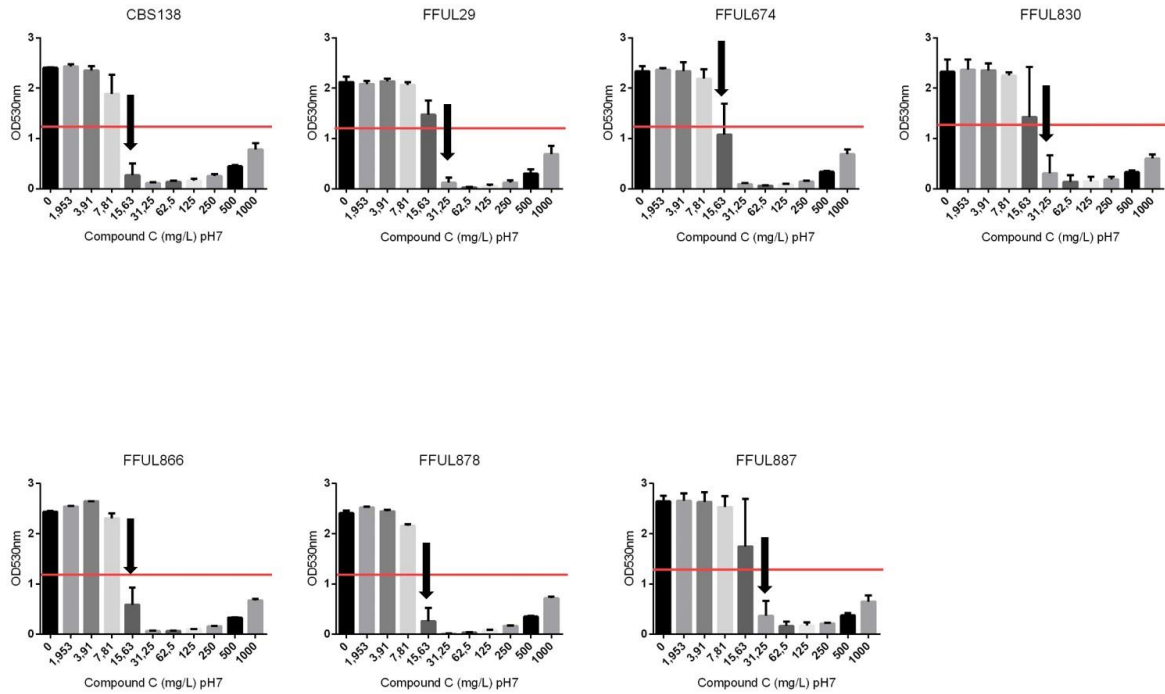
Annex J

Antifungal activity of compound B against the resistant clinical isolates, FFUL29, FFUL674, FFUL830, FFUL866, FFUL878, FFLU887 and the reference strain CBS138. The MIC₅₀ was determined comparing the values of the different isolates in the supplemented medium with chemical and the one registered in control conditions after 24 h of cultivation at 37 °C in RPMI growth medium (pH 7), as described in materials and methods. The MIC₅₀ value is indicated by a black arrows and the 50 % reduction of the growth registered in the absence of the chemicals is indicated by the red line.



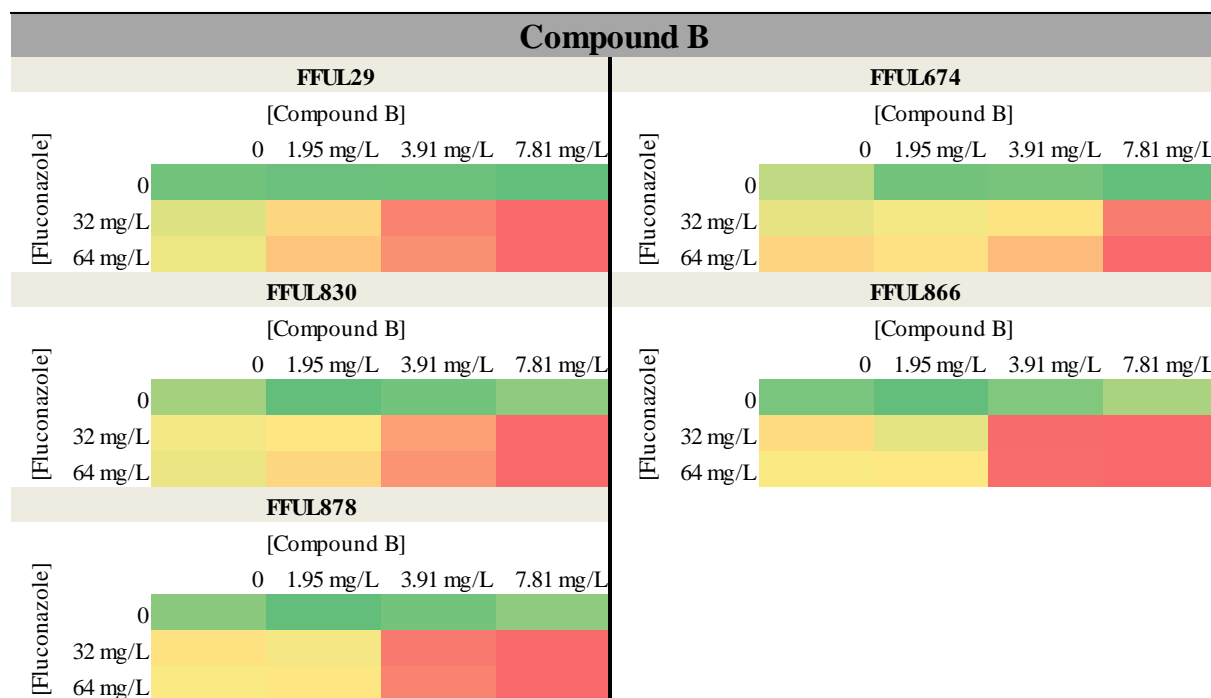
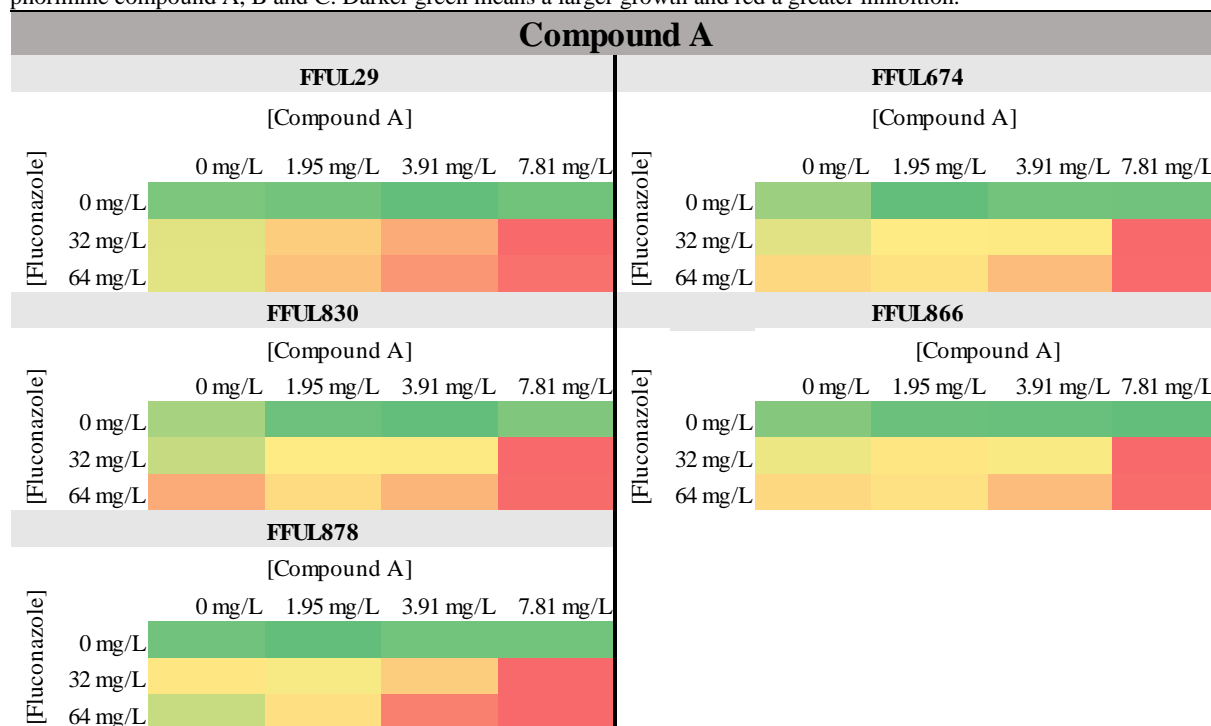
Annex K

Antifungal activity of compound C against the resistant clinical isolates, FFUL29, FFUL674, FFUL830, FFUL866, FFUL878, FFLU887 and the reference strain CBS138. The MIC₅₀ was determined comparing the values of the different isolates in the supplemented medium with chemical and the one registered in control conditions after 24 h of cultivation at 37 °C in RPMI growth medium (pH 7), as described in materials and methods. The MIC₅₀ value is indicated by a black arrows and the 50 % reduction of the growth registered in the absence of the chemicals is indicated by the red line.

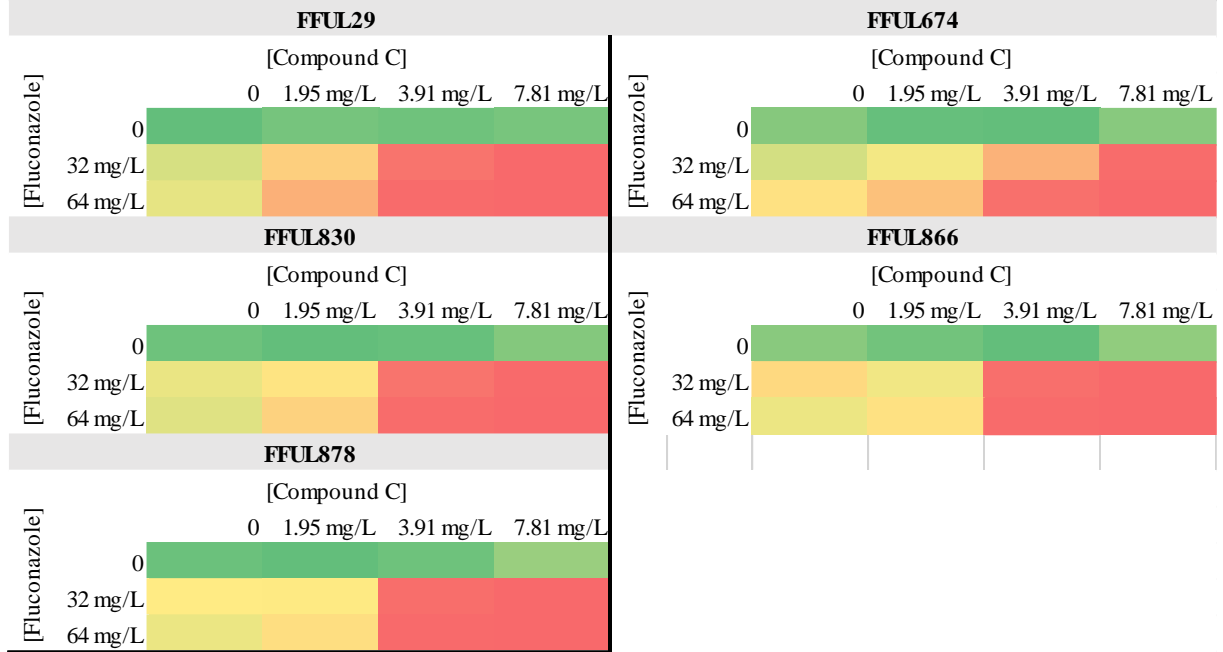


Annex L

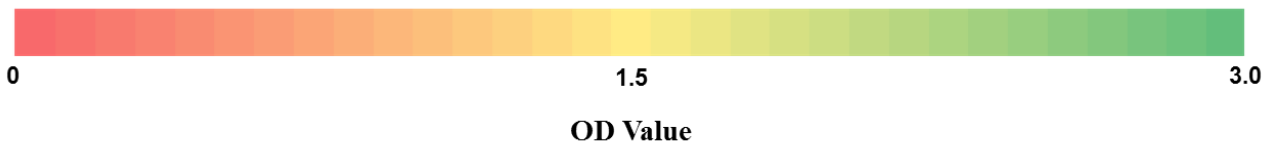
Heatmaps obtained in the synergism assay used to assess the potential of the synergistic effect of fluconazole and camphorimine compound A, B and C. Darker green means a larger growth and red a greater inhibition.



Compound C

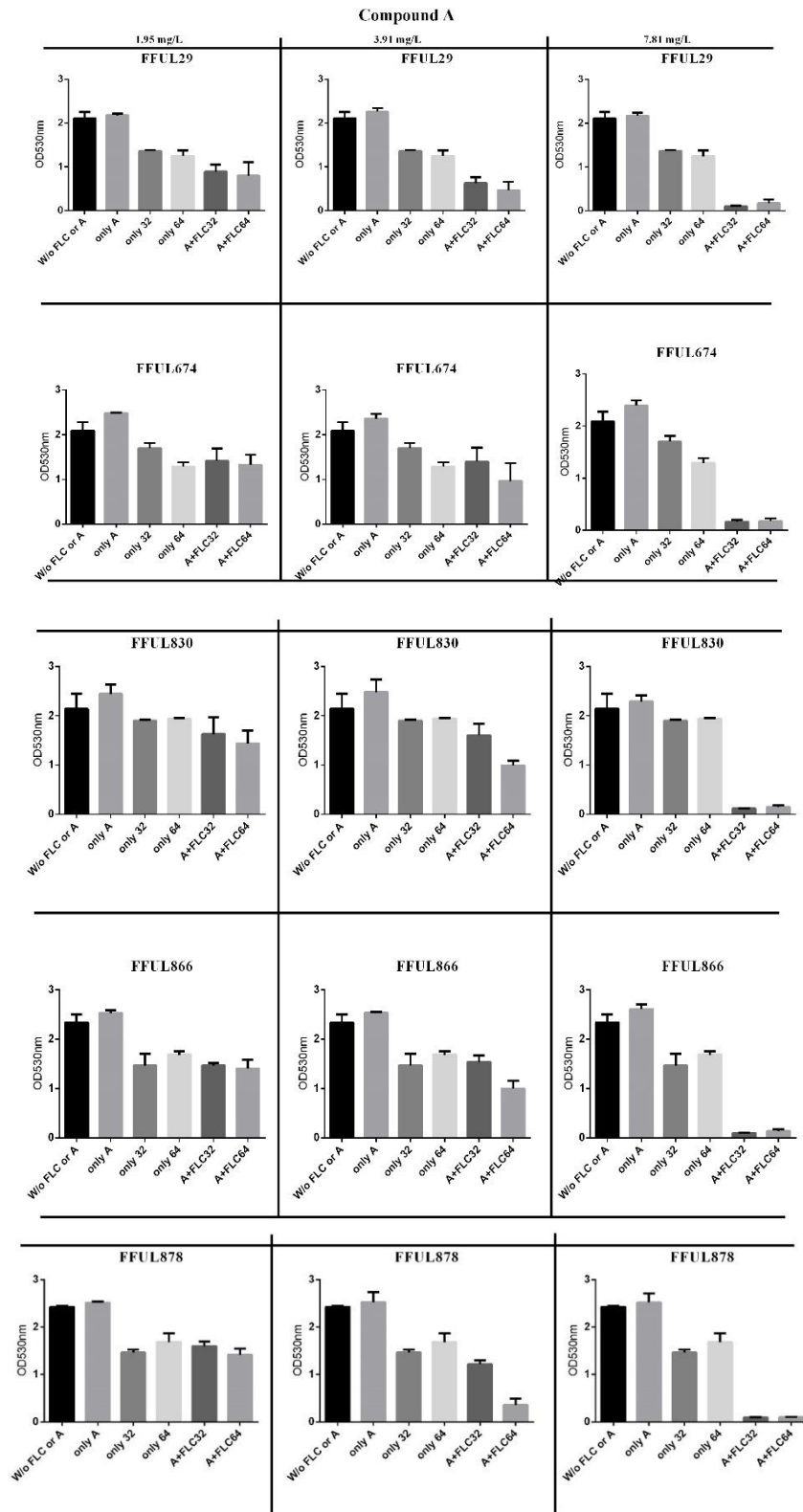


Color Key



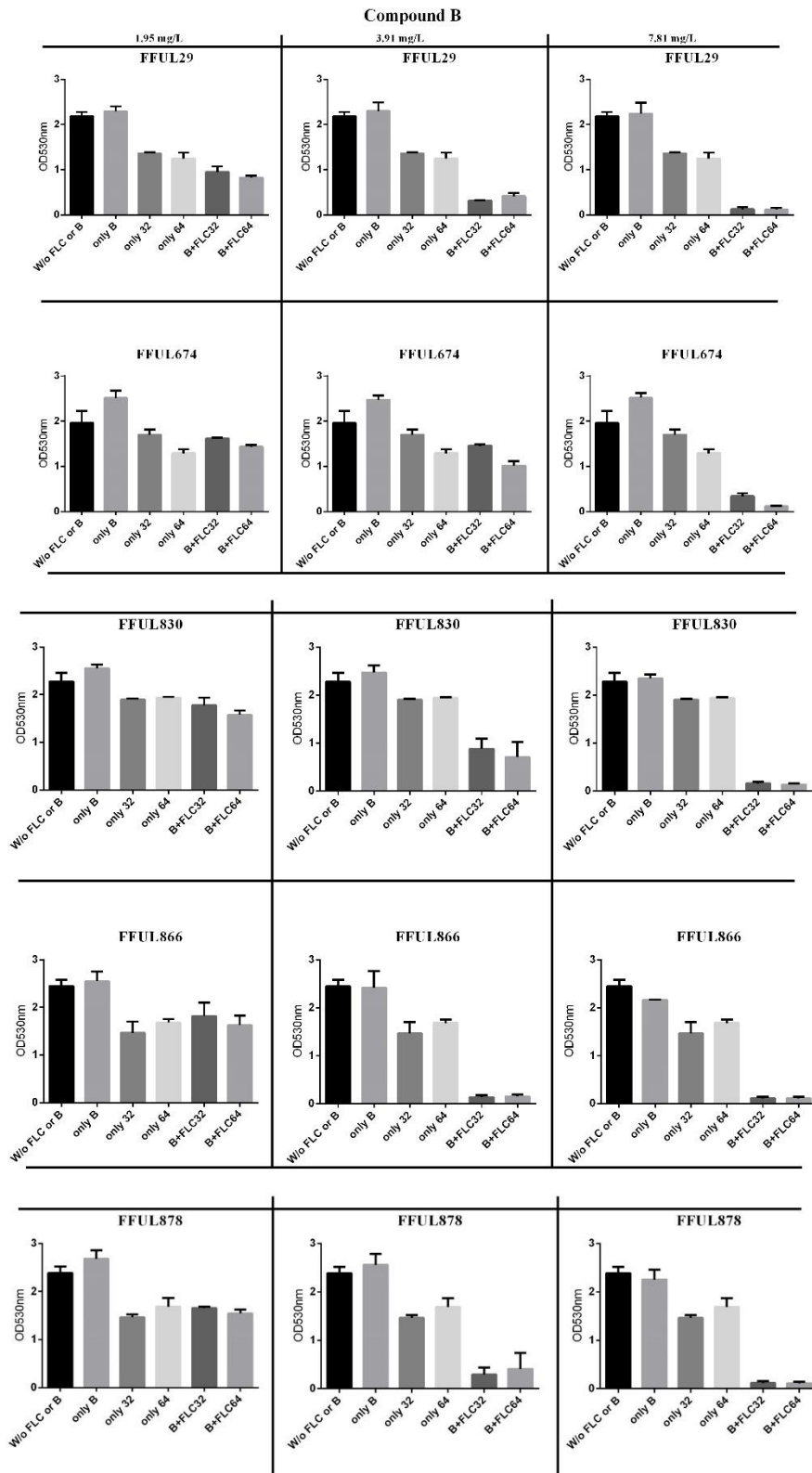
Annex M

Graphic representation of the ODs obtained in the assays to assess the effects of the potential synergistic combination of compound A and fluconazole against *C. glabrata* clinical isolates. In the graphic is represented a control column (w/o FLC or A) with the growth medium without stress, or the medium supplemented only with compound A (only A), or with the concentration of the breakpoint value (32 mg/L for CBS138 (only 32) and 64 mg/L for the resistant isolate (only 64)), and one concentration below (16 mg/L for CBS138 (only 16) and 32 mg/L for the resistant isolate (only 32)) and at last a combination of the compound plus each one of the concentrations of fluconazole. Three non-inhibitory concentrations of the compound was used, 1.95 mg/L, 3.91 mg/L and 7.81 mg/L.



Annex N

Graphic representation of the ODs obtained in the assays to assess the effects of the potential synergistic combination of compound B and fluconazole against *C. glabrata* clinical isolates. In the graphic is represented a control column (w/o FLC or B) with the growth medium without stress, or the medium supplemented only with compound B (only B), or with the concentration of the breakpoint value (32 mg/L for CBS138 (only 32) and 64 mg/L for the resistant isolate (only 64)), and one concentration below (16 mg/L for CBS138 (only 16) and 32 mg/L for the resistant isolate (only 32)) and at last a combination of the compound plus each one of the concentrations of fluconazole. Three non-inhibitory concentrations of the compound was used, 1.95 mg/L, 3.91 mg/L and 7.81 mg/L.



Annex O

Graphic representation of the ODs obtained in the assays to assess the effects of the potential synergistic combination of compound C and fluconazole against *C. glabrata* clinical isolates. In the graphic is represented a control column (w/o FLC or C) with the growth medium without stress, or the medium supplemented only with compound C (only C), or with the concentration of the breakpoint value (32 mg/L for CBS138 (only 32) and 64 mg/L for the resistant isolate (only 64)), and one concentration below (16 mg/L for CBS138 (only 16) and 32 mg/L for the resistant isolate (only 32)) and at last a combination of the compound plus each one of the concentrations of fluconazole. Three non-inhibitory concentrations of the compound was used, 1.95 mg/L, 3.91 mg/L and 7.81 mg/L.

